S

FACULTY OF SCIENCE AND TECHNOLOGY
MASTER THESIS

Author:
Selam Abraha Gebre

Selam Abraha
(Signature author)

Faculty supervisor: Sudath C. Siriwardane
External supervisor: Bruno Villoria

Thesis title:

Fatigue Life Assessment of Rib to Deck Welded Joint of the Hardanger Bridge – a Realistic Traffic Loading of FEM

Fatigue Life Assessment of Rib to Deck Welded Joint of the Hardanger Bridge – a Realistic Traffic Loading of FEM

Selam Abraha Gebre

Faculty of Science and Technology
UNIVERSITY OF STAVANGER, SPRING 2022

Preface

This thesis was written as a finalization of my master´s degree in structural engineering at the Department of Mechanical and Structural Engineering and Materials Science at the National University of Science and Technology in Stavanger (UiS), Norway. The thesis covers 30 out of 120 ECTs required for a master's degree. The finite element model creation and analysis for this thesis was conducted from January to June 2022.

I would like to thank my supervisor at the University of Stavanger, Professor Sudath C. Siriwardane, for his guidance throughout the semester. I also would like to thank my external supervisor, in The National Public Roads Administration, PhD Candidate Bruno Villoria for his guidance on finite element modelling, traffic loading, and stress extraction from Abaqus.

Abstract

The orthotropic steel decks in the Hardanger Bridge, as is common for long span suspension bridges, have welded joints that are susceptible to fatigue cracks. The rib-to-deck welded joints under the wheel load are the most common crack initiation sites. Crack in the weldment accelerates the degradation of other components of the bridge deck and ultimately shortens the fatigue life of the road bridge. The fatigue life of the rib-to-deck welded joint is determined by using Miner's damage accumulation rule of the rainflow cycle counted stress ranges of the nominal and Hot Spot stresses.

A full-scale 20 m long finite element model of the box girders in the Hardanger Bridge was built following the design drawings provided by the Norwegian Public Road Administration (NPRA). The model was loaded with fatigue load models (FLM) in Abaqus. A realistic dynamic design of the FLM traffic loading on the bridge was achieved by user subroutine. The thesis compared the fatigue life of two fatigue load models, the national (FLM-N) and Eurocode's FLM4. The effect of velocity on fatigue life of the welded joint was assessed by simulating vehicle with three different velocities while ensuring equal sampling rate. A validated whole span global model of Hardanger Bridge was provided for this thesis. The global model was loaded by vehicle equivalent concentrated load and corresponding moment of FLM-N and FLM-4. Stress response calculated from moment and axial force was used to estimate fatigue life.

The fatigue load models cause high cycle fatigue damage on the welded joints of the orthotropic steel decks of the Hardanger Bridge. The Hot Spot stress fatigue life of the welded rib-to-deck joint was 135 years (FLM-N) and 24 years (FLM4). The corresponding nominal stress fatigue life was 1180 years (FLM-N). Stresses from loading the global model with a single vehicle at a time did not induce fatigue damage. The effect of velocities of the vehicles loaded resulted in insignificant changes of the fatigue life of the welded joint.

Table of contents

Abbreviations

AADT   Annual average daily traffic

CAE   Computer Aided Engineering

CAFL   Constant Amplitude fatigue Limit

DNV   Det Norske Veritas

ECS   European Committee for Standardization

FEA   Finite Element Analysis

FEM   Finite Element Method

FLM   Fatigue Load Model

FLM4   Fatigue load model 4

FLM-N   Fatigue load model National (H-185)

HCF   High Cycle Fatigue

HSS   Hot Spot Stress

IIW   International Institute of Welding

LCF   Low Cycle Fatigue

Nobs   Total number of heavy lorries crossing the road bridge

NPRA   The National Public Roads Administration

RP   Reference Point

Symbols

A	Cross-sectional area
D	Damage accumulation factor
m	Negative slope of fatigue strength curve
n	Number of stress cycles
N	Fatigue life (cycles)
$N_{f,FL}$	Endurance number of cycles
$N_{f,LCF}$	Number of cycles to fatigue failure of the
N_i	Number of fatigue failures
$\Delta\sigma$	Stress range
$\Delta\sigma c$	Reference value of fatigue strength
$\Delta\sigma_D$	Constant Amplitude Fatigue Limit stress range
$\Delta\sigma_L$	Cut-off Limit stress range
$\Delta\tau$	Shear stress range
$\Delta\tau_R$	Shear Stress fatigue strength
γ_{Ff}	Partial factor for equivalent constant amplitude stress ranges
γ_{MF}	Partial factor for fatigue strength
σ_{hs}	Hot Spot stress
σ_{nom}	Nominal Stress
σ_x	Normal stress perpendicular to welding
σ_y	Normal stress parallel to welding

1. Introduction

1.1. <u>The finite element models</u>

1.1.1. *Hardanger Bridge*

The Hardanger Bridge is the longest suspension bridge in Norway and the 17th longest suspension bridge in the world today[2]. The bridge is 1380 m long, making it 30 m longer than the Golden Gate Bridge in San Francisco[3]. The bridge was constructed between 2009 and 2013, and it is the most attractive and quickest highway between Oslo and Bergen across the Hardanger fjord in Norway. The bridge was built with the intention of better regional transportation and ferry free east-west and north-south communication[4]. It has replaced the ferry connection between Bruravik and Brimnes on the highway *Figure 1* and made both local and regional transport easier.
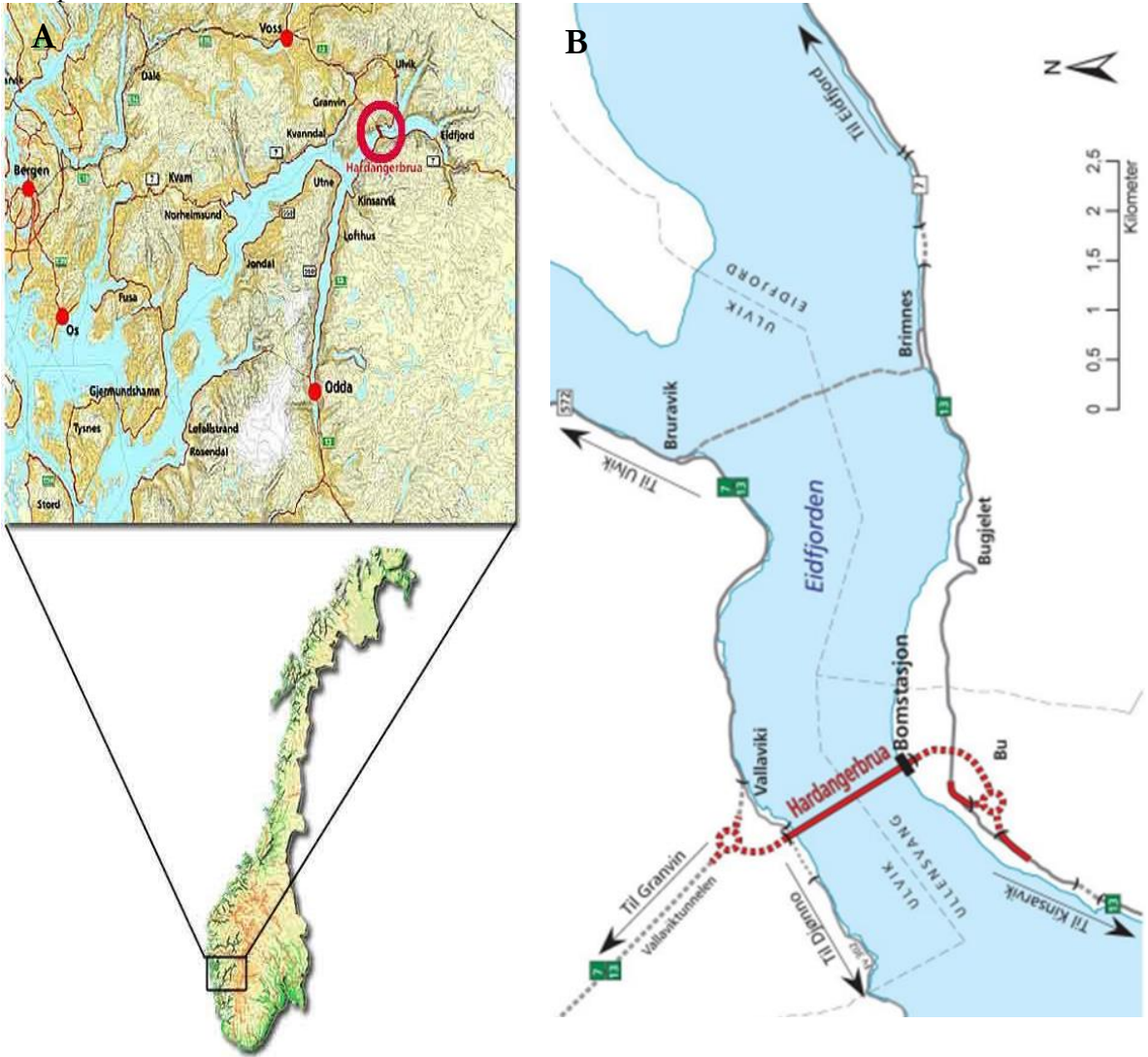
Figure 1 (A) The location of Hardanger Road Bridge in Norway and the Hardanger Fjord. (B) The bridge (red) crossing the Eid fjord, inner branch of the Hardanger fjord [5].
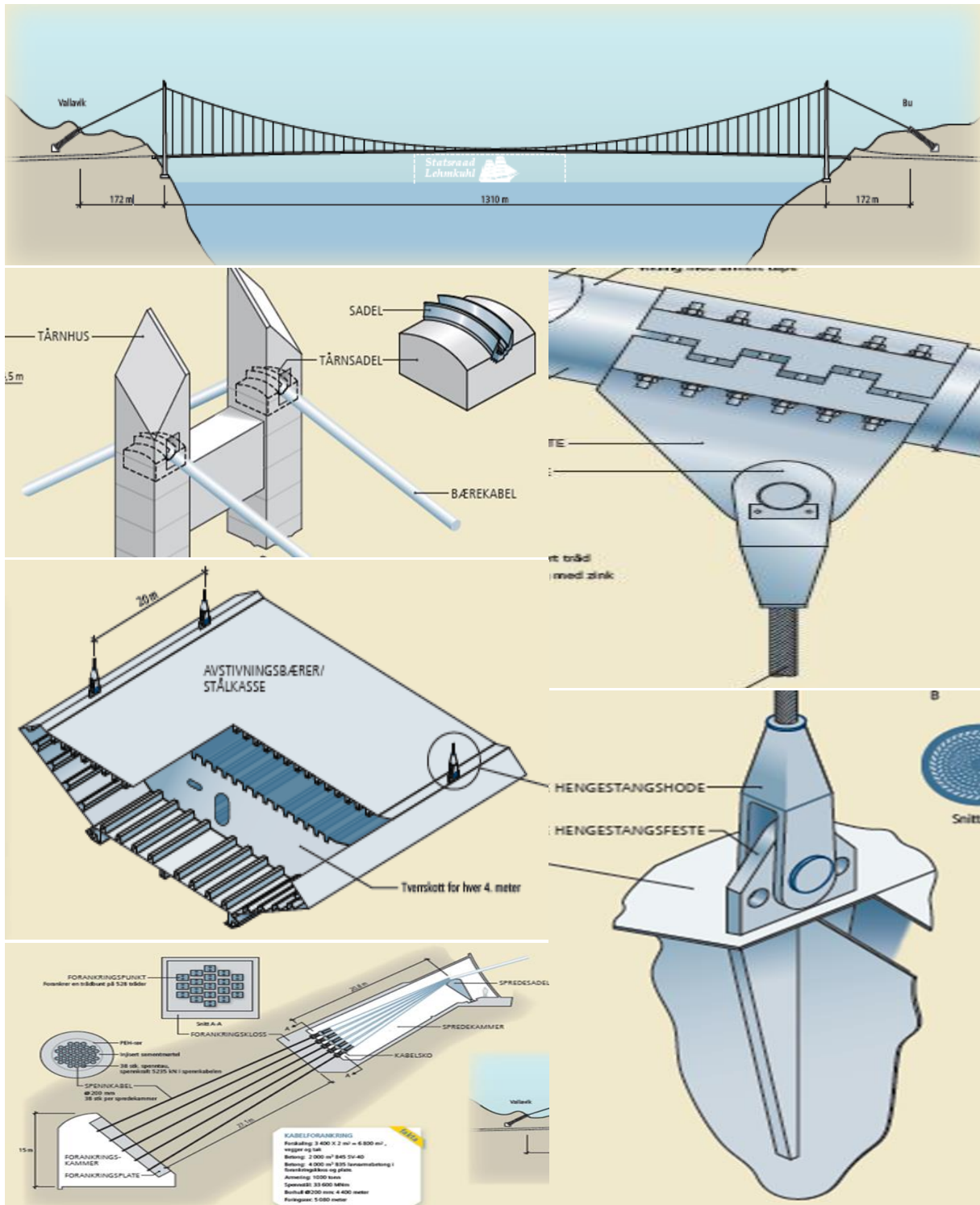
Figure 2 Hardanger bridge design drawings. The span of the suspension bridge. The main cables pass through the saddle-housing in the pylons and anchored to the mountain. The box girder is carried by the hangers, which again are attached to the main cable [6].

The main components of the suspension bridge are the box girder, the hangers, the main cables, the pylons, and the anchorage *Figure 2*. The traffic lanes are on the upper deck of the box girder. The hangers suspend the box girder on the main cable, with hangers' clamps on each side of the box girder placed 20 meters apart. The main cables pass through the saddle housing at the top of the pylons and are anchored at the anchorage piers of the mountain's solid rocks.

1.1.2. The global model

The global FEM of the suspension bridge of Hardanger Bridge was provided by external supervisor for this thesis. It was loaded with equivalent concentrated load of each vehicle moving the total span of the suspension bridge, one vehicle at a time.

1.1.3. The rib-to-deck welded joint

The FEM of the box-girder was created, loaded, and analyzed by the author for this thesis. The local stress variation at a welded detail of the orthotropic steel deck of Hardanger Bridge, was calculated from a detailed finite element model (FEM) of a segment of the bridge box girder. Closed trapezoidal stiffeners are taken as the study objects for fatigue problem of orthotropic steel decks (OSDs), because they are the most common support beams of OSDs. The most common fatigue affected details in OSDs are the (1) stiffener-to-diaphragm and (2) rib-to-deck welded joints *Figure 3*. This thesis investigates the fatigue life of the rib-to-deck welded joint.
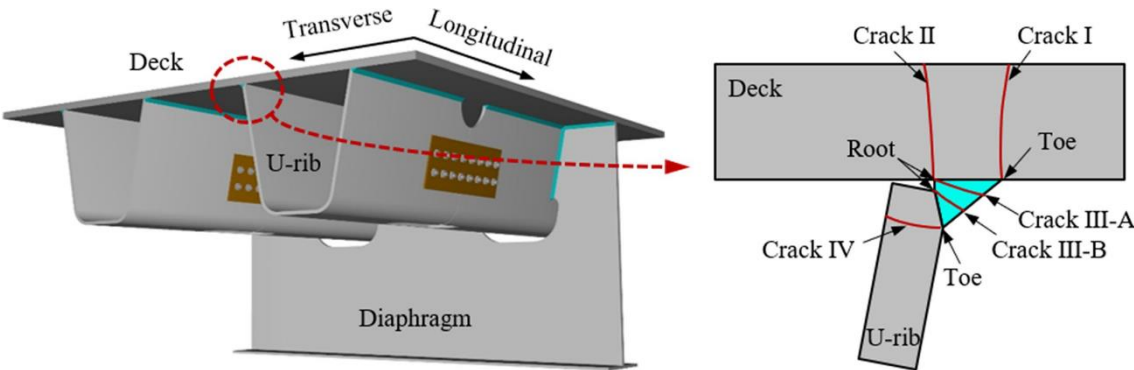
Figure 3 The rib-to-deck welded joint. The typical crack propagation paths (Crack I - IV). Image from[7].

1.2. Fatigue assessment

Fatigue is the main determinant factor of the service life of steel bridges. Most suspension bridges today use steel, due to their low price, low self-weight, high load carrying capacity[28]. high fatigue resistance. Reliably determining the fatigue life, i.e., the length of safe and maintenance free service life, of a steel bridge is complex.

1.2.1. Traffic loading of the bridge

A realistic fatigue traffic loading was defined using Fortran code (DLOAD user subroutine) to simulate fatigue load model induced damage. The national fatigue load model (FLM-N) specified by the Norwegian Public Road Administration (NPRA)[49] and the fatigue load model 4 (FLM-4) specified by Eurocode 3[10] are used for fatigue loading.
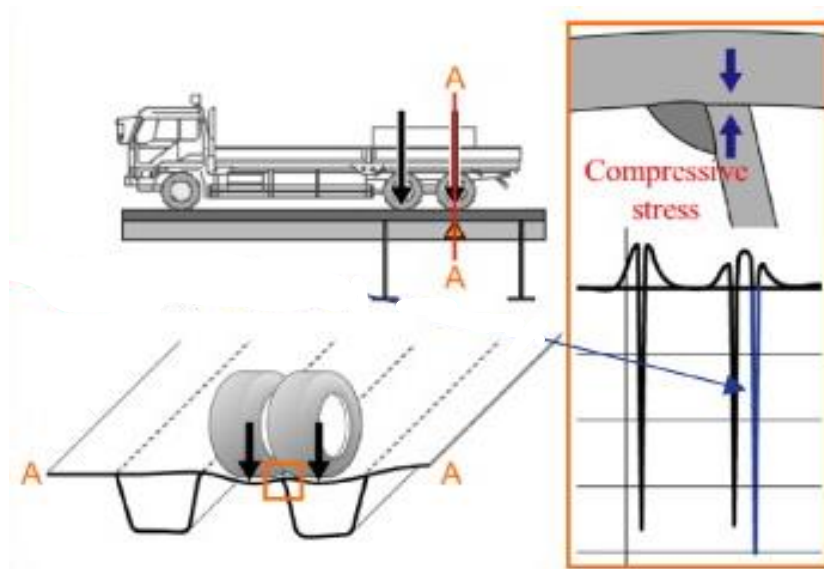
Figure 4 Stresses at the rib-to-deck welded joint due to traffic loading of OSDs. The three stress peaks correspond to the three axles of the vehicle. Image from[11].

1.2.2. The stresses from the local model

Two stress life methods are applied in this thesis to determine the fatigue life. The Hot Spot method is widely accepted as a reliable method for fatigue assessment of welded joints in orthotropic steel decks of road bridges. It is linearly extrapolated from two reference points in accordance with guidelines[12,13]. The nominal stress method, being the traditional fatigue assessment method, was also evaluated. A node at the local model, located further from the Hot Spot reference nodes is employed to calculate the nominal stresses[14,15].

1.2.3. Fatigue life estimation

The stress time histories at the welded joint of the local FEM model and the stress influence lines from the global FEM model of the Hardanger Bridge were cycle counted using rainflow method. The fatigue inducing stress ranges were applied to determine the fatigue life of the detail using Miner's damage accumulation rule **Figure 5**.
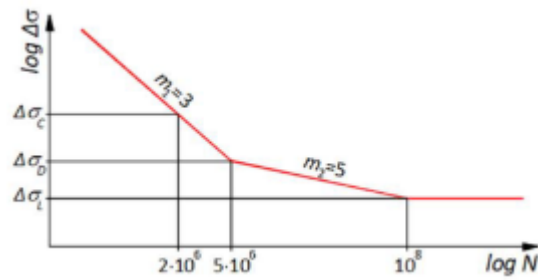
Figure 5 The trilinear S-N curve[16]

1.3. <u>Overview</u>

1.3.1. The aim of the thesis

The aim of this thesis is to determine the fatigue life of the rib-to-deck welded joint of the orthotropic steel deck of the Hardanger bridge.

This simple task required extensive pre- and postprocessing work across multiple platforms. For this thesis a finite element model of the box girder of the bridge was built and meshed in Abaqus. The fatigue load models (FLM-N and FLM-4) were designed in DLOAD subroutine in Fortran programming language. The finite element analysis of the traffic simulation on the bridge gave the Hot Spot and nominal stresses relevant for the rib-to-deck welded joint. The linear extrapolation of the Hot Spot stress and the calculation of the principal stress was done in X-Y data operations functionality in Abaqus Visualization module. Rainflow counted fatigue cycles from the stress history by using Python. The fatigue life calculated from the trilinear S-N curve of the welded joint in excel.

1.3.2. Limitations

The performance of the finite element model of the box girder built by the author for this thesis is not validated. The results of the finite element analysis are more reliable if the built model is calibrated by experimental study results. Examples of FEM validation of the relevant detail may be found in reference[17].

1.3.3. Structure of the thesis

Chapter 2 Fatigue theory introduces basic concepts of fatigue damage and the recent research topics on the fatigue pathologies in orthotropic steel decks (OSDs). The fatigue loads and the structural design are discussed as the main contributors of fatigue in OSDs. The factors that make the welded joints vulnerable to fatigue are briefly discussed, especially the geometric profile and the residual stress.
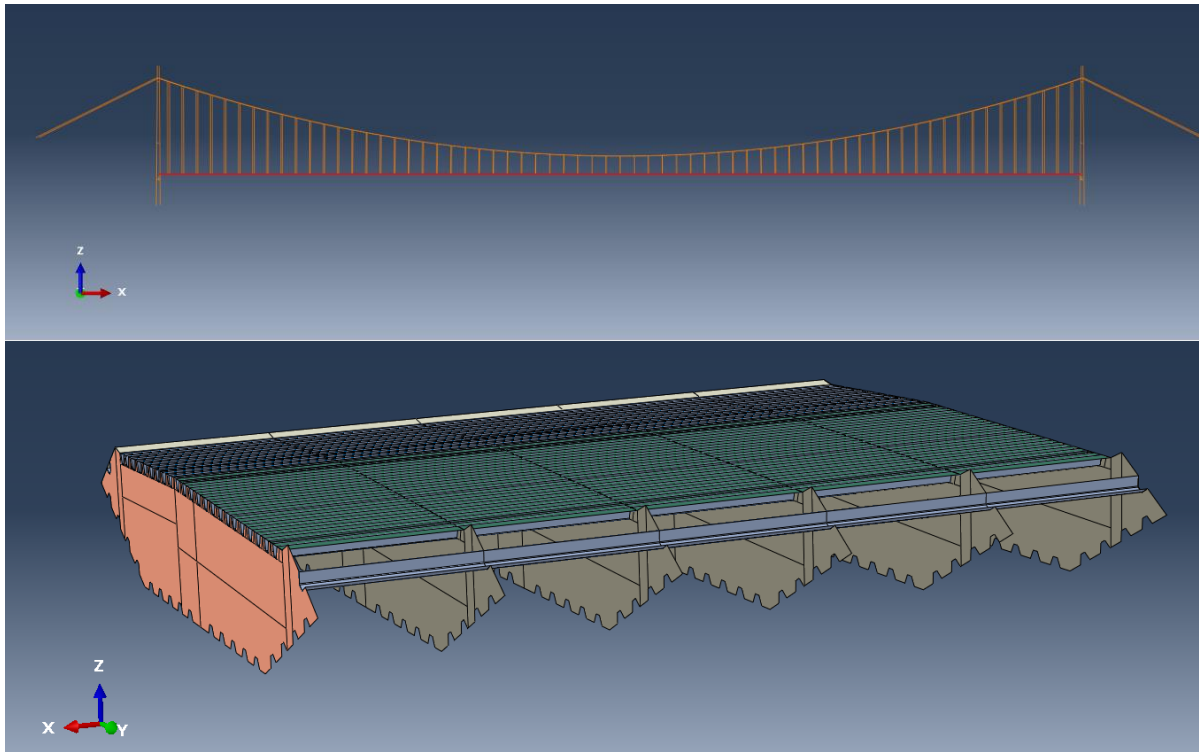
Figure 6 The finite element models in the thesis. The global model provided by NPRA, and the local model (box girder) built by the author.

Chapter 3 Stress based fatigue assessment. **Overview** of the relevant theory on the stress life approach in determining fatigue life of the welded detail, the fatigue load models, and the fatigue assessment method employed in this thesis is proved in this chapter.

The major work on this thesis is on building the finite element model of the local model (Chapter 4), traffic loading the model (Chapter 5), and fatigue analysis from the stresses of the local model (Chapter 6). Overview of the contents of these chapters is given in **Figure 7**. Chapter 4 Creating the local model discusses building the shell element model on Abaqus. The boundary conditions and interactions between components of the local model are sketched. Meshing rules for Hot Spot stress analysis is demonstrated. Chapter 5 the fatigue load models are loaded on the local model. The traffic lane that is loaded, the location of the vehicles in the lane, the placement of the wheel load in relation to the Hot Spot are demonstrated.

Chapter 8 addresses the global model. The model was provided by supervisor B.V. Traffic loading is designed as equivalent concentrated loads. The weak and strong moments and axial force influence lines are used to calculate the normal stress response. An attempt is made to calculate fatigue life from the global model by loading one vehicle per simulation. Chapter 9 and 10 are discussion and conclusion. Chapter 11 is appendix.

Overview of Chapter 4 – 6

4. Creating Local Model

- Shell element model
- Fine local meshing w/ gradient coarse mesh
- Reference points in fine mesh

5. Traffic Loading

- Determining the asphalt (lane)
- Traffic loading: FLM-N vs FLM4
- Different velocities compared

6. Fatigue Analysis

- Linearly extrapolated Hot Spot
- Stress transformation
- Rainflow cycle counting
- Miner's fatigue damage accumulation rule
- Fatigue Life (years)

Figure 7 Overview of chapter 4 to chapter 6.

2. Fatigue theory

2.1.   Introduction

The thesis deals with fatigue on steel bridges and therefore the theory on fatigue is limited to fatigue on steel structures, especially welded joints of steel structures. Fatigue is the most common failure mode of steel bridges[18]. Fatigue failure of machines in service led the initial advancements in the history of fatigue theory[19,20]. Fatigue failures of conveyor chains used in mines helped Wilhelm Albert publish the first article on fatigue. The unpredictable failure of train axles in service and the devastating loss of human lives that followed, helped August Wöhler[21] successfully introduce his theory on the relationship of load magnitude to number of cycles to failure. The 20th century research made clear that repeated fatigue loading initiates and propagates the fatigue mechanism, i.e., crack initiation and crack propagation. Investigations are ongoing to solve the remaining questions on fatigue assessment methods, design of fatigue resistant details, and prediction of fatigue life under variable amplitude loading[21,22].

2.1.1. The basic fracture mechanisms

Fatigue is one of the six basic failure mechanisms of steel structures. The other five base steel failure mechanisms are static or dynamic overload, instability, creep, stress corrosion, and brittle fracture. Static overload or impact and instability are both almost entirely eliminated by conventional design methods[23] and mainly occur due to human errors[24]. Failure due to creep is easily predictable. Stress corrosion is one of the most important failure modes in humid environments[25] and brittle fracture mainly depending on quality of steel, but also common at localized heat affected zone (HAZ) at weldment of steel bridge decks[26].
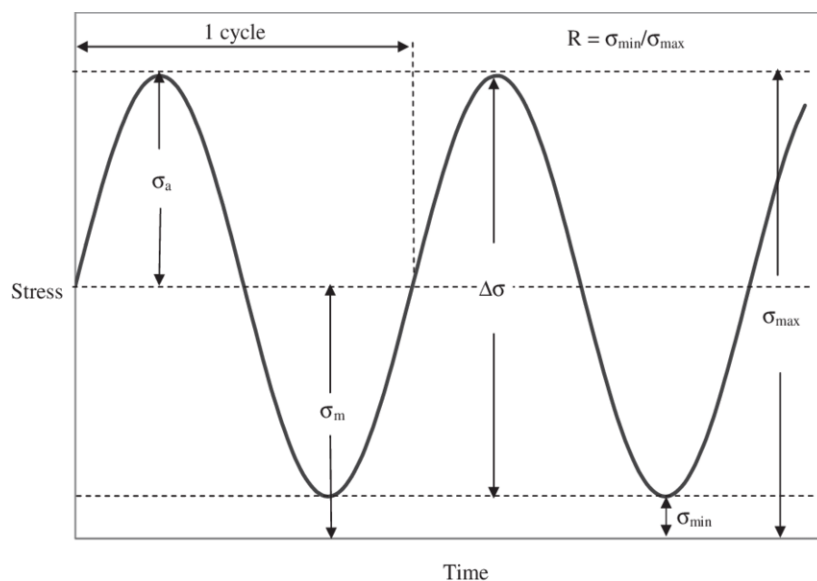
Figure 8 Sinusoidal stress time history due to cyclic loading.

2.1.1. Definition of fatigue

Any steel structure that is designed to carry repeated loads may become weaker after a given number of loading cycles. A material is said to be weak if it fails at loads less than the material's tensile strength. This weakness due to repeated loading is referred to as fatigue, i.e., the study of the relationship of the number of fatigue-inducing load cycles to the magnitude of the load. Fatigue can be defined as a progressive localized accumulation of damage as the result of cyclic loading *Figure 8*. The definition of a cyclic loading is a repeated continuous loading, giving a stress time history resembling the sinusoidal curve. The mean stress, the stress range, the stress amplitude, and the stress ratio are calculated using *Eq.(1)-(4)* respectively.

$$\sigma_m = \frac{(\sigma_{max} + \sigma_{min})}{2} \tag{1}$$

$$\Delta\sigma = \sigma_r = \sigma_{max} - \sigma_{min} \tag{2}$$

$$\sigma_a = \frac{(\sigma_{max} - \sigma_{min})}{2} \tag{3}$$

$$R = \frac{\sigma_{min}}{\sigma_{max}} \tag{4}$$

Around 90% of metallic failures are from fatigue[27]. Historically fatigue failure used to occur suddenly and without warning, and often lead to catastrophic events. Unlike other failure mechanisms, fatigue was difficult to detect. This remains to be true for internal cracks, for example crack initiation at rib-to-deck weld-roots in orthotropic steel decks is often detected due to water leakage from upper surface of deck into the box girder[28].

2.1.2. Fatigue failure

The structure[11] of the parameter governing fatigue are based on the experimental testing critical values for fatigue strength or service life assessments *Table 1* Parameters governing fatigue failure11 and *Figure 9*. Fatigue strength is described using S-N curve, the nominal stress versus number of cycles to failure curve, using (a) unnotched smooth specimen have longest life. The S-N curve of (b) notching specimen is gained by considering the stress concentration at the notch, which shortens fatigue life. Additional consideration of shape and surface of the structure (c) other structural complications further reduce the S-N curve, i.e.,
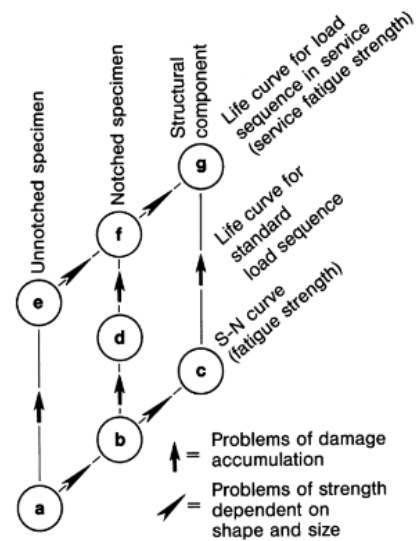
Figure 9 Parameters that cause fatigue failure[11]

shorten the fatigue life. The effect of shape and surface are connected to the behavior of the structure when exposed to constant amplitude loading (d) which further accelerates degradation of the structure, connecting (a), (b), and (c) to (e), (f), and g respectively.

Table 1 Parameters governing fatigue failure[11]

Structural member	Surface	Material
Shape	Roughness	Type
Size	Hardness	Alloy
Dimensions	Residual stress	Microstructure
Loading type	**Loading course**	**Environment**
Stress amplitude	Amplitude spectrum	Temperature
Mean stress including residual stress	Amplitude sequence	Corrosion
Multiaxiality including phase angle	Rest periods	

2.2. <u>Fatigue phases</u>

Fatigue has three phases, crack initiation phase, crack propagation phase and final fracture under cyclic loading ***Figure 10.*** Cracks usually initiate from the surface of a component. The crack may propagate (i.e., grow) perpendicular to the direct stress and finally the component may fracture. There is a relationship between the magnitude of the fatigue inducing loads and the number of cycles to failure. This relationship is termed fatigue life (see section: S-N curves).
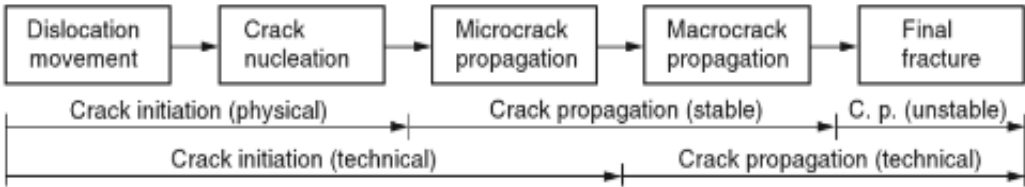
Figure 10 The process of failure due to fatigue can be described by the following phases. Crack initiation, propagating, and final fracture.

2.2.1. Crack initiation

For a crack to initiate, some **local plasticity** must occur during some part of the load history. Local stress-strain theories and critical location are fields in modern fatigue theories that relate fatigue endurance to local stresses and strains. The local

approaches to fatigue assessment can be approximately described by a macroscopic elastic stress analysis according to continuum mechanics[11], i.e., cyclic deformation causing initiation and propagation of the crack and ultimately causes final fracture, **Figure 10**. A crack is said to have been initiated if crack surface length reaches detectable values, for example above 1 mm.

2.2.2. Crack propagation

Crack propagation by cyclic loading is primarily governed by the amplitude of the cyclic stress intensity factor. Most of the parameters which determine the critical value of stress, at the crack tip causing crack propagation, are identical to those which cause crack initiation. Only the influence of the surface diminishes, while crack shape, crack size and crack growth rate become more important. Crack growth rate is related to a single load parameter, usually the stress intensity factor ΔK, using fracture mechanics approach. With the exception of high and low ΔK levels, the crack growth rate (da/dN) is predictable, referred as the linear region of crack propagation (phase 2 in **Figure 11**), approximated by the Paris Law **Eq.(5)**, where C is the material constant and m are the slope of the log-log curve **Figure 11**.
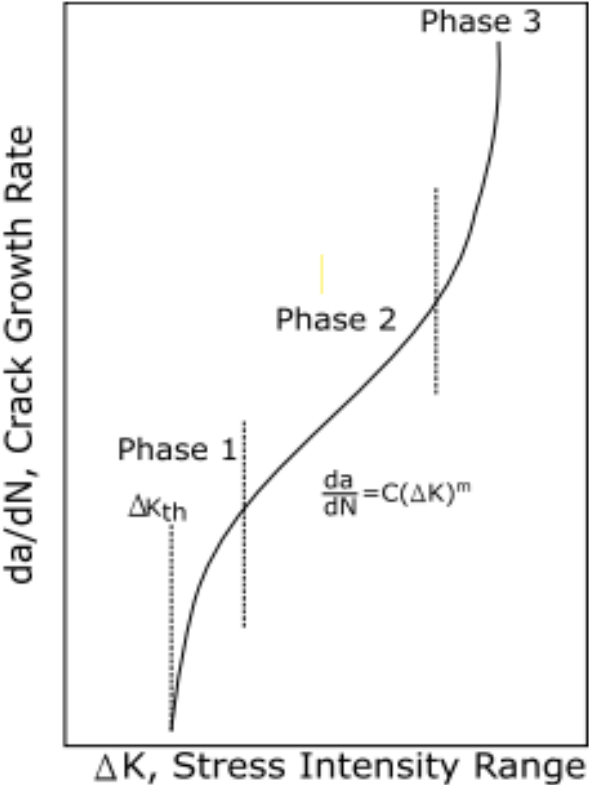
Figure 11 Fatigue crack growth behavior in metals

$$\frac{da}{dN} = C\Delta K^m \qquad (5)$$

11

2.2.3. Final Fracture

A fatigue loaded structure will finally fracture after the fatigue crack grows beyond a critical size. The stress level, the crack size, and the material toughness are the main determinators of fracture. The fatigue life in S-N curves of codes include the life until fracture[29]. This last fatigue phase is a very small part of the fatigue life of a structure, and it is usually neglected, compared to crack initiation and crack propagation phases.

2.3. <u>Fatigue on the rib to deck welded joint</u>

This section addresses the theories on why fatigue cracks commonly occur in rib to deck weld joints of OSDs[30]. For the fatigue assessment method employed on this thesis refer to *Chapter 4 – 6*. The 20 m long full-scale finite element model (FEM) of the box girders have a 12 mm thick OSD that carries the traffic. Fatigue pathologies on the component of the local model is addressed in this subsection. Relevant details of the principal factor that increase fatigue development on welded joints are addressed in detail.

2.3.1. Orthotropic steel deck

The orthotropic steel deck bridges (OSBDs) are the main stay in long span bridge constructions, because they substantially reduce the self-weight while providing superior load carrying capacities[31]. The proportions of the steel bridge construction in France, Japan, America, and China are 85%, 41%, 35%, 1% respectively[32]. The ability utilization rate of OSBDs is expected to increase with the worldwide modernization trends. However, the problems of bridge deck's fatigue cracks and the damage of pavement layer caused by the structure's characteristics and its service requirements, have restrained the rate of production of OSBDs for a long time.

Although the OSBDs are extensively applied worldwide in long span bridges due to their light self-weight and accelerated construction and repairing of existing bridges, they are vulnerable to fatigue cracking especially due to unexpected increase of traffic amount. Fatigue cracks occur often at the rib-to-deck welded joint near the crossbeam as well as in span[33]. Thicker deck plates and better welding techniques are often implemented in the new structural designs to improve the fatigue life of those bridges.

Zhang et al, 2017[32] and Villoria et al, 2021[34] reviewed the OSD's research topics in the aspect of the reliability of fatigue performance, evaluation methods, structural details and new-type OSDs, maintenance and reinforcement of fatigue cracks, etc. The main conclusions and suggestions including the ongoing research to improve steel bridge structure's life-cycle performance, to optimize cost, and the sustainability potential of the bridges. This thesis builds on the current research methods of OSDs' fatigue analysis and prediction.

2.3.2. Fatigue failure on OSDs

Orthotropic steel bridge decks, like most other welded steel structures which are subjected to fluctuating loads, are vulnerable to metallic fatigue. Even though fatigue may occur in any metal component, weldments are the most frequent fatigue sites because they are stress concentrators. Despite 150 years of research and over hundred thousand of studies of steel weldment fatigue, the problem remains only partially solved. This is due to the infinite variety of welded joints, each of them is partially unique, and have complex stress responses[35]. The variety and complexity of the welded rib to deck joints introduces uncertainty to the fatigue assessment results. Early attempts to create S-N curves for welded joints from physical curves created a great deal of scatter. The major parameters that govern fatigue life of the welded joints on OSBDs include the following:

1. Wheel load (fatigue load)
   a. Traffic volume
   b. Ratio of heavy vehicles
2. Structural design of the OSDs
   a. Geometric profile of welded joints
   b. Manufacturing quality and steel property

The action of wheel loads on OSDs belongs to 3-dimensional structural fatigue problems[32]. OSDs fatigue problem differs from that of skeletal structures such as main girder and main trusses, as those structures have unidirectional primary stress state and fatigue life can be calculated from the effects of the principal stress. Direct application of the principal stress method to solve fatigue problems on OSDs might be inaccurate[32]. The principal stress is recalculated from the plane stress using equation.

Fatigue load: Fatigue loading of OSBDs mainly depends on traffic volume, ratio of heavy vehicles, and their axle weight and axle spacing. Structural detail: the angle of welded joints of these components. Steel property: The steel's material strength, fracture toughness, solderability. Manufacturing quality: Quality of material, precision of assembly of parts and welding technique.

Structural design: the design of orthotropic decks is dominated by fatigue resistance. Fatigue cracks are seen at closed rib to deck welded joints due to their sensitivity to fatigue loads. Thickness of deck, thickness and spacing of longitudinal rib and transversal diaphragm are often improved to increase the fatigue life of the OSDs. Increasing the thickness of deck, at the expense of increased steel consumption and weight gain of the main box girder, is the current design approach for improving the fatigue life of the OSDs[32]. Fatigue tests performed on a full-scale orthotropic deck comparing 20 mm with 12 mm thick deck plate did not find a significant improvement on fatigue strength.

2.3.3. Welded joint

In steel structures, welding provides high-strength joints, improves manufacturing efficiency, and can be adapted to various environmental conditions[17]. However welded joints are also stress concentrators, see *Figure 12*. They affect the load-carrying capacity and fatigue life of steel bridge structures. The fatigue cracks in welded structures start at welds rather than the base material[36,37].

2.3.3.1.   Geometric Profile

Welding geometry strongly influences the fatigue life of the welds[38]. A field study attributes all the rib-to-deck weld cracks found in OSDs with closed ribs on two bridges in Germany and one bridge in UK, were located at the rib-to-deck welds and other locations. The cause of the cracks was suggested to be due to inappropriate details and welds that were not suitable for transmitting stresses between the deck components at these joints. There were no weld failures or cracks found in OSDs with correct details[39], i.e., infinite fatigue life.

Physical testing complex geometry of OSDs: When cracks occur on the orthotropic deck, replacement of the deck panel for rehabilitation of bridge is an alternative. To test whether the replacement plate fatigue life, one used to build full-scale prototype of the bridge and the replacement panel, and the fatigue resistance of the common weld-location at welded rib-to-deck, rib-to-diaphragm connection details would be studied by physical testing. Alternative details were also physically tested to determine the superior detail. Design specifications for OSDs depended on such studies[40]. Physical testing is expensive and time consuming, and replacement fatigue analysis using finite element models is advantageous.

The complex structure, the many weld joints, and the local wheel load directly influence the deck, leading to high stress concentration at specific locations. The highest stress concentrations are found in places of discontinuity of geometric configuration, such as welded joints, even higher stress concentrations may arise due to welding defects and manufacturing errors. The actual fatigue life of the OSDs is highly dependent on design parameters and production defects, due to the complex geometrical shape of the welded joints at the interaction of bridge decks, longitudinal stiffeners, and diaphragm[32]. With the repeated traffic loading, fatigue cracks are initiated and propagate in fatigue details (or fatigue Hot Spot) where the stress concentration problem is the main cause of fatigue damage of OSDs.
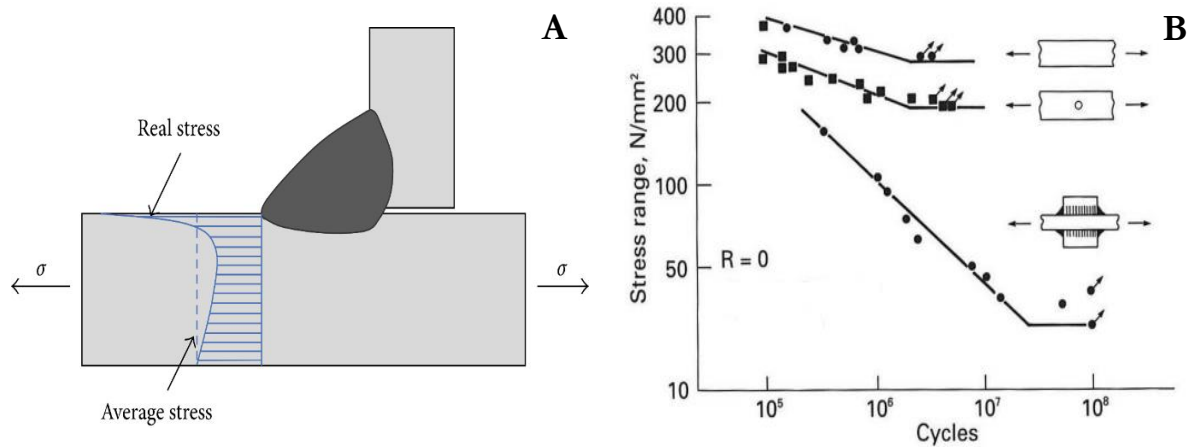
Figure 12 (A) Welded joints are stress concentrators[30]. (B) Fatigue strength of plain, notched, and welded structure.

The geometric profile of welded joints is one of the primary factors that limit the fatigue life of the joints. In addition to post-welding operations like grinding, peening, water-jet eroding, and remelting that greatly improve of fatigue life the welded joint, techniques that improve the welding geometry have been demonstrated to significantly improve the geometrical profile of longitudinal fillet weld, and lower the stress concentrations prior to post-weld operations[41].

Axial and angular misalignments may significantly magnify or reduce the Hot Spot stress. The influence of misalignment is especially strong for transversally loaded thin-walled structures[11]. The structural stress change due to misalignment may be calculated for simple cases using engineering formulas given in guidelines. The procedure selected for welding and quality assurance have predominant influence on the stress concentration effect at the Hot Spot.

All fatigue cracks initiate at vulnerable fatigue details, such as welded joints or geometric discontinuities, due to steep stress concentration gradient[32]. Crack initiation and propagation are further influenced by preproduction factors and loading history, at those locations are fatigue stress amplitude, number of cyclic loadings, and resistance force of structural details[32].

Production process may significantly affect the fatigue life of the welded joint. Improving geometry is as crucial as applying automated and reliable welding techniques[41]. Take for example laser welding, which is gaining favor due to their ease of process automation and high welding speed and increased process reliability. They can achieve full-penetration welds in one pass. A sharp radius can substantially reduce fatigue life of a high-quality full-penetration weld, solely due to the geometry of the weld profile. Laser welded joints are modern technology and the fatigue life of these welds has yet to be verified in the real world. Efforts are made to quantify the actual fatigue life of laser welded joints with various geometrical profiles. To

15

fabricate laser welds with stress concentration factors near unity is costly, and tradeoffs must be made regarding desired weld geometry, operation speed, and amount of filler material[41].

2.3.3.2. *Residual stress*

Welded joints show several peculiarities that complicated the local approach. Inhomogeneous material is characteristic of welded joints. Weld defects and imperfections typical of welded joints are, for example, cracks, pores, cavities, inadequate penetration etc. Welding residual stress are important characteristic of welded joints that are still studied by experimental measurements and numerical simulations[17].

Residual stress reduces the load carrying capacity of the detail and increases the fatigue crack growth rate[42]. Residual stress, a permanent state of stress in a structure, can arise from rolling stresses, cutting process, welding shrinkage, and lack of fit between members, and from any load that causes yielding of the structure. The heating, the welding process, and the following rapid cooling produce residual stresses. These welding residual stresses have a low-level stress outside the weld area but produce local stress concentrations at the weld. The effect of residual stress is especially prominent on high-cycle fatigue strength of welded joints[11]. Ongoing research distinguishes the fairly understood surface residual stress from the equally important, yet not well understood internal residual stress[17].

2.3.3.3. *Fatigue on welded joints*

The connections between steel components, usually welded joints, are the main accumulators of fatigue damage. The last century's research on fatigue has provided successful new and advanced technology that made steel bridges affordable. The lightweight orthotropic steel decks (OSDs) on hollow box girders are a hot topic in research fatigue on steel bridges. The U-shaped longitudinal stiffeners are the main components that support the OSDs. They are connected by welding that produces complex welding residual stress. During the service life of the bridge the residual stress of weldment in addition to the working stress produces cumulative local damage, that inevitably reduces the fatigue strength of the welded joint[43].

Fundamental understanding of the impact of welding on fatigue life of the structure may broaden the understanding existing of steel bridges that are under regular maintenance and inspection by today's engineers. The presence of joints, particularly welded joints, play a crucial role in fatigue failure. This is due to:
    (a) the stress concentration they produce,
    (b) the residual stress caused by welding, and
    (c) the metallurgical changes produced by welding.

3. Stress Based Fatigue Assessment

3.1. Introduction

The stress-based approach is chosen for its simplicity and applicability for the expected high cycle fatigue of traffic loading on bridges. At long lives and mainly elastic strain deformations, the stress-based approach is equivalent to the alternative strain-based approach[44]. Strain-based fatigue is typically preferred for low cycle fatigue, where there is predominant plastic deformation. In the stress-based fatigue life approach the S-N curve is used to predict fatigue life from the stress ranges.

3.1.1. The evaluating process of fatigue performance

The major factors that influence fatigue performance include structural design, fatigue load, and structural details. Modern bridges consider fatigue in their structural design. Variation in the magnitude of the fatigue load, the eccentricity of wheel loads in relation to the lane, and the amount of traffic flow are difficult to regulate. Different location of the wheel load on the lane may result in different modes of fatigue failure of the same fatigue detail. In road bridges load cycles in the order of millions per year are common, making stresses well below the fatigue limit of the structure relevant for fatigue damage. The increasing complexity of structural details in bridge design, require special care in the evaluation of fatigue failures at sites of high stress concentrations, especially at weldment of load carrying joints.

Two methods for fatigue assessment are suggested by EN 1993-1-9: the damage tolerant method and the safe life method. Fatigue life using damage tolerant method assumes regular inspections, maintenance, and reparation of fatigue damage. The fatigue life is determined using the safe life method reliable performance of structure without regular maintenance of fatigue damage. "*The safe life method should be applied in cases where local formation of cracks in one component could rapidly lead to failure of the structural element or structure*"[10].

Fatigue life prediction may be achieved using either the S-N curve approach or the fracture mechanic's approach. The relationship of these two approaches on the aspect of the total fatigue life is shown in **Figure 13**. While the S-N curve is mostly used to study fatigue in crack initiation phase, the fracture mechanics studies crack propagation.
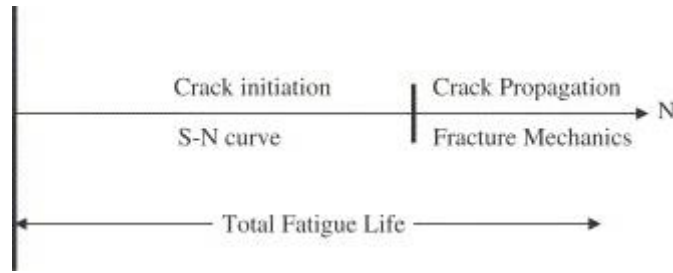
Figure 13 The relationship between the S-N curve and the fracture mechanics method for predicting fatigue life.
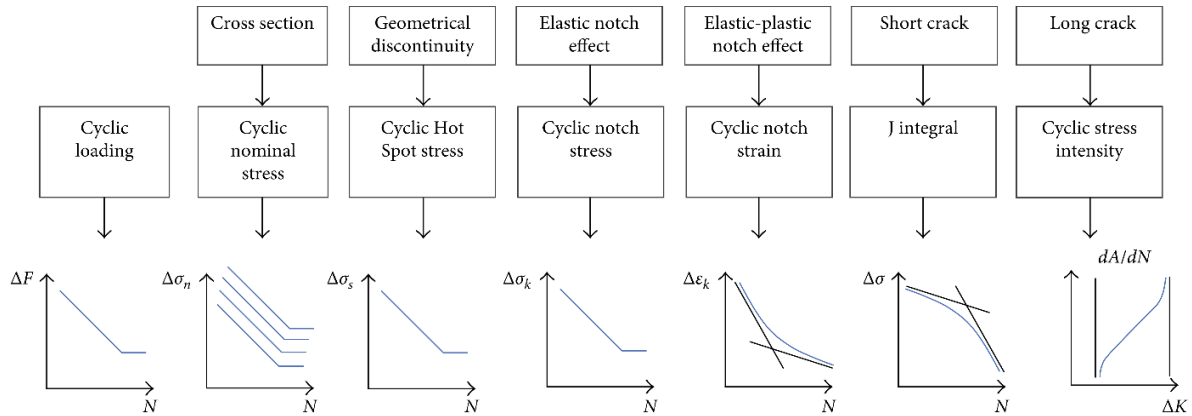
Figure 14 Global and local approaches for fatigue strength and fatigue life assessment. Image is modified from Fustar 2018 [1,22].

Strength assessments are made up of comparison of stresses with their critical values that cause a defined damage. The loads including forces, moments, stresses, and strains are nominal or Hot Spot type. The stresses and strains are derived from the forces and moments according to elasticity theory. The fatigue critical stress values are designated as strength values. The strength values are determined from loading tests on FEM of the component. Fatigue relevant tests are constant amplitude test, the variable amplitude test, and the corresponding crack propagation test. The component life is determined at the given critical stress values, thus the number of cycles to failure depends on load amplitude[11].

The local fatigue assessment is derived from local stress parameters. It considers the local process of damage by material fatigue, i.e., cyclic crack initiation, propagation, and final fracture, as mentioned above. Time to crack initiation can be predicted and studied using Hot Spot stress approach or notch stress approach. While crack propagation is studies using crack propagation approach the Hot Spot approach is considered a link
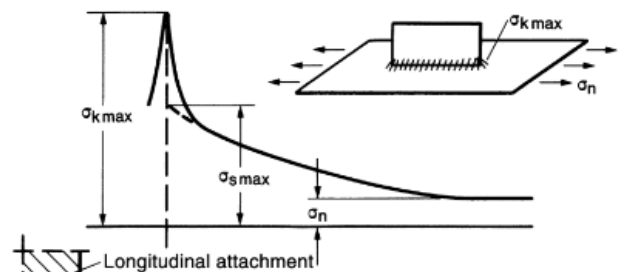
Figure 15 Hot spot stress ($\sigma_{s\ max}$) functions as the link between the notch stress ($\sigma_{k\ max}$) and the global or nominal stress (σ_n) concepts of fatigue evaluation. Figure from[11].

between the global and the local concepts, which reflects the stress concentrations originating from the microgeometry at the welded joint.

3.1.2. The S-N curve

The fatigue performance of the most typical steel structures has experimentally determined S-N curve, i.e., they have a clearly defined relationship between the magnitude of the stress (S) and the number of cycles (N) the load may be applied before fatigue failure of the component occurs. The data from the S-N curve is collected from a series of laboratory tests by subjecting a specimen to stress cycling at a given stress, and the number of cycles to failure is recorded. The procedure is repeated with different stress levels, until the S-N curve of the component is sufficiently determined. Experimentally determining the S-N curve components with complex geometry often gives diverse results, often referred to as the S-N scatter. Steel components loaded with constant stress amplitude usually have fatigue limit, also called the endurance limit, where the component may not suffer fatigue damage at stress levels below cutoff limit[45].

The fatigue life of a steel structure depends on the fatigue life of its structural components, which can be acquired from the detail's fatigue resistance represented by the corresponding S-N curve. The S-N curves categorize each detail according to its fatigue resistance, which depends on corresponding geometry, quality of performance, environmental influence, and the way of loading that are obtained from experimental measurements and finite element analysis[30]. The multitude of user specific fatigue assessment approaches from local stresses remain incomplete in respect of generalizability, and the local parameter data for most part lack statistical proof[11].

3.1.3. Trilinear vs bilinear S-N curves
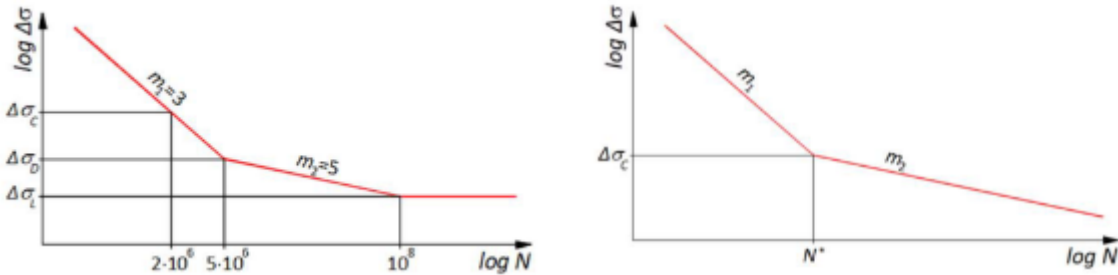
Figure 16 The trilinear and bilinear S-N curves[16]

The S-N curve neatly shows that the fatigue resistance decreases with an increase in the number of stress amplitudes N. The straight lines of the S-N curves are gained by logarithmic scaling the curves. The classical trilinear S-N curve is usually adopted when calculating fatigue damage. It is characterized by two inclined lines (m_1 and m_2) and a horizontal line see **Figure 16.** The slope $m_1=3$ for $\Delta\sigma_i \geq \Delta\sigma_D$ and **Eq. (6)**. The slop $m_2 = 5$, for $\Delta\sigma_D > \Delta\sigma_i \geq \Delta\sigma_L$ and **Eq. (7)** . The cutoff limit ($\Delta\sigma_L$) corresponds

to $N = 10^8$ the cycles to failure. It is given by the horizontal line. This cutoff limit assumes infinite life of a detail when loaded with constant amplitudes less than the limit.

$$N_i = \left(\frac{\Delta\sigma_C/\gamma_{Mf}}{\gamma_{Ff} \times \Delta\sigma_i} \right)^3 2 \times 10^6 \qquad (6)$$

$$N_i = \left(\frac{\Delta\sigma_D/\gamma_{Mf}}{\gamma_{Ff} \times \Delta\sigma_i} \right)^5 5 \times 10^6 \qquad (7)$$

The bilinear fatigue resistance S-N curve have two slopes[16]. If a specimen is subjected to variable stress amplitudes (VA) lower than the cutoff limit each element will in practice ultimately fail and the slope m_2=22 (**Figure 16**) may better approximate the fatigue performance of the component, especially in very high cycle fatigue[30].

The welded joints have fatigue strength that is different from the base material's yield strength[12,37,46]. The fatigue strength of the welded joint is referred as the detail category of the component. The fatigue strength is given at $2*10^6$ cycles and is defined by the stress range value in MPa that results in fatigue failure of the given welded joint geometry. The same structural component has different S-N curve depending on the stress approach applied. For Hot Spot stress approach, the rib-to-deck welded joint has the detail category of 100 MPa is recommended[10]. Correspondingly, for nominal stress the detail category 71 MPa is recommended[10]. *See **Appendix D.2.** for the detail categories and their respective constructional details.

Constant Amplitude Fatigue limit (CAFL) **Eq.(8):**

$$\Delta\sigma_D = \left(\frac{2}{5} \right)^{1/3} \Delta\sigma_C = 0{,}737\Delta\sigma_C \qquad (8)$$

Cut off limit **Eq.(9):**

$$\Delta\sigma_L = \left(\frac{5}{100} \right)^{1/5} \Delta\sigma_D = 0{,}549\,\Delta\sigma_D \qquad (9)$$

3.2. <u>Stress life approach</u>

To predict fatigue life for welded joints three main stress life approaches are available, those are the nominal stress approach, the Hot Spot stress approach, and the notch stress approach[47]. The structural complexity of the welded joint determines the level

of accuracy and the amount of working effort required for fatigue analysis[38]. These approaches differ in accuracy, where the nominal stress is the least precise in predicting the fatigue life of the welded joint. They also differ level of effort they require in the model design, where the Hot Spot stress approach requires more effort in strain gauge placement or mesh size than the nominal stress approach. To predict the fatigue life of the welded joints in orthotropic steel decks, the precision of the Hot Spot Stress is well worth the effort.
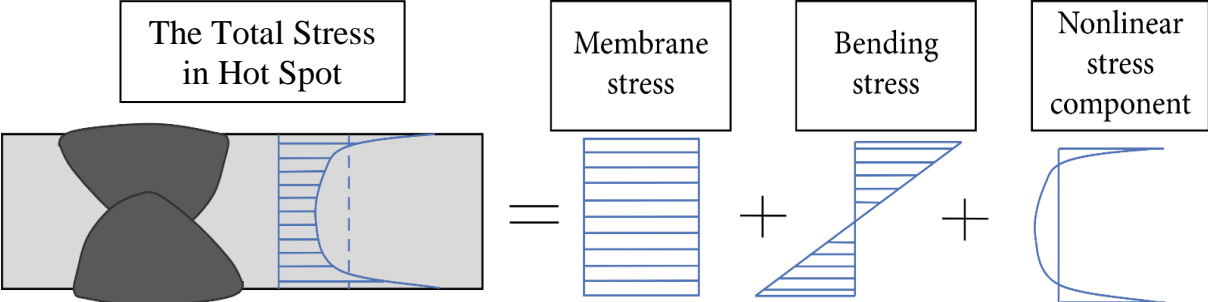
Figure 17 The Hot Spot stress approach includes the membrane stress (nominal stress) and the bending stress (stress concentration at the weld approximated by linear extrapolation). Image from [22]

3.2.1. Nominal Stress

Nominal stress is the average stress calculated in the sectional area of the specimen considered **Figure 18**. It disregards the local stress raising effects, such as discontinuities at welded joints, but includes the stress raising effects of the macro-geometric shapes. They are stresses derived from simple beam theories and linear elastic behavior and can be assessed using coarse mesh finite element models[47]. The nominal stress-based approach is not accurate for geometrical complex details; therefore, it is necessary to use approaches that consider local effects.
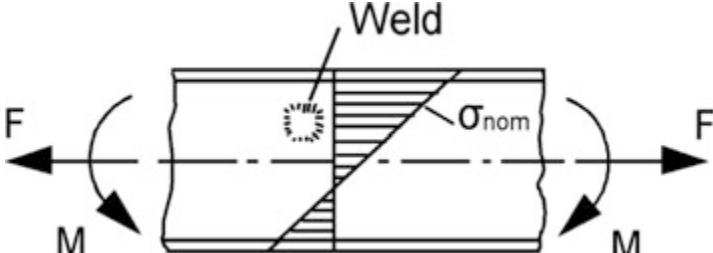
Figure 18 Nominal stress in beam-like component[12].

The nominal stress approach of determining fatigue life assumes that fatigue damage accumulation is a linear phenomenon[41]. Experimental fatigue testing of a smooth structural detail, with a generalized connection geometry, generates S-N curves unique to the structural detail. The nominal stress approach uses these connection specific S-N curves, and it does not include the stress concentrations due to welding as it assumes the S-N curve of a detail already characterizes this effect. The stress (y-

axis) in the S-N curve is the nominal stress, σ_{nom}, which is the stress due to forces[35] and moments at the potential site of cracking. The local geometry of the weld toe and the local material properties are not considered in the nominal stress. The nominal stress depends on the size of the applied loads and macro-geometric changes of the component, while the effect of welded connections is not accounted for.

3.2.2. Hot Spot Stress

Hot Spot refers to the rib to deck welded joint studied in this thesis where a fatigue crack is expected to occur. The weld is not modeled in the shell finite element model; therefore, it is not possible to distinguish the weld toe from the weld root. Fatigue failure of structural members is an extremely localized process; therefore, the local parameters, such as geometry and loading of structural members must be as close to reality as possible when performing fatigue strength assessments[11].

The Hot Spot stress, σ_{hs} is computed at the welded joint, where the fatigue stress is the highest. The stress at the transition point is usually a singularity, therefore linear extrapolation from the points in the vicinity, the reference points, is calculated according to a validated stress extrapolation rule. The Hot Spot stress is computed from a fine mesh finite element analysis of the connection. It will include global effects and partial influence of the local geometry.

Linear stress extrapolation (theory)
The linear surface stress extrapolation technique is used to predict the stress in the Hot Spot as prescribed elsewhere[13]. This is the most common procedure to derive the Hot Spot stress from FE-analysis. This method excludes the extremely high stress concentration at welded joints. The distance of the reference points, at which the weld stress effects are diminished, is defined as a function of plate thickness (**t**). The location of stress extrapolation points is also dependent on the mesh density in FE models *Figure 20*. For a model with fine mesh, the first reference point (RP1) closest to the weld toe could be defined as 0.4**t** and the second reference point (RP2) is positioned at 1**t** from the weld toe. Other rules are used for coarse mesh and other weld types. The two reference points on the stress curve are located normal to the welded toe.
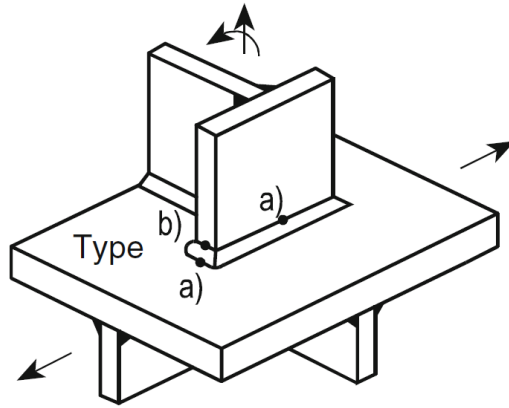
Figure 19 Types of Hot Spots[12]

Table 2 Types of hot spots illustrated in **Figure 19**

Type	Description	Determination
a	Weld toe on plate surface	FEA or measurement and extrapolation
b	Weld toe at plate edge	FEA or measurement and extrapolation

Table 3 Surface stress extrapolation at the welded joint recommended by IIW

Hot Spot point	Linear extrapolation	
	Fine mesh	**Coarse mesh**
Type a	0,4 **t** and 1,0 **t**	0,5 **t** and 1,5 **t**
	$1{,}67\,\sigma_{0,4t} - 0.67\,\sigma_{1.0t}$	$1{,}5\,\sigma_{0,5t} - 0.5\,\sigma_{1.5t}$
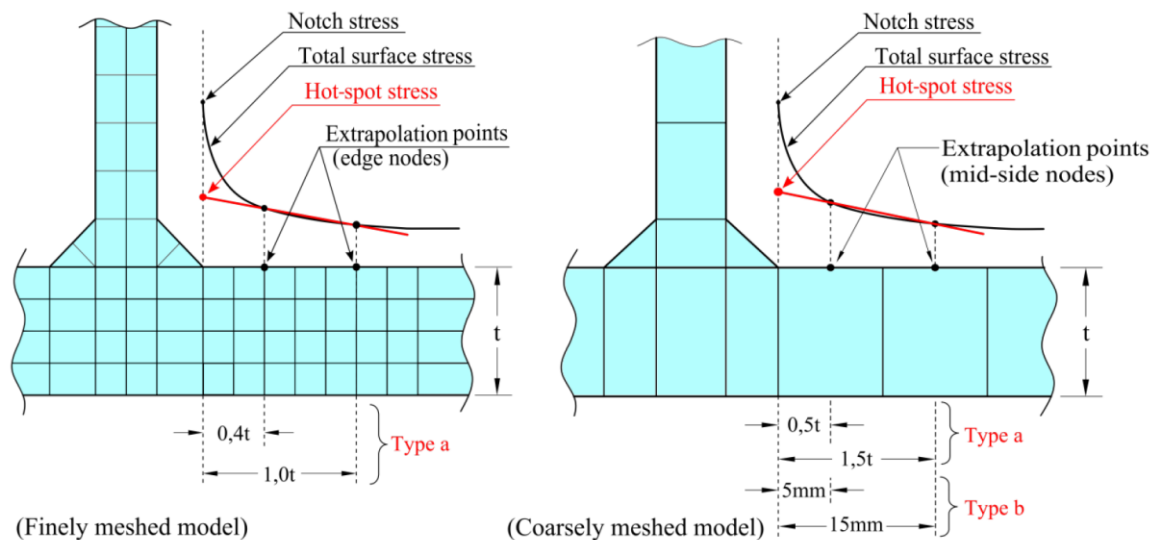
Figure 20 Hot Spot stress extrapolation is mesh sensitive. Figure from [13].

$$\sigma_{hs} = 1.67\,\sigma_{0.4\,t} - 0.67\,\sigma_{1.0\,t} \tag{10}$$

23

3.2.3. *Notch Stress*

The notch at the weld toe produces a non-linear stress peak which is addressed by the notch stress approach. It is the sum of the non-linear peak stress and the Hot Spot stress. The notch stress requires a more complex modeling of the welded detail, with extreme fine meshing. It is not employed in this thesis and will not be further discussed. For review on notch stress approach in fatigue assessment of welded detail see reference [13].

3.3. <u>Fatigue design method</u>

Eurocode allows for the application of two principal methods for the fatigue design of bridges: the equivalent damage method, also known as λ-coefficient method, and the more general cumulative damage method, i.e., Miner rule[13].

3.3.1. *Principles of fatigue design method (Eurocode)*

The fatigue life of the rib-to-deck welded joint of the Hardanger road bridge from traffic loading is in accordance with Eurocode recommendations. It is as follows:

- A long span suspension bridge (Hardanger bridge) is simulated for responses to traffic flow
- Rib-to-Deck weld toes are selected as structural details for Hot Spot fatigue analysis along with their fatigue resistance curves.
- FLM-N and FLM4 are used for traffic loading.
- Python script (rainflow.py) is used to count fatigue cycles from the stress history, and the fatigue inducing stress ranges are extracted.
- Fatigue damage is calculated by applying Miner's damage accumulation rule.
- Results are given as fatigue life (years) of the rib-to-deck welded joint.

3.3.2. *Stress transformation*

Stresses from shell element model are essentially plane stresses. The components of the plane stresses are transformed into the principal stresses to account for the potential directional loading changes in the load cycles. The principal stresses are calculated using[48,49] ***Eq. (11) & (12).*** To get the principal stresses from the plane stresses (σ_{yy} and σ_{xx}) are rotated by the angle ϕ (σ_1 and σ_2) such that the shear stresses (σ_{yx} and σ_{xy}) are zero ***Figure 46***. Rotating the stress element will vary the normal and shear stress components. Rotation of the stress element only rotates the axes of the coordinate system, and it does not change the actual stress state of the large body. The magnitude of principal stresses σ_1 and σ_2 is calculated from the linear extrapolated Hot Spot plane stresses (*see **Appendix C.4.***). The stresses applied in this thesis for fatigue analysis are maximal principal stresses ***Eq. (12).***

$$\sigma_1 = \frac{\sigma_{xx} + \sigma_{yy}}{2} + \frac{1}{2}\sqrt{\left(\sigma_{xx} - \sigma_{yy}\right)^2 + \sigma_{xy}^2} \qquad (11)$$

$$\sigma_2 = \frac{\sigma_{xx} + \sigma_{yy}}{2} - \frac{1}{2}\sqrt{\left(\sigma_{xx} - \sigma_{yy}\right)^2 + \sigma_{xy}^2} \qquad (12)$$

3.3.3. Cycle counting

The response of steel to a cycle of constant loads stabilizes, after initial softening and hardening, into its stress-strain hysteresis loop, and the number of cycles the specific load can be applied until the material fails is the fatigue life. Fatigue cycles can be described as closed stress-strain hysteresis loops.

The stress history in response to variable amplitude loading often have a complex arrangement of fatigue cycles of various stress ranges, therefore it is necessary to implement a cycle counting method to accurately determine how many fatigue cycles are in the stress history. A good fatigue cycle counting method counts every part of every overall range once and only once, and it also counts smaller ranges down to some predetermined threshold once and only once[50]. Several methods for cycle counting can result in inconsistencies and large differences between predicted and actual fatigue lives. Rainflow counting is said to be one of the most consistent and the most widely used[44,51,52].

Transformation of the variable amplitude loading into a representative constant amplitude loading is usually done by cyclic counting method. The "rain flow" and the "reservoir" stress counting methods, being the most common counting methods, do not always lead to the same result, but give very close results, especially for "long" stress histories. In this thesis the rainflow cycle counting method using a python script (*Code 1*), rainflow.py v.3.1.1[53], that implements the algorithm provided by ASTM Standard E1049-85[54]. This is simply done:

```
import rainflow

rainflow.count_cycles("Max principal stress history")
```

Code 1 Sample python code showing the cycle counting program

3.3.4. Equivalent stress range

The fatigue damage caused by several loading blocks with variable amplitude loading can be simplified into a single equivalent stress range. The definition of equivalent stress range is that constant amplitude stress range which if applied with the same total number of loading cycles of the variable stress range ($\sum n_i$) would cause the same

total damage as the variable amplitude loading block. Equivalent stress range is calculated from the cycle counted stress ranges using **Eq. (13)**

$$\Delta\sigma_E = \left[\frac{\sum_{i=1}^{n} n_i \times \Delta\sigma_i{}^3}{\sum_{i=1}^{n} n_i}\right]^{\frac{1}{3}} \tag{13}$$

3.3.5. *Palmgren - Miner damage accumulation*

Using the new set of representative constant amplitude loading to perform the fatigue design or analysis is done by applying the Palmgren-Miner damage accumulation rule[55], **Eq. (14)**. The principle of the damage accumulation rule (Palmgren-Miner) is presented in more detail in reference[13]. S-N curve, relation between the stress range and the total number of cycles to failure, N_i. in other words, a specific detail with a certain fatigue strength (represented by an S-N curve) will fail after N_i cycles of a stress range $\Delta\sigma_i$. At failure D=1. The adjusted stress ranges are then computed directly on the S-N curve to give the damage index. The accumulated damage is used to calculate the fatigue life.

$$D = \sum_i D_i = \sum_i \frac{n_i}{N_i} \tag{14}$$

4. Creating Local Model

The finite element modeling, traffic loading and stress analysis is performed on *FEM platform Abaqus/CAE 2020* [56]. Stress analysis for the closed rib to deck joint is carried out at midspan (x=10m) between diaphragm 3 and 4.

4.1. Components of the local model

4.1.1. Dimensions of the box girder

The bridges' slender structure owes to its thin orthotropic steel deck on the box girders. The bridge deck consists of a series of hollow suspended box girders. They are suspended through the vertical hangers which are connected into two main cables which again are anchored into mountains on both sides of the bridge. The suspension cables are continuously extended from one end to the other, and they are supported at the top of the pylons on each side of the bridge [4]. A full-scale orthotropic steel deck and box girder segment is modeled in Abaqus for fatigue testing. The FEM of the Hardanger Bridge's box girder and its dimensions shown in **Figure 21.**
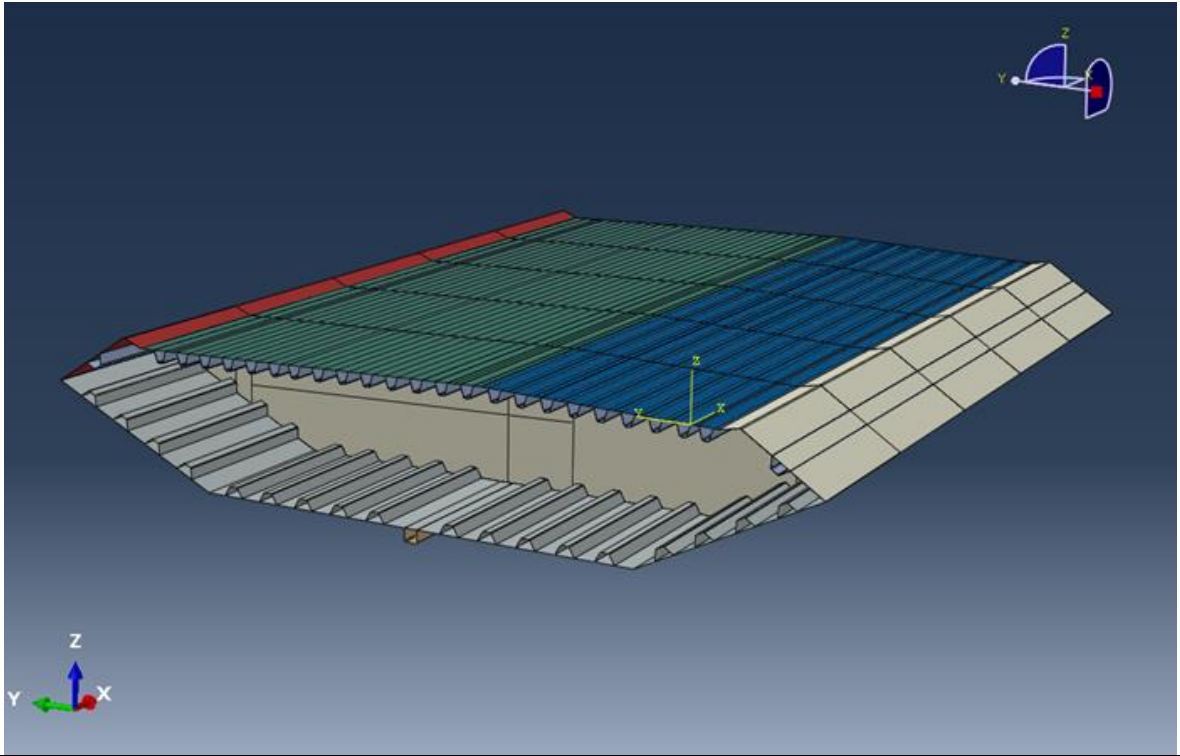
Hight	3.3 m	Hight/Width ratio	0.18
Width	18,3 m	Slenderness	0.0025
Length of model	20 m	Main span of the bridge	1310 m

Figure 21 The dimensions of the box girders in Hardanger bridge[57]. The girder is not entirely symmetric, due to the inclination criteria from two road lanes and one pedestrian lane (3% inclination).
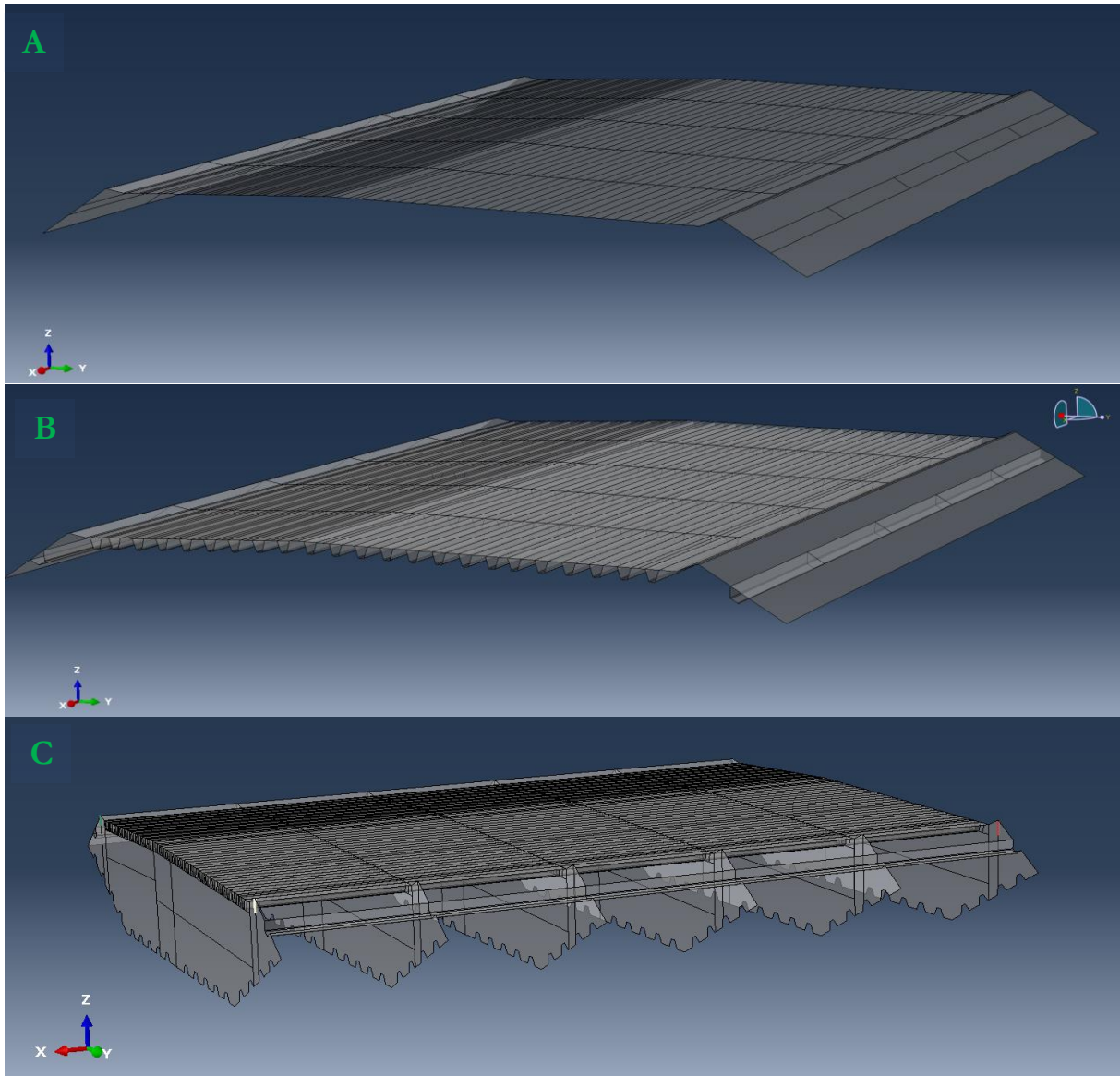
Figure 22 The FEM of the Orthotropic Steel Deck (OSD) of Hardanger bridge. (A) The upper steel deck of the road bridge, (B) The deck is supported by the longitudinal stiffeners (ribs), (C) which again is supported by the six transversal diaphragms.

4.1.2. The modeled OSD

The orthotropic steel decks are incorporated in the box girder to increase both stiffness and strength **Figure 22**. The components of the OSD in the model are the deck plate, the longitudinal U-ribs, and the diaphragms. The upper and lower deck plates have different thicknesses. The upper deck, which is 12 mm thick, serves as the bridge floor. The upper deck is supported by longitudinal closed trapezoidal stiffeners. There are 23 evenly spaced longitudinal closed rib stiffeners that support the upper deck. The longitudinal stiffeners penetrate the diaphragms. The 6 diaphragms in the modeled box girder function as vertical and transversal stiffeners. These components give the OSD its structural stiffness and traffic load carrying capacity.

4.2.   <u>Boundary conditions</u>

The boundary conditions are placed in accordance with the design drawing provided by the NPRA (***Appendix A***). Applying correct boundary condition is especially important if the fatigue critical components are close to the boundary condition[38]. The effect of boundary condition is strongest on the fatigue critical locations that are closest to the boundary condition.
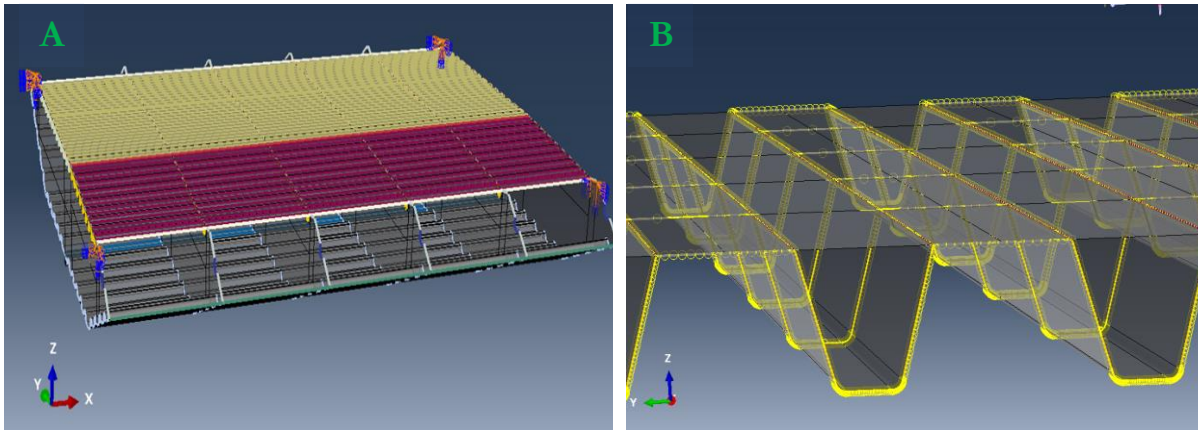
Figure 23 Boundary Conditions. (A) Suspension. The box girder is suspended in mid-air. This is done via the four hanger clamps at the corners of the outer most diaphragms. (B) Weldment. Tie connections (yellow rings) function as weldment. Rib to deck welded joints are highlighted in using red line. The remaining tie connections are weldment between rib-to-diaphragm and deck-to-diaphragm.

4.2.1. Suspension

Suspension of the box girders on the hangers is very close to the design drawings. The four relevant edges that are expected to be in contact with the hanger clamps are fixed, and do not have translation or rotation in any direction ***Figure 23A***. The rest of the components of the local model ultimately transmit their loads to these four edges.

4.2.2. Weldment

The rib-to-deck welded joints are modeled as a longitudinal tie connection between the deck plate and the U-rib ***Figure 23B***. The longitudinal tie connections are equal to the 20 m long segment of a box-girder. The 12 mm thick upper deck plate and the 6 mm trapezoidal stiffener wall thickness are "glued" at contact edges The detailed design drawings of the box girder are shown in appendix ***Figure 40*** and the corresponding FEM of the box girder. The six crossbeams are glued to the continuous ribs using tie connections. All the rib to diaphragm contact surfaces is tie connected modelling continuous weldment along the edge.

29

4.3. <u>**Meshing**</u>

4.3.1. *Shell element model*

The hot spot stress in welded steel structures is determined using a finite element analysis. FE models of welded joints can be constructed with thin/thick shell elements or solid elements ***Figure 24***. In thin-shell element models the elements are arranged in the middle plane of the individual plates. The weld need not be modeled by separate elements. Modeling the weld is needed only in special cases of weld arrangements, for example closely neighboring welds with expected interaction effects and high local bending at weldment[12]. Thin shell elements are used for modeling of the box girder. Thin-shell elements naturally have a linear stress distribution over the thickness, which suppresses the notch stresses at "welded joint" node. The Hot Spot stress is often extrapolated to the welded joint from the reference points recommended in guidelines[10,12].
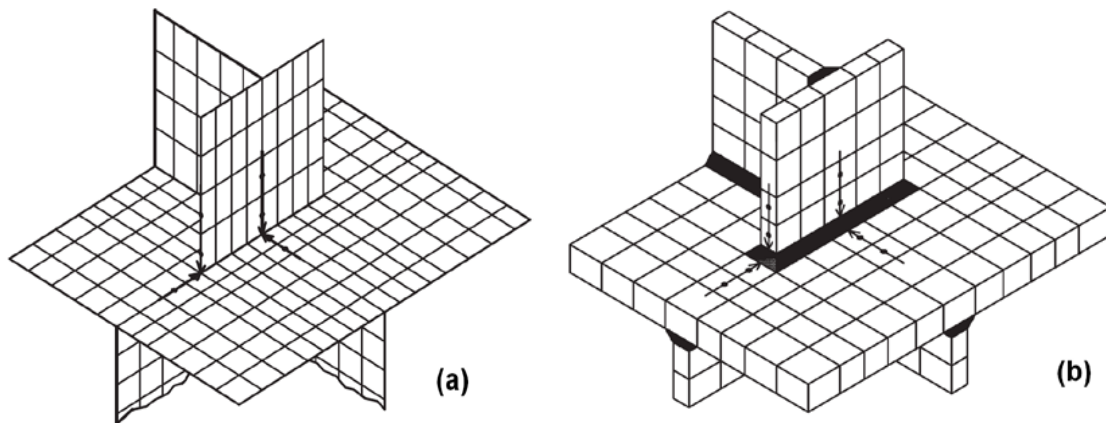
Figure 24 Three- dimensional FE modelling to the weld toe (a) Shell model (b) Solid model including weld[13].

Linear quadrilateral type S4R element including bending and membrane effects is used. Material properties of the steel plates used in the model is defined in ***Table 4***. The steel plates are isotropic and linearly elastic. Thin shell structures are analyzed using the four-node element and its six degrees of freedom per node. The requirements on mesh size and type of elements depend on the size of the studied structural components and the magnitude of load[15].
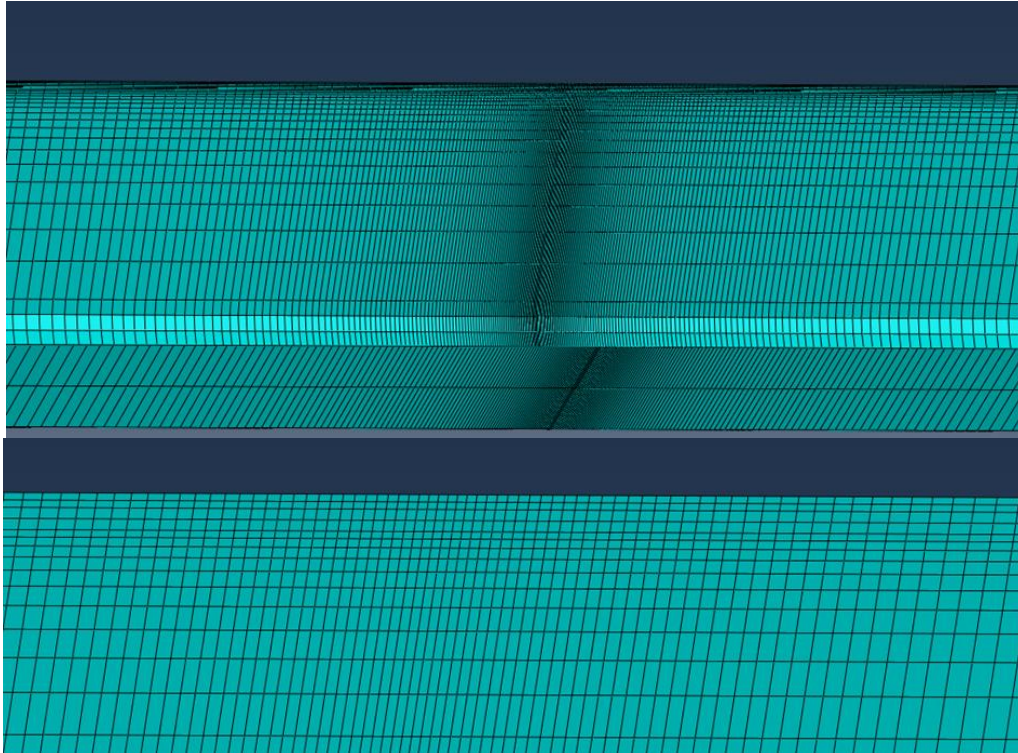
Figure 25 Fine local meshing. (A) Gradual increasing mesh size from fine to coarse. (B) magnified, showing the fine mesh is equilateral 1,2 x 1,2 mm.

4.3.2. Fine local mesh

The acquisition of precise stress response in fatigue analysis of structural components using Hot Spot stress approach is a highly mesh size sensitive process. This is due to studying the stress variations at the vicinity of welded joints. The discontinuities at the joints often result in high stress concentration gradients and stress singularities. Fine mesh size is a requirement for Hot Spot stress analysis, as the resultant stresses may differ depending on element size. The increased number of elements in the model ultimately increases the computational cost. The local mesh for Hot Spot analysis was linear S4R fine local mesh at the studied rib-to-plate connection (1.2 mm), with gradual increase to coarse global mesh (60 -120 mm) was employed **Figure 25**.

Table 4 Material data used in Abaqus

Material	Young`s modulus (GPa)	Poisson's ratio	Mass density (kg/m^3)	Yield strength (MPa)
Steel	**210**	**0.3**	**7800**	**355**

4.3.3. Reference points for Hot Spot stress

Two different sets of reference points of the Hot Spot stress at the deck-to-rib weld joint were compared. These are (1) **deck plate** and (2) **stiffener wall** near the joint. The reference points at the stiffener wall, resulted in shorter fatigue life, and were therefore chosen to calculate the Hot Spot stress and the fatigue life of the welded

joint for the reminder of the thesis. **Figure 26**: shows the location of the reference points for linear extrapolation of the Hot Spot stresses.

4.3.1. Linear stress extrapolation

The nodal stress at two reference points read out from Abaqus are used to linearly extrapolate the stress at the Hot Spot, i.e., at the weld toe. As the mesh element size around the Hot Spot is fine mesh, the first reference point (RP1) closest to the weld toe could be defined as 0.4**t** and the second reference point (RP2) is positioned at 1**t** from the weld toe, where **t** is the plate thickness. The stress at the Hot Spot is calculated using the linear extrapolation (**Eq.(10)**) [58]. The nodal stresses output by Abaqus for shell element model are plane stresses. These stresses from each of the reference points were used to linearly extrapolate the Hot Spot plane stresses.
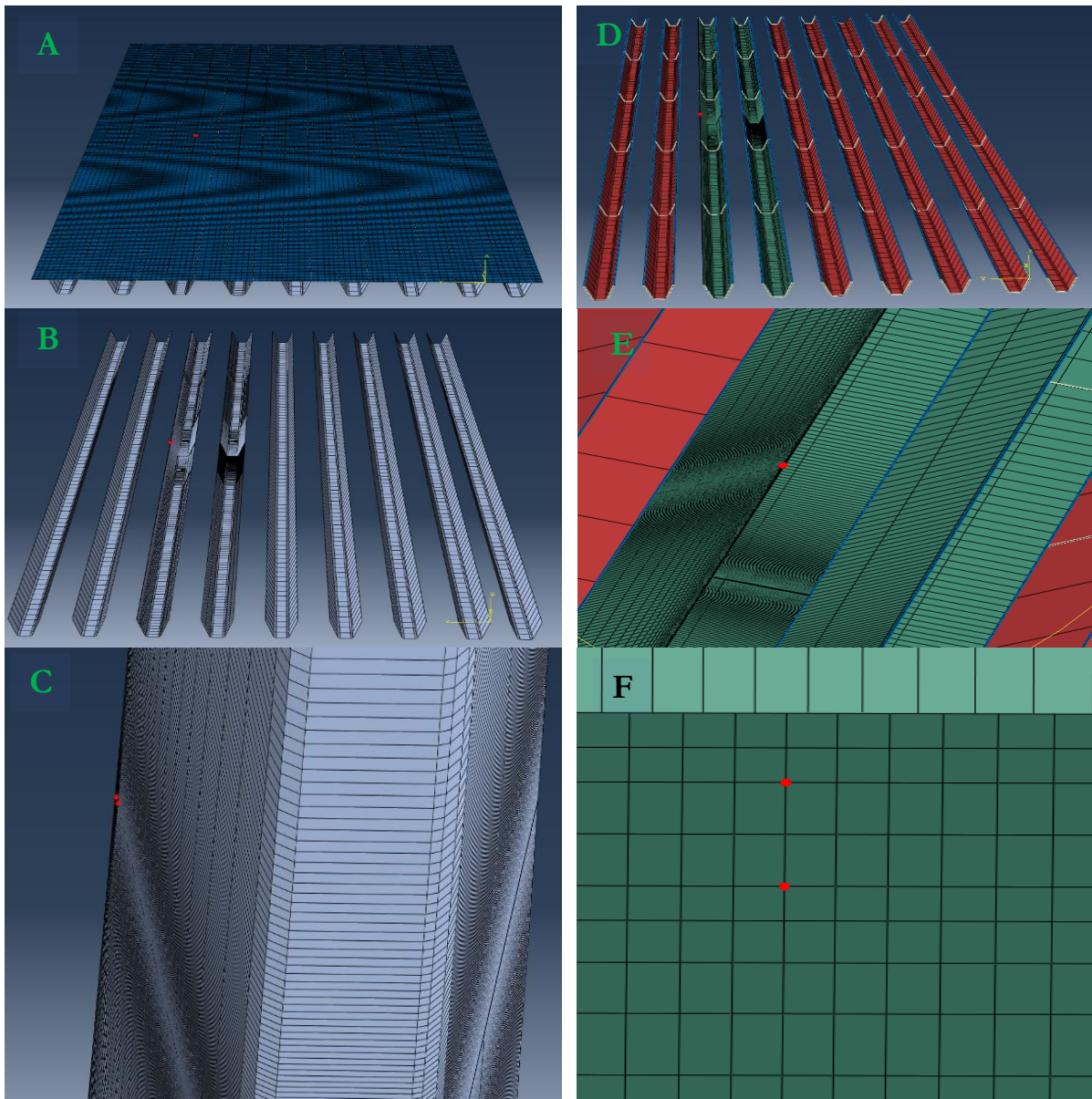
Figure 26 Location of the reference points for Hot Spot stress extrapolation (red nodes).

5. Traffic Load Models

Traffic load causes fatigue damage on bridges depending especially on the magnitude of the axle load and the composition of the traffic[59]. Traffic loading is complex due to the variable load amplitude and the random nature of the loading sequence[13]. Fatigue load models proposed by standards, significantly simplify the traffic loading, yet reflect the actual load conditions accurately when assessing fatigue damage on road bridges. In this thesis Fatigue Load Model according to the NPRA (FLM-N)[9] and Fatigue Load Model according to Eurocode (FLM4)[60] were loaded for comparison.

5.1. <u>Fatigue load models</u>

The fatigue load models are generated from field measurements of traffic flow and vehicle weight frequency on bridges. The lightweight vehicles that do not cause fatigue damage are neglected, and the heavier lorries that cause fatigue damage are defined in the fatigue load models. A fatigue load is a load on a structure that is well below the static resistance of a structure, i.e., it does not cause any damage during static loading, but causes failure of the structure when cyclically loaded on the structure. If the number of fatigue load cycles to failure is low (<1000 cycles), the fatigue load causes low cycle fatigue, which is characterized by plastic deformation. If the number of fatigue load cycles to failure is high (10^6 cycles), it causes high cycle fatigue, and it is characterized by elastic deformations[61].

5.1.1. FLM-N

Accurate determination of the fatigue load models is required to make useful approximation of fatigue. The specifications of the fatigue load model, including the geometry of the load model vehicle, its axle loads, axel spacing as well as composition of traffic and its dynamic effects follows the requirements of fatigue loading on bridge as specified by the National Public Roads Administration[49]. The lorries in FLM-N have 3 axles, with equal axle spacing as defined in **Table 5**. The axle load and probability of the lorries is shown in **Table 6**. The number of vehicles expected to cross the Hardanger bridge in a year, **Table 7**, is calculated from the annual average daily traffic (AADT = 3650) as recommended by NPRA[49].

Table 5 Axle distance for vehicles classes in FLM-N

FLM-N	Axle distance (m)	
	Axle 1-2	Axle 2-3
Lorry1-5	2,5	6

Table 6 FLM-N axle load and corresponding probability distribution

Vehicles	Probability	Yearly traffic flow	Axle load (kN) A1 / A2 /A3
Lorry1	0.75	999187,5	60 / 60 /60
Lorry2	0.10	133225	80 / 80 /80
Lorry3	0.05	66612,5	100/100/100
Lorry4	0.05	66612,5	125/125/125
Lorry5	0.05	66612,5	145/145/145

Table 7 Number of cycles per year for each model

Fatigue load models	Number of cycles per year
FLM-N	$1,3 \times 10^{6}$
FLM 4	$0,5 \times 10^{6}$

5.1.2. *FLM4*

Eurocode (EN 1991-2:2003) proposed five fatigue load models, FLM 1-5 for road bridges[13,60]. The choice of appropriate load model depends on the fatigue verification or assessment method used in design. The thesis aims to determine the fatigue life of a component of the road bridge using the safe-life design and cumulative damage. The safe life design assures that the structure will perform satisfactorily throughout its design life, without being dependent on regular in-service inspection for fatigue damage[13]. The FLM4 is chosen in this thesis as it satisfies the requirements.

The axle weight and frequency of the lorries in FLM4 is given in **Table 6**, the axle spacing in **Table 8**. The Hardanger road bridge belongs to the road category 2 of "Roads and motorways with medium flow rates of lorries"[62]. Accordingly, the expected number of lorries per year and per slow lane is given in **Table 7** .

Table 8 Axle distance for vehicle classes in FLM 4

FLM 4	Axle distance (m)			
	Axle 1 – 2	*Axle 2 - 3*	*Axle 3-4*	*Axle 4-5*
Lorry1	4,5	-	-	-
Lorry2	4,2	1,3	-	-
Lorry3	3,2	5,2	1,3	1,3
Lorry4	3,4	6,0	1,8	-
Lorry5	4,8	3,6	4,4	1,3

Table 9 FLM4 axle load and corresponding probability distribution

FLM-4	Probability	Yearly traffic flow	Axle load (kN) A1/A2 /A3 /A4 /A5
Lorry1	0.40	200000	70/130/ - / - / -
Lorry2	0.10	50000	70/120/120/ - / -
Lorry3	0.30	150000	70/150/ 90/ 90 / 90
Lorry4	0.15	75000	70/140/ 90/ 90 / -
Lorry5	0.05	25000	70/130/ 90/ 80 / 80

```fortran
subroutine DLOAD("preamble")
!variable definition
Velocity = 10000 !(mm/s)
ecc=2500 !Eccentricity (mm)
Y_ax=2000 !Wheel spacing (mm)
Xp = Velocity * TIME(1) !Dynamic position

!First Axle definition
!Left Wheel definition
if (X.le.(Xp+100).and.X.ge.(Xp-
100).and.Y.le.(ecc+300+Y_ax/2).and.Y.ge.(ecc -
300+Y_ax/2)) then
F=0.25 ! Wheel load (MPa)

!Right Wheel definition
elseif (X.le.(Xp+100).and.X.ge.(Xp-
100).and.Y.le.(ecc+300-Y_ax/2).and.Y.ge.(ecc-
300-Y_ax/2)) then
F=0.25
else
F=0.0
endif
RETURN
END
```

*Code 2 Moving load definition in Fortran code. Xp= Velocity * Time defines the time dependent location (i.e., motion).*

5.1.3. FLM in Fortran programming language

To dynamically load the vehicles on the lane, a user defined subroutine in Fortran programming language was used. **Code 2** shows a simple script that defines the moving load. Each lorry is explicitly defined in user subroutine (**Appendix B**). The axle weight and the axle spacing are defined as listed in **Table 8 & Table 6**. The vehicles are defined as moving surface loads using DLOAD user subroutine. The axle loads are converted to pressure loads by dividing with the surface area of the wheels. The rectangular contact surface area (width x length) of each wheel is 0.2 m x 0.6 m for FLM-N and 0.32 m x 0.22-to-0.44 for FLM-4 (**Appendix B**).

5.2. __The lane__

The Hardanger bridge has a total of two road lanes. Only one lane is loaded for this thesis. The asphalt weight was accounted for as a uniformly distributed load on the upper deck in accordance with the recommendation by the NPRA[49].

5.2.1. *Eccentricity*

The fatigue loads drive in the direction of the lane with an eccentricity 2.5 m from centerline of bridge to centerline of axle. The 6 offsets of vehicle location on the lane were simulated using a single lorry (lorry 5 – FLM-N) *Figure 44*. These locations of the axel mid-point in relation to bridge centerline are common according to traffic data[9,63]. They are defined as eccentricity of 2.5 m $\pm$ 0.3 [2.20, 2.80] m *Figure 27*. The location of vehicle that gave the highest stress at the Hot Spot was chosen for all vehicle loading simulations for fatigue life estimation. This eccentricity was found to be 2.5 m. It gave the highest principal stress at the Hot Spot. Therefore, the model is loaded with this eccentricity.
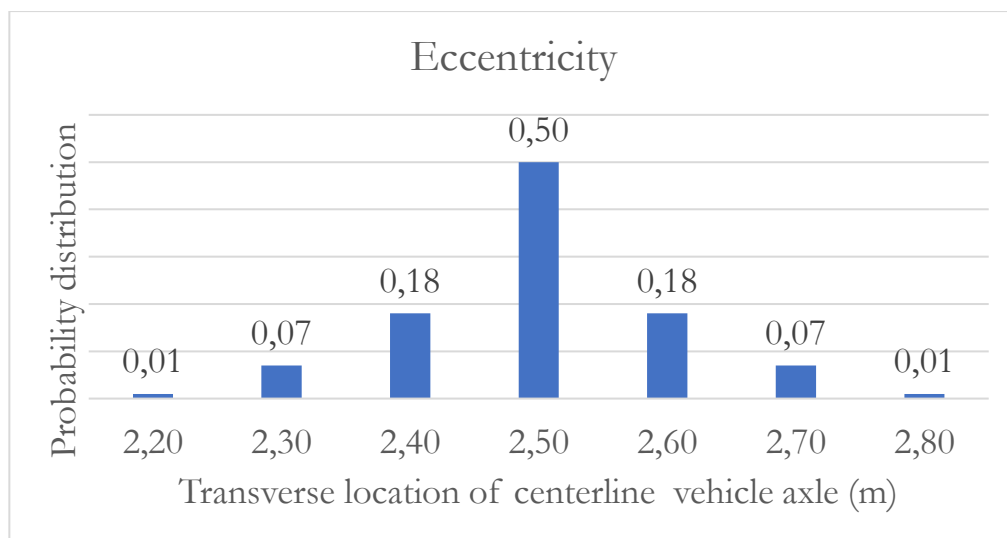
Figure 27 Probability distribution of transverse location of center line of vehicle[63].

5.2.2. *Location of the Hot Spot under the wheel load*

The welded connection of the rib to deck of the OSD was selected for Hot Spot analysis as it is the main load transmitters in transferring the wheel loaded from the OSD to the remaining structures of the box girder. The most unfavorable rib to deck connection was selected for fatigue assessment due to traffic loading. The box girder was loaded by two wheel per axle of each lorry. The reference points for Hot Spot extrapolation are located at the longitudinal rib under the wheel loads *Figure 42*.

6. Fatigue analysis

6.1. Stress time history

Max principal stress time history calculated from the linearly extrapolated Hot Spot plane stresses is shown in *Figure 28*. The traffic loading method is defined in **the dynamic vehicle loading section**. Five lorries are loaded, one lorry at a time. In the FLM-N, Lorry 1 is the lightest and produces the shallowest valley in the stress time history, while lorry 5 is the heaviest and produces the deepest valley on the time history. Each lorry of the FLM-N has three axles and each valley in the stress history corresponds to each axle *Figure 28*.
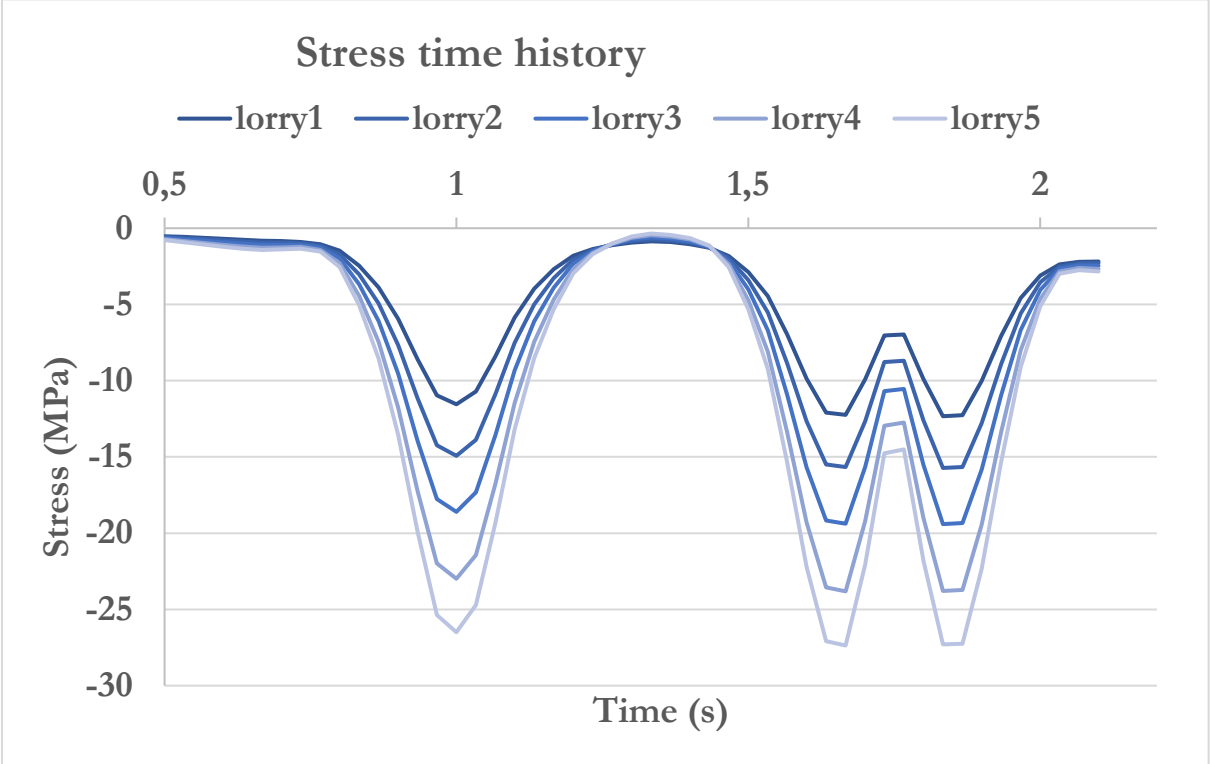
Figure 28 Stress time history for the 5 different lorries loaded on the model.

Each lorry in the Eurocode's FLM4 has different axle numbers and the corresponding valleys in stress history are shown in *Figure 29*.
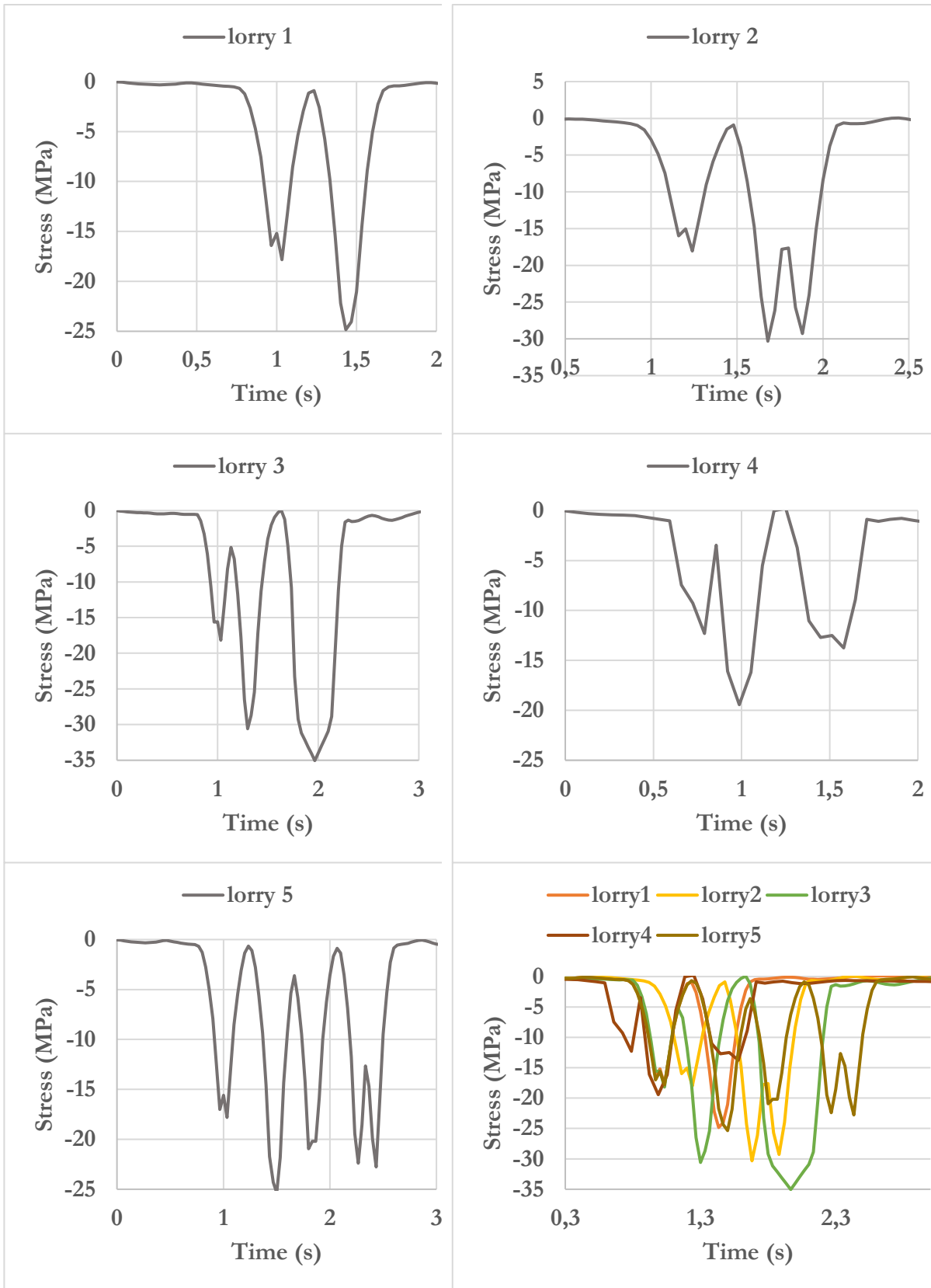
Figure 29 Stress time history at hotspot for FLM4

6.2. Stress Ranges

The fatigue relevant stress ranges are acquired by **cycle counting** the stress histories. Python script (rainflow.py) is used for cycle counting method to transform the maximal principal stress history into a stress histogram with a few variable amplitude stress ranges. The safe life assessment method is used in this thesis, as it is recommended for bridges with high consequence of failure[13]. The cycle counted stress ranges are further adjusted using the partial factor (γ_{mf}) for fatigue strength 1.35. Damage is then calculated using the damage accumulation rule (Palmgren-Miner rule) of the sequence of stress ranges obtained from the fatigue traffic loaded model.

The series of stress ranges from each stress history can be simply represented by a single equivalent stress range for each lorry. For comparison the equivalent stress ranges of each lorry from both FLM-N and FLM4 loading are shown[30].
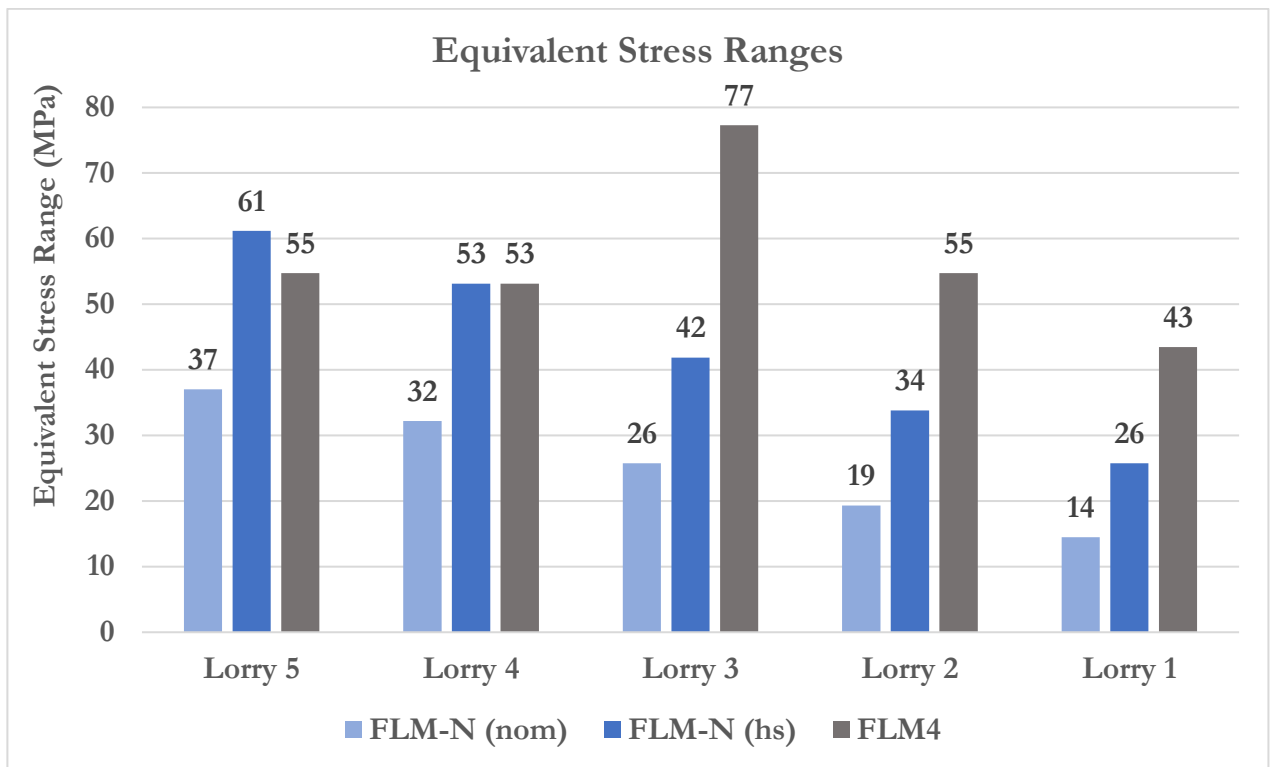
Figure 30 Equivalent stress range at the Hot Spot. Abbreviations: nom: nominal, hs: Hot Spot
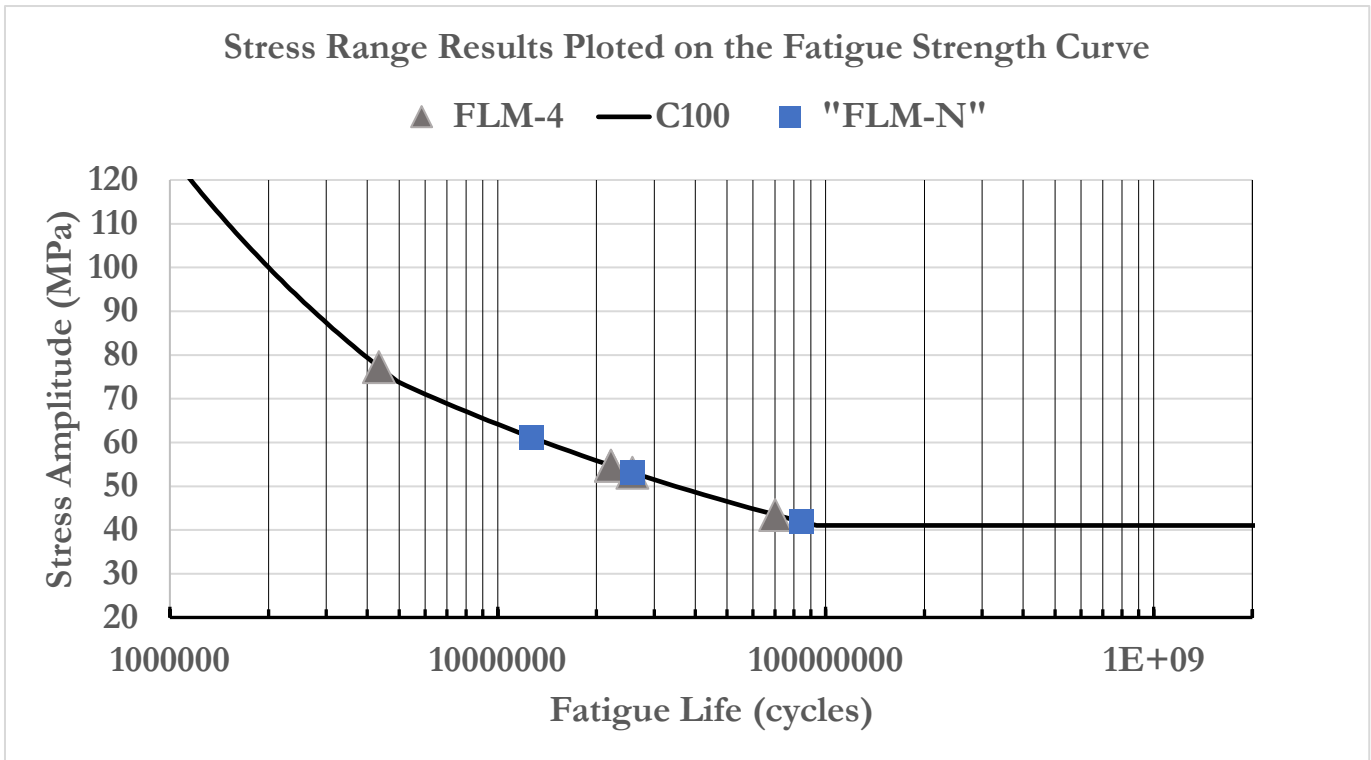
Figure 31 Fatigue inducing stress ranges plotted on the fatigue strength curve (C100).

6.3.   Fatigue life

The cycle counted stress ranges when plotted on the detail category 100 curve demonstrate that the fatigue damage induced by the traffic model is high cycle fatigue ***Figure 31***. Comparing the fatigue life of the longitudinal rib-to-deck welded joint when loading with the National FLM-N and Eurocode's FLM4, the results show 135 years and 24 years respectively.
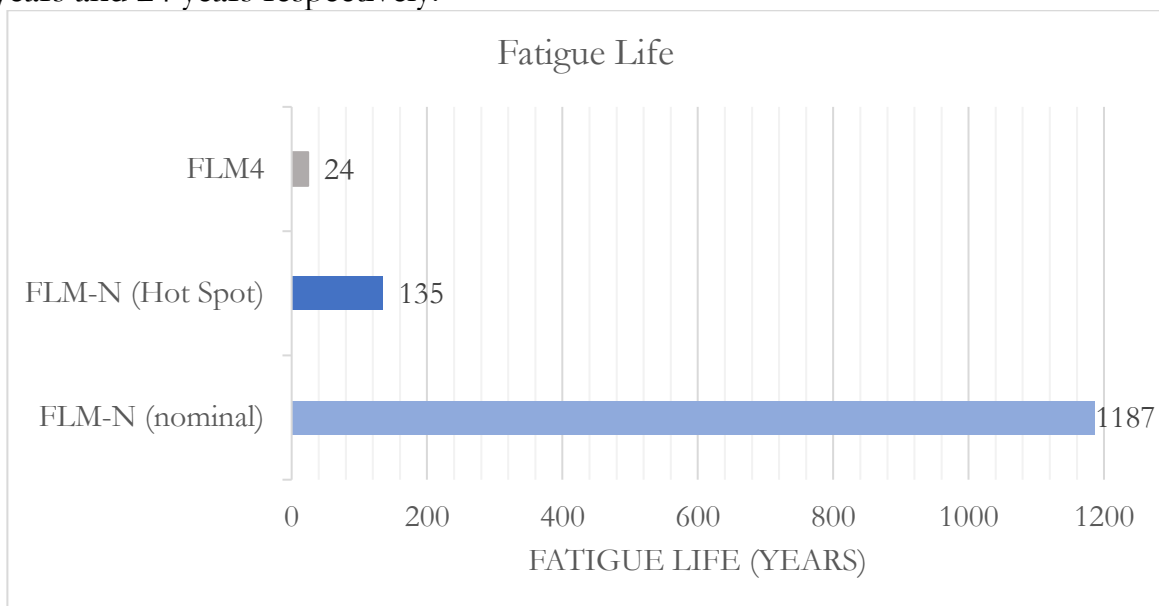
Figure 32 Fatigue life (years) of the rib-to-deck welded joint

To evaluate the effect of velocity of fatigue life of the welded joint, the vehicles were run with three different velocities. The fatigue life of the weld after loading the vehicles with a single velocity at a time was compared. Care must be taken when simulating a moving load with relatively high velocity. The sampling frequency matched the speed of the vehicle, by using the timepoint algorithm in Abaqus can be used, where sampling interval was defined as distance per frame
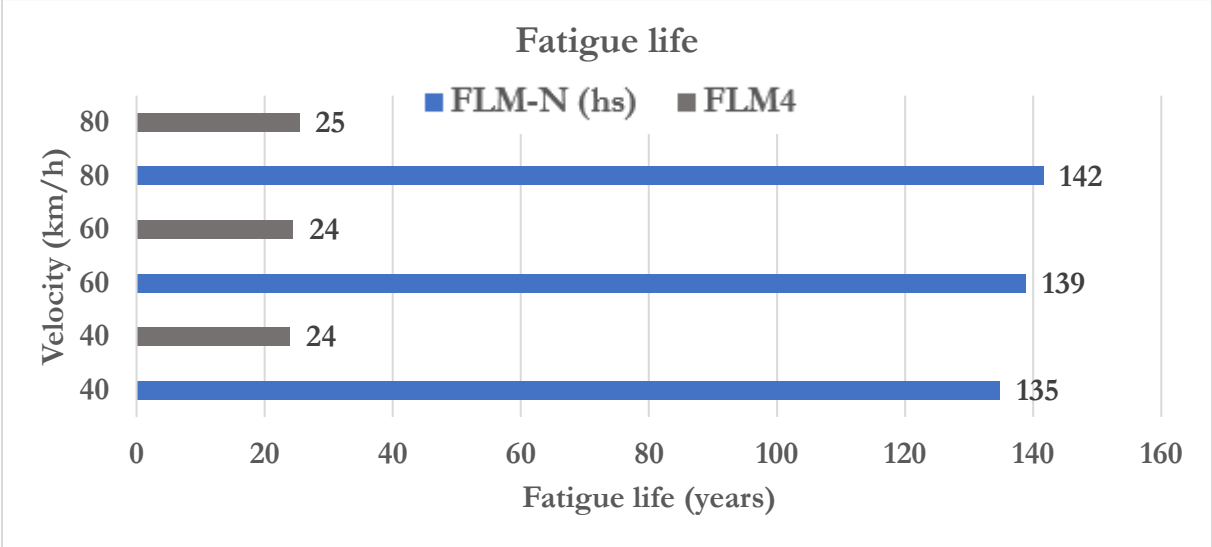
Figure 33 The effect of vehicle velocity on fatigue life of the welded joint.

7. Global model

7.1.   The structure of the FEM

The Hardanger bridge was modeled as a single span suspension bridge, and simplified into the two cables, as-built number of vertical hangers and a horizontal beam representing the box-girders **Figure 34**. The two cables, if considered identical and vertical, make the cable plane, i.e., x-z plane. The suspension bridge is subjected to three main loads: self-weight, traffic load, and wind load.
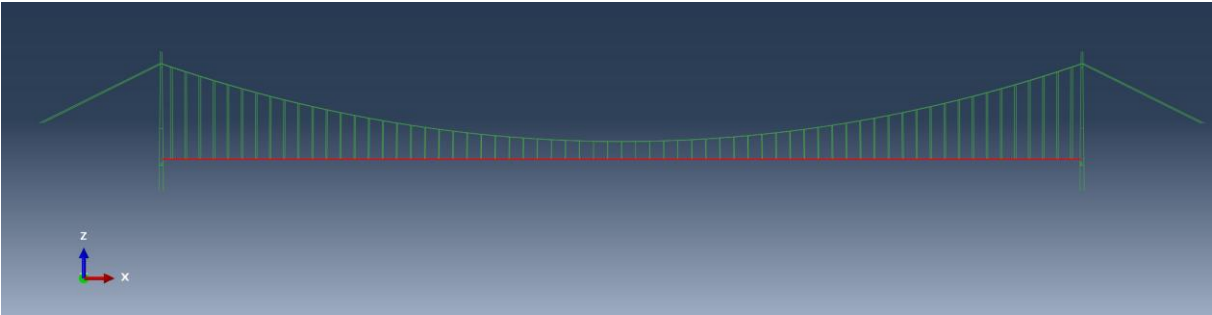
Figure 34 The global FE-model of Hardanger Bridge. The red line is the beam model of the box girders.

7.2.   Traffic loading

Table 10 Total weight for each lorry in FLM-N and FLM4 for the Global model

Lorries	Total lorry weight (kN)	
	FLM-N	**FLM4**
Lorry1	120	200
Lorry2	240	310
Lorry3	300	490
Lorry4	375	390
Lorry5	435	450

7.2.1. Vehicle loads

The traffic load was simulated by applying a moving point-load of the total weight of FLM-N and FLM 4 (see **Table 10**). The passage of a single lorry across the global model is simulated as a passage of a single moving concentrated load. The load corresponds to the total weight of the passing lorry. The moving load was stepped over the full length of the bridge with a pre-defined stepping distance. The response from each loading scenario was extracted for each of the selected five nodes along the span of the bridge. The location of the selected nodes is given in **Table 11**. The extracted responses created the influence line for the nodes.

Influence lines are curves that show the variations of various functions such are the axial force and moment at a given section, or the stress in each beam, due to passage of a single unit load across the span. Use of influence lines is common in the study of the effect of concentrated loads.
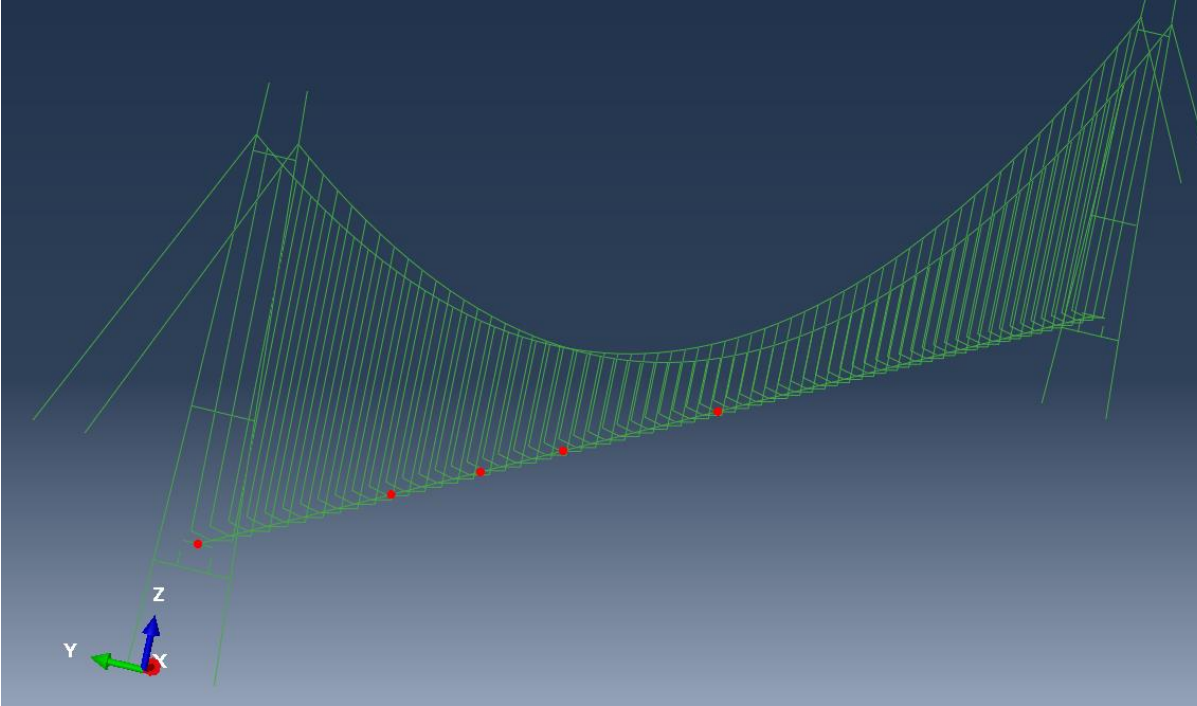
Figure 35 Stress is calculated for five output nodes along the span of the bridge.

Table 11 Stress measurements from selected nodes along the bridge span length.

Node number	L=1310 m (Main span length of the bridge)	Distance in x-direction (m)
1	0	0
198	L/6	218
248	L/4	328
296	L/3	437
395	L/2	655

7.2.2.Location of sensors

The five nodes highlighted in **Figure 35** and listed in **Table 11** function as section moment and section force sensors on beam model of box girder. Due to symmetry of the bridge, all the nodes are selected at one half of the suspension bridge. The output measurements are due to traffic loading, and they are used to calculate the stress response the global model of the bridge.

43

7.3.   <u>Stress fatigue life</u>

7.3.1. *Calculating normal stress*

The normal stresses (σ) at different location along the span of the global model in the global model in Abaqus are shown in. Normal stresses (σ) at a given node along the span of the suspension bridge is calculated from force components (force and moment) and section resistance (section area and section modulus). Navier's equation shown in the ***Eq. (15) & (16)*** is used to calculate normal stress. N: axial force, A: cross-section area of the box girder, My: moment about the weak axis, Mz: moment about the strong axis, input table for values of A, Iy, Iz, y and z. The nodal measurements are acquired from the nodes in the global model in Abaqus and are listed in ***Table 11***.

A_{tot}	I_y	I_z	y_{top}	y_{bottom}	z
m^2	m^4	m^4	m	m	m
0.5813	0.972	16.448	1.607	1.953	8.53^*
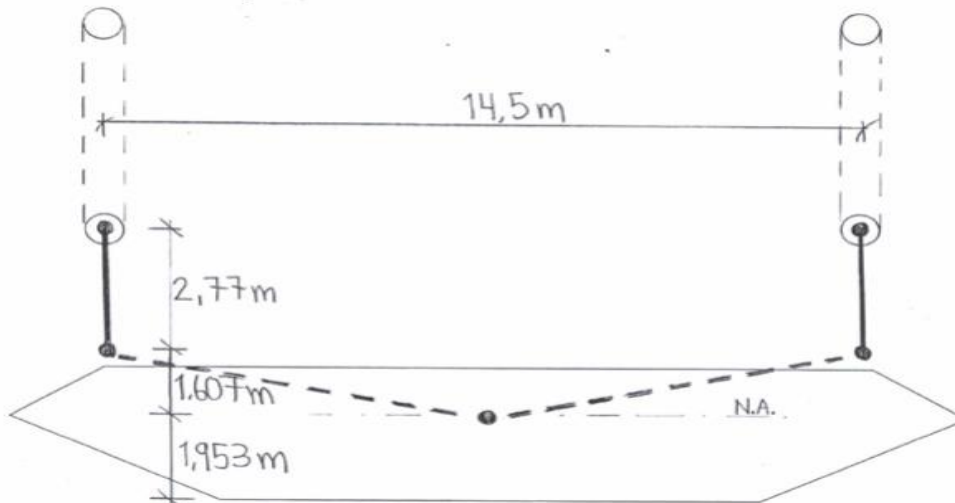
Figure 36 Input data for calculation of stress from global model simulation output.
*$^*Z=8.53m$ gave the largest stress response, for calculation see (**appendix E.1**).*

$$\sigma = \frac{N}{A} + \frac{M_y}{I_z} z + \frac{M_z}{I_y} y \qquad (15)$$

$$\sigma = \frac{N}{0.5813} + \frac{M_y \times 1.953}{0.972} + \frac{M_z \times 8.53}{16.448} \qquad (16)$$
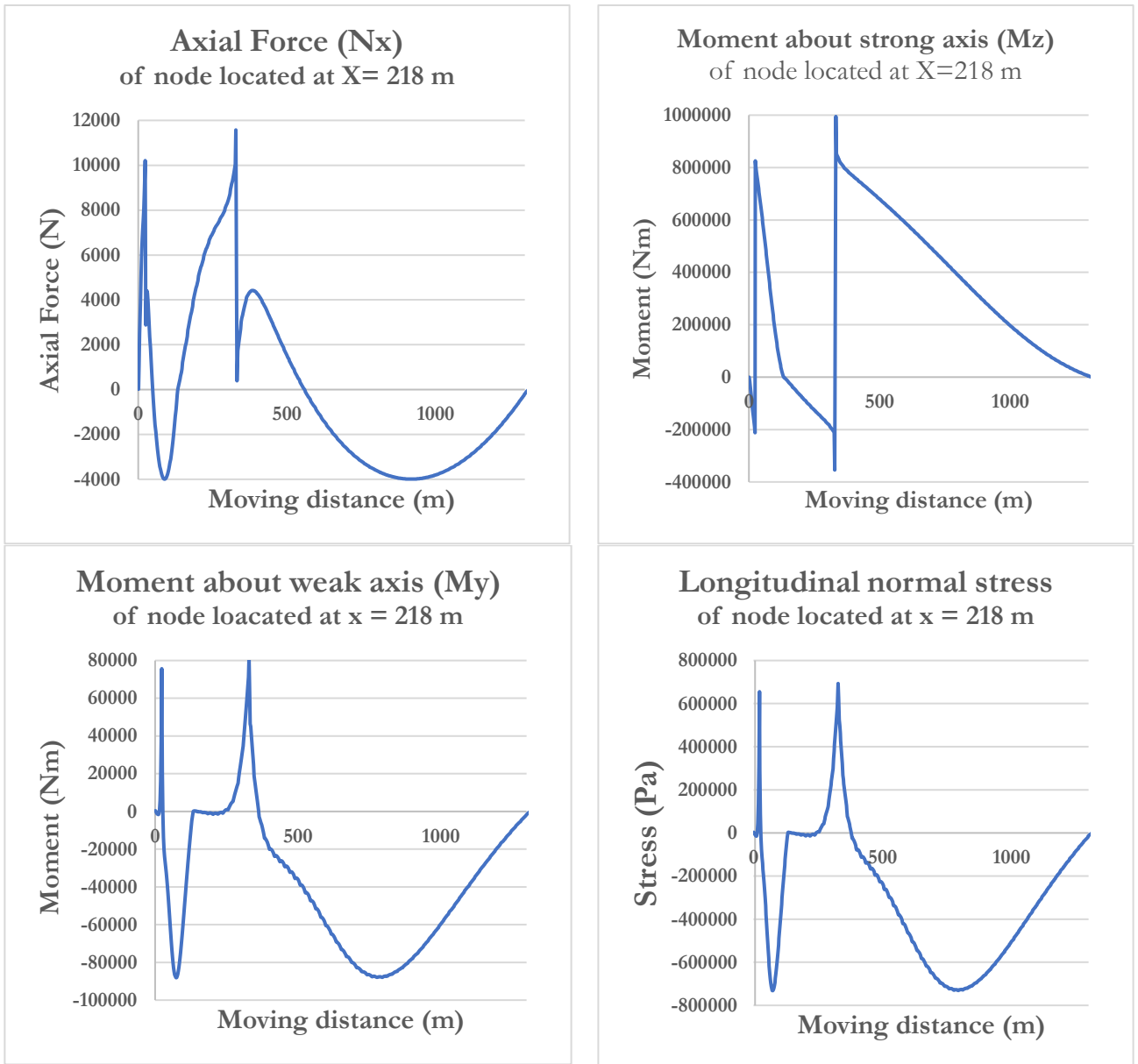
Figure 37 The relationship between the calculated normal stress and the axial force, weak moment, and strong moment. The influence lines are measured at the node that gave the largest stress range (at x=218 meter; L/6) by loading with Lorry 5 of FLM-N.

7.3.2. Stress influence lines

The normal stresses (σ) at different locations along the span of the global model is shown in **Figure 38**. The relationship between the calculated influence line of the normal stress and axial force, weak moment, and strong moment influence lines of at the node that gave the strongest normal stress range is shown in **Figure 37**.

The longitudinal normal stress of a node at x=218 m

The longitudinal normal stress of a node at x=328 m
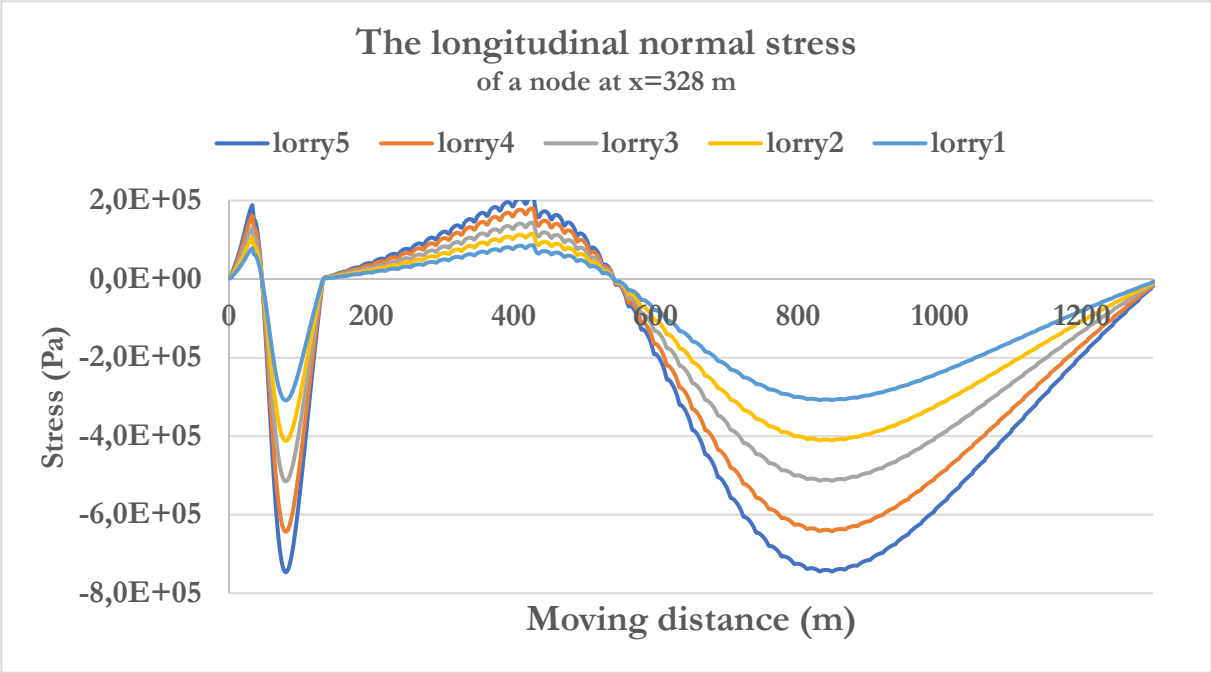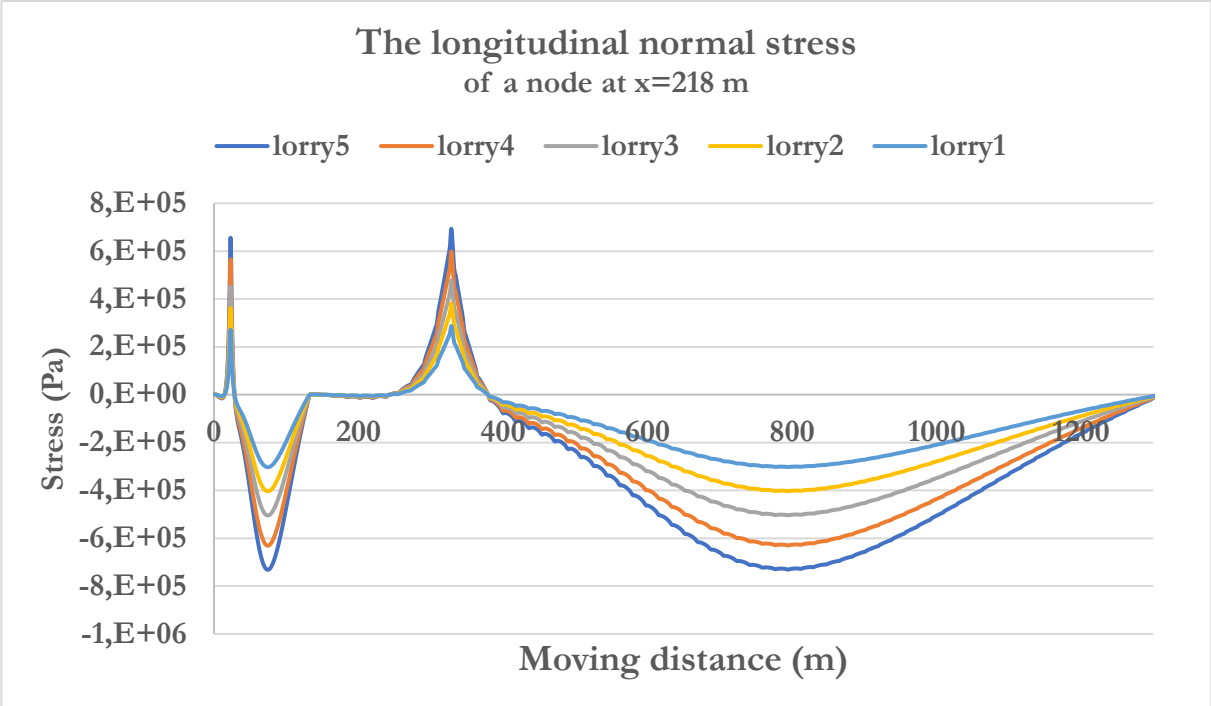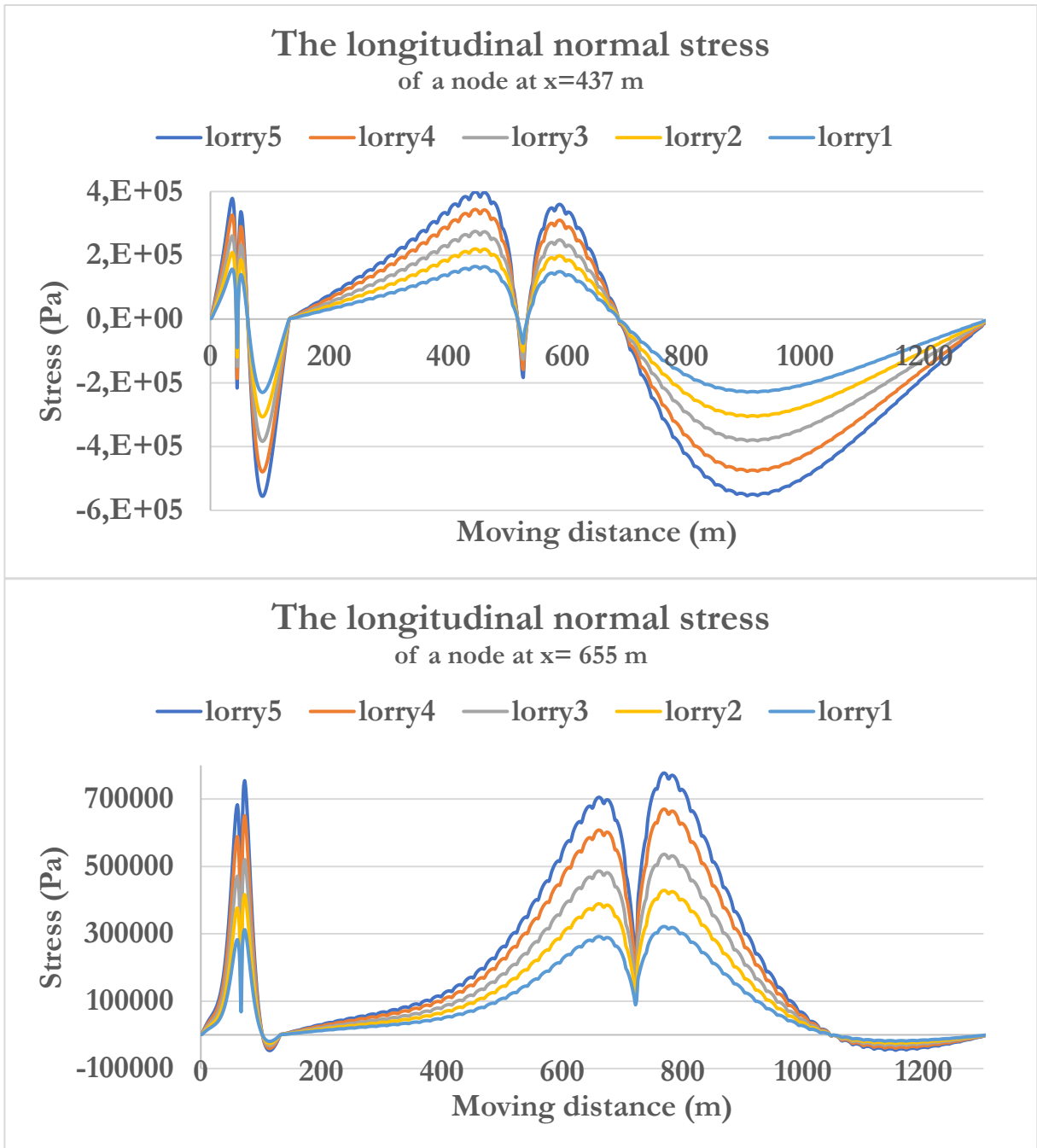
Figure 38 The longitudinal normal stress at nodes along the span of the bridge.

7.3.3. Fatigue life

The equivalent stress ranges, *Figure 39*, were calculated from the cycle counted normal stress influence lines at the five locations along the span of the global bridge model *Figure 35*.
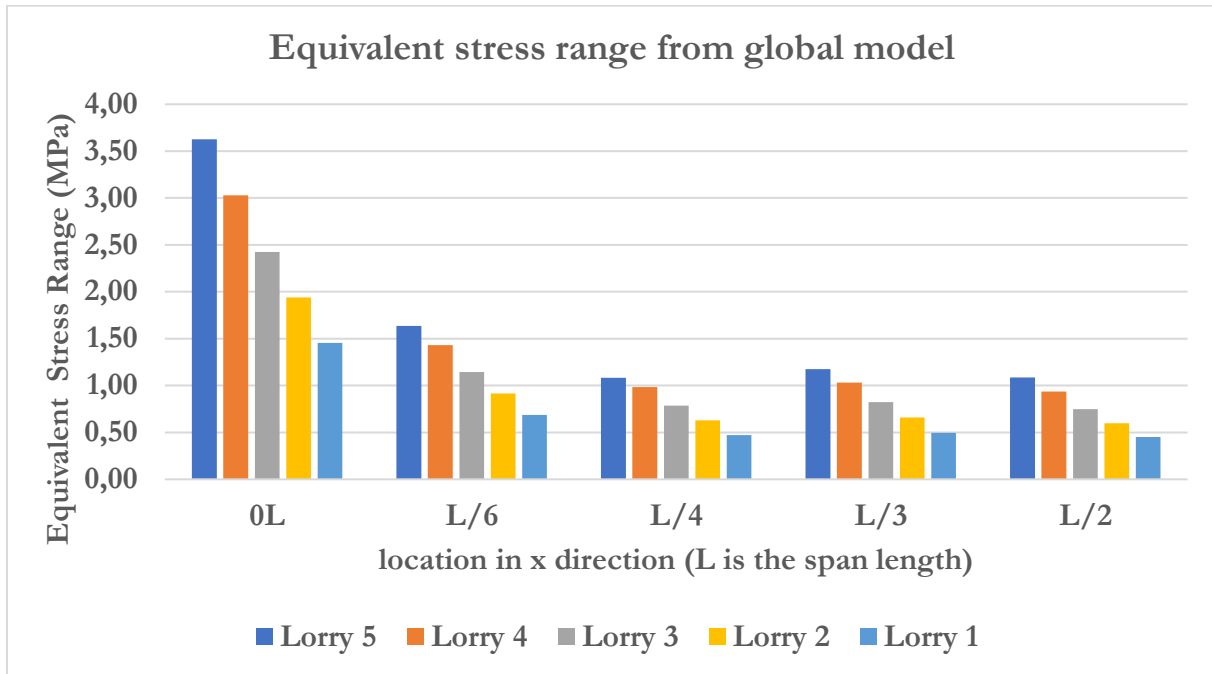
Figure 39 Equivalent stress ranges from the selected nodes along the span of the bridge.

The stress ranges from the global model, after loading the whole bridge with single vehicle at a time, are too small and do not induce fatigue damage. Fatigue life of the detail would be infinite.

8. Discussion

8.1.   <u>Discussion on the finite element model</u>

The rib-to-deck welded joint under the wheels is studied in this thesis. The welded joints between the longitudinal stiffeners and the upper decks located in the direct rolling area of the vehicle loads are chosen for numerical analysis. The location was chosen because cracks are often found there on monitoring the orthotropic steel decks[32]. They are difficult and expensive to repair as they may require traffic interruption.

The distribution and magnitude of stresses in a welded joint traditionally determined by experimental testing can be simulated, i.e., imitatively represented[64] in a finite element model of the joint. Determining fatigue life from experimental tests has its own challenges. Detecting crack initiation on specimen is often determined by visual inspection, which introduces some uncertainty. Experimental study of crack propagation of welded joints of OSDs report difficulty detecting crack propagation with certainty when using small increments of load[28]. The finite element fatigue design aids the precision and reliability of the experimental fatigue design. Fatigue assessment of road bridge components using finite element method has been applied in real life decision making of fatigue damage monitoring. The fatigue crack monitoring frequency and repair prioritization of fatigue damaged bridges are increasingly being based on results from FE-analysis[15].

The precision of fatigue predictions from finite element analysis may be ensured by verification method. Direct comparison of the experimental tests with the finite element numerical analysis is complex, in part due to randomness of material inhomogeneity in the steel that is difficult to reproduce by finite element method. Studies often use an indirect verification method, by comparing the stress-strain curves and fatigue test results between the simulated and experimental specimens[65], or by comparing the simulation results with field monitoring data from structural health monitoring system[15]. Unfortunately, traffic loading field data from the Hardanger bridge was not available for this thesis, and direct verification of the model was therefore not done.

Shell element model of the box girder was built. The components of the box girder are "glued together" using tie connections. As is common for shell element models of weldment[12,61], the weld geometry was not modeled in model. This type of modeling is considered adequate to make Hot Spot stress-based estimation of fatigue life.

For fatigue life prediction of complex welded components, the hotspot stresses have better precision than the nominal stress. The Hot Spot stresses are sensitive to the stress concentrations on the at the weldment. They vary along the weld toe, while

49

less variability is observed in the nominal stresses. Hot Spot and nominal fatigue life estimation of the welded components are compared[15], as it is simpler to determine and is widely applied in fatigue analysis. The nominal stress method can be adequately estimated by using coarse mesh. It is the most common fatigue life assessment approach[30], applied in standards, is still being used in fatigue research to determine the fatigue life of welded joints[65].

Stress analysis at the welded joint (Hot Spot) studied using FEA is mesh sensitive, therefore the meshing recommendations in literature[12,61] were strictly followed for consistency. A consistent and standardized mesh sensitive Hot Spot stress extrapolation need not be replaced by a mesh insensitive approach. Local fine mesh is employed at the Hot Spot, to meet the required mesh size for linear extrapolation of Hot Spot using. The Hot Spot stress concentration was calculated using linear extrapolated from reference points (0.4t and 1t) from the local fine mesh. The local fine mesh size is gradually increased to coarse global meshing by a linear mesh rule. Coarse mesh is used for the rest of the box-girder model for computational efficiency.

8.2.   Discussion on the traffic load model

Independent of the precision of FEM for fatigue assessment
The vehicle weight was taken as constant unite values for its respective vehicle type specified by the NPRA[9] and Eurocode[13]. Although alternative traffic modeling exists that model the traffic very close to the realistic traffic loading by using probability distribution curves and gross vehicle weight. They use traffic data analysis that includes variation in the distribution of the vehicles. The traffic loading employed in this thesis is a simplified, yet very realistic loading. The vehicles are defined precisely as specified in the standards. The standards specify the axle space, the wheel space, the axle load and probability distribution of each lorry. The percentage of the average daily traffic (AÅDT) corresponding to each lorry is used to determine the number of cyclic loadings of the stress range calculated from the simulation.

Traffic scenarios that induce negligible stress response and consequently negligible fatigue damage are systematically excluded by using the fatigue load models provided by the Norwegian national annex and the Eurocode's FLM-4. The five lorries in each of those fatigue models with their selected distribution and yearly flow rate are representative of the fatigue inducing traffic loads that approximate the vehicles that travel on Norwegian road bridges and its equivalent regional European highway bridges. Stress ranges under variable amplitude traffic loads were cycle counted from the principal stress time history. The fatigue load models of the NPRA and Eurocode are compared. The difference in loading comparing surface load and single wheel loading and effect on damage was evaluated.

8.3. Discussion on fatigue assessment

This study presents numerical simulation of the fatigue behavior of rib-to-deck welded joints of OSD. The fatigue assessment was carried out in compliance with the Eurocode recommendations on fatigue design of bridge decks. **The rib-to-deck joint** is one of the components of bridge decks with longitudinal stiffeners that should be checked: deck plate, stiffeners, diaphragms, and stiffener-to-diaphragm connections.

Fatigue of welded details remains an inadequately understood steel pathology[30]. The long-term performance studies of steel bridge components are important in the prediction of the sustainability of the steel bridge. One main research aspect in the study of long-term performance of such bridges is fatigue performance studies: where a full-scale steel bridge deck is modeled to study the fatigue behavior of its components. The most commonly researched fatigue prone components of steel bridges are the welded joints[66]. The durability defects can be studied using finite element simulation analysis and the resulting fatigue life prediction may be used to guide maintenance and reinforcement measures.

The stress-life method is used in this thesis for fatigue life assessment. It is one of the three classical fatigue analysis methods: the strain life method, and the stress life (S-N) method, and the fracture mechanics method[67]. The traffic loading simulated in this thesis on orthotropic steel decks of the bridge produces stresses and strains in elastic range, and results in high cycle fatigue on the bridge. The stress-life method was chosen because it is the best suited fatigue assessment method of structures loading that give high cycle fatigue. The two main fatigue design methods proposed by the International Institute of Welding (IIW): the nominal stress method and the Hot Spot stress method have been applied to predict the fatigue life of the welded joint.

Fatigue life of the rib-to-deck welded joints were predicted using Miner's Rule. When damage of a structure is evaluated based on the linear damage accumulation rule, the actual damage state tends to be overestimated in the early stage of fatigue damage accumulation, and the evaluation results on this thesis may therefore be conservative. Alternative nonlinear fatigue damage accumulation models may be explored depending on the level of accuracy required[68]. For the scope of this thesis the accuracy achieved by Miner's Rule was considered adequate[10].

8.4.   <u>Discussion of the results</u>

The fatigue life of the welded joint was 135 years when loaded with the National fatigue load model (FLM-N). The orthotropic steel deck (OSD) of the Hardanger bridge is like all other OSDs prone to fatigue cracking due to unexpected increase in traffic volume. Therefore, for comparison, the heavier Eurocode's fatigue load model 4 (FLM4) was loaded to account for potential increase in traffic volume and assess the fatigue response of the welded joint. The fatigue life of the stiffener to deck welded joint is shortened from 135 to 24 years when loaded by FLM4. This is less than one fifth of the life found when loading with FLM-N. Fatigue life using nominal stress was found to be 1187 years.

Loading the whole span of the global model with one vehicle per simulation gave no relevant fatigue damage. The stress ranges from the global model, after loading the whole bridge with single vehicle at a time, are too small to induce any fatigue damage. Calculating the fatigue life using the trilinear S-N curve with cutoff-limit would give infinite fatigue life of the welded detail.

Fatigue life evaluation methods based on S-N curves recommended by different national specifications often result in diverse fatigue lives[68]. In this thesis we compare the National specifications for fatigue loading with those specified in Eurocode. Yu et al. 2022[68], studied fatigue on an OSD when exposed to real traffic by studying the data and a finite element analysis of the bridge. They found the fatigue life of the deck plate stiffener welded joint had significant variability ranging between $2 - 12$ years depending on different national specifications. Eurocode 3 evaluation criteria gave one of the shortest fatigue life predictions (ca. 3 years) for weldment at the plate deck of the OSD. Visible fatigue cracks are found on the rib-to-deck welded joint of existing bridges after a service life of 2 years[69], 7 years[70], 9 years, and 10 years. Other studies report similar findings to that found in this thesis, with shorter fatigue life the welded rib-to-deck joint when using the Eurocode's fatigue loading recommendations compared to other national specifications[68].

9. Conclusion

This thesis estimates the fatigue life of the rib-to-deck welded joint of OSD of Hardanger Bridges, solely due to traffic loading of the finite element model of a box girder of the bridge.

1. The Hot Spot stress approach was applied on a healthy bridge to estimate the fatigue life under normal service spectrum traffic load frequency and distribution. Compared two different sets of reference points for extrapolation of the Hot Spot and found the reference points on the stiffener wall gave shorter fatigue life than reference points at the deck plate.

2. The fatigue life of the rib-to-deck welded joint based on the Hot Spot stress approach was 135 years when loaded with the national FLM-N. The fatigue life was shortened to 24 years when loaded with Eurocode's FLM 4. The nominal stress-based calculation prolonged the fatigue life to 1187 years.

3. Comparing the velocity of the vehicle in relation to fatigue life found no significant difference in fatigue life.

4. The stress responses from the global model when loaded with a single vehicle per simulation were too small to induce and fatigue damage on the detail.

Recommendations for future work

Verifying the finite element model will improve the reliability of the fatigue life determined from simulation on the box girder. This is done by calibrating the results of simulation to the experimental study results and/or real-life data.

Sub-modeling and combination formulas may help in combining results from the global and local models.

Fatigue assessment of the detail from global model may better approximate the fatigue damage from the local model, if the global model is loaded by multiple vehicles per simulation, loading both lanes simultaneously, and additionally considering wind load may result in fatigue life that is more realistic. This is excepted to significantly reduce the fatigue life of the weldment.

This thesis relies heavily on semi-manual post-processing work for fatigue analysis. Abaqus works well with FE-SAFE fatigue analysis software. It reduces the post-processing work: where the simulation output file is directly inputted into the FE-SAFE and fatigue life easily calculated in on a single software. In addition, the outputted fatigue analysis may be plotted on the model on Abaqus, and the stress concentration and fatigue damage may visually be assessed, and new fatigue relevant Hot Spots detected (Machine Learning).

10. Bibliography

1. Radaj D, Sonsino CM, Fricke W. *Fatigue assessment of welded joints by local approaches*. Woodhead publishing; 2006.
2. Wikipedia.org. https://en.wikipedia.org/wiki/List_of_longest_suspension_bridge_spans. Accessed 11.06.22.
3. RoadTraffic-Technology. Hardnager Suspension Bridge. 2013; https://www.roadtraffic-technology.com/projects/hardangerbridge/. Accessed 02.june 2022, 2022.
4. Andersen RC, Aunemo ER. *Traffic induced vibrations of cable-supported bridges*, NTNU; 2016.
5. Wifstad K, Haugland LM, Aalen P, et al. Evaluering av Rv. 13 Hardangerbrua. 2018.
6. Vegvesen S. Hardangerbrua, teknisk brosjyre. In: Hentet fra http://www. vegvesen. no/_attachment/113344; 2011.
7. Li J, Zhang Q, Bao Y, Zhu J, Chen L, Bu Y. An equivalent structural stress-based fatigue evaluation framework for rib-to-deck welded joints in orthotropic steel deck. *Engineering Structures*. 2019;196:109304.
8. Chen L, Li S, Chen H, Saylor DM, Tong S. Study on the design method of equal strength rim based on stress and fatigue analysis using finite element method. *Advances in Mechanical Engineering*. 2017;9(3):1687814017692698.
9. Statens vegvesen V. Bruprosjektering: Eurokodeutgave: veiledning [Håndbok 185]. In:2011.
10. -1-9 E. Eurocode 3: Design of steel structures-Part 1-9: Fatigue. *European Committee for Standardization: Brussels, Belgium*. 2005.
11. Kainuma S, Yang M, Jeong Y-S, Inokuchi S, Kawabata A, Uchida D. Experiment on fatigue behavior of rib-to-deck weld root in orthotropic steel decks. *Journal of Constructional Steel Research*. 2016;119:113-122.
12. Hobbacher AF. *Recommendations for Fatigue Design of Welded Joints and Components*. Springer Cham; 2016.
13. Al-Emrani M, Aygül M. Fatigue design of steel and composite bridges. *Göteborg: Chalmers Reproservice*. 2014.
14. Zamiri Akhlaghi F. Fatigue life assessment of welded bridge details using structural hot spot stress method. 2009.
15. Mashayekhi M, Santini-Bell E. Fatigue assessment of a complex welded steel bridge connection utilizing a three-dimensional multi-scale finite element model and hotspot stress method. *Engineering Structures*. 2020;214:110624.
16. Croce P. Impact of road traffic tendency in europe on fatigue assessment of bridges. *Applied Sciences*. 2020;10(4):1389.
17. Qiang B, Wang X. Determination of the Welding Residual Stresses in Welded Joints and Their Effects on SIFs for Surface Cracks: A Review of Recent Progress. Paper presented at: International Conference on Offshore Mechanics and Arctic Engineering2021.
18. Alencar G, de Jesus A, da Silva JGS, Calcada R. Fatigue cracking of welded railway bridges: A review. *Engineering Failure Analysis*. 2019;104:154-176.
19. Heshmati M. *Fatigue life assessment of bridge details using finite element method* 2012.
20. Schütz W. A history of fatigue. *Engineering Fracture Mechanics*. 1996;54(2):263-300.
21. Schijve J. Fatigue of structures and materials. Editorial Kluwer. In: Academic Publishers Dordrecht; 2004.
22. Fuštar B, Lukačević I, Dujmović D. Review of fatigue assessment methods for welded steel structures. *Advances in Civil Engineering*. 2018;2018.
23. Weck R. Failure of steel structures: causes and remedies. *Proceedings of the Royal Society of London Series A Mathematical and Physical Sciences*. 1965;285(1400):3-9.
24. Alpsten G. Causes of structural failures with steel structures. Paper presented at: IABSE Symposium Report2017.

25. Mohtadi-Bonab MA. Effects of Different Parameters on Initiation and Propagation of Stress Corrosion Cracks in Pipeline Steels: A Review. *Metals.* 2019;9(5).

26. Wang B, Nagy W, De Backer H, Chen A. Fatigue process of rib-to-deck welded joints of orthotropic steel decks. *Theoretical and Applied Fracture Mechanics.* 2019;101:113-126.

27. Langeland JH. *Finite Element Analysis of the fatigue strength of a big-end bolt*, The University of Bergen; 2017.

28. Wang D, Xiang C, Ma Y, Chen A, Wang B. Experimental study on the root-deck fatigue crack on orthotropic steel decks. *Materials & Design.* 2021;203:109601.

29. Radaj D, Sonsino CM, Fricke W. Recent developments in local concepts of fatigue assessment of welded joints. *International Journal of Fatigue.* 2009;31(1):2-11.

30. Ji B, Liu R, Chen C, Maeno H, Chen X. Evaluation on root-deck fatigue of orthotropic steel bridge deck. *Journal of Constructional Steel Research.* 2013;90:174-183.

31. Yan F, Chen W, Lin Z. Prediction of fatigue life of welded details in cable-stayed orthotropic steel deck bridges. *Engineering Structures.* 2016;127:344-358.

32. Zhang Q, Bu Y, Li Q. Review on fatigue problems of orthotropic steel bridge deck. *China Journal of Highway and Transport.* 2017;30(3):14-30.

33. Wu W, Kolstein H, Veljković M, Pijpers R, Vorstenbosch-Krabbe J. 09.04: Fatigue behaviour of the closed rib to deck and crossbeam joint in a newly designed orthotropic bridge deck. *ce/papers.* 2017;1(2-3):2378-2387.

34. Villoria B, Siriwardane SC, Lemu HG. Review on fatigue life assessment methods for welded joints in orthotropic steel decks of long-span bridges. *IOP Conference Series: Materials Science and Engineering.* 2021;1201(1):012036.

35. Munse WH, Wilbur TW, Tellalian ML, Nicoll K, Wilson K. *Fatigue characterization of fabricated ship details for design.* Illinois Univ at Urbana Dept of Civil Engineering;1982.

36. Fricke W. Recommended hot-spot analysis procedure for structural details of ships and FPSOs based on round-robin FE analyses. *International Journal of Offshore and Polar Engineering.* 2002;12(01).

37. Niemi E. Structural Hot-Spot Stress Approach to Fatigue Analysis of Welded Components : Designer's Guide. In: Fricke W, Maddox SJ, eds. 2nd 2018. ed. Singapore: Springer Singapore : Imprint: Springer; 2018.

38. Martinsson J. *Fatigue assessment of complex welded steel structures*, KTH; 2005.

39. Wolchuk R. Lessons from weld cracks in orthotropic decks on three European bridges. *Journal of Structural Engineering.* 1990;116(1):75-84.

40. Tsakopoulos PA, Fisher JW. Full-scale fatigue tests of steel orthotropic decks for the Williamsburg Bridge. *Journal of Bridge Engineering.* 2003;8(5):323-333.

41. Caccese V, Blomquist PA, Berube KA, Webber SR, Orozco NJ. Effect of weld geometric profile on fatigue life of cruciform welds made by laser/GMAW processes. *Marine Structures.* 2006;19(1):1-22.

42. Qiang B, Li Y, Yao C, Wang X. Through-thickness welding residual stress and its effect on stress intensity factors for semi-elliptical surface cracks in a butt-welded steel plate. *Engineering Fracture Mechanics.* 2018;193:17-31.

43. Wang F, Lyu Z-d, Zhao Z, Chen Q-k, Mei H-L. Experimental and numerical study on welding residual stress of U-rib stiffened plates. *Journal of Constructional Steel Research.* 2020;175:106362.

44. Dowling N. Mechanical Behaviour of Materials. ed Pearson Prentice Hall. *Upper Saddle River, NJ, USA.* 2007.

45. Callister WD, Rethwisch DG. *Materials science and engineering: an introduction.* Vol 9: Wiley New York; 2018.

46. Leitner M, Stoschka M. Effect of load stress ratio on nominal and effective notch fatigue strength assessment of HFMI-treated high-strength steel cover plates. *International Journal of Fatigue.* 2020;139:105784.

47.   Lee J-M, Seo J-K, Kim M-H, et al. Comparison of hot spot stress evaluation methods for welded structures. *International Journal of Naval Architecture and Ocean Engineering.* 2010;2(4):200-210.

48.   Wermundsen T. *Efficient evaluation of fatigue and damage in welded joints from finite element analysis*, NTNU; 2014.

49.   DNV G. Class guideline DNVGL-CG-0129:"fatigue assessment of ship structures". *DNV GL, Oslo.* 2015.

50.   Fuchs HO. Metal fatigue in engineering. *Wiley.* 1980.

51.   Dowling NE. *Fatigue failure predictions for complicated stress strain histories.* Department of Theoretical and Applied Mechanics. College of Engineering …;1971. 0073-5264.

52.   Suresh S. *Fatigue of materials.* Cambridge university press; 1998.

53.   Sheridan C. *The Python language reference manual.* Lulu Press, Inc; 2016.

54.   Standard A. E1049-85. *Standard Practices for Cycle Counting in Fatigue Analysis, ASTM.* 2011;339.

55.   Miner MA. Cumulative damage in fatigue. 1945.

56.   ABAQUS. *ABAQUS FEM CAE solving engine.* 2020.

57.   Ekern E, Bang D. *Aerodynamic Stability of a Suspension Bridge with an Aluminum Girder-Wind Tunnel Testing and Numerical Predictions*, NTNU; 2020.

58.   Yokozeki K, Tominaga T, Miki C. The effects of rib shape and slit on fatigue properties of orthotropic steel decks. *Welding in the World.* 2021;65(4):601-609.

59.   Norge S. NS-EN 1991-2: 2003+ NA: 2010: Eurokode 1: Laster på konstruksjoner, Del 2: Trafikklast på bruer. *Brussel: CEN.* 2003.

60.   Standard B. Eurocode 1: Actions on structures—. In:2006.

61.   FESAFE. Fatigue Theory Reference2019.

62.   -2 E. Eurocode 1: Actions on structures–Part 2: Traffic loads on bridges. In:2003.

63.   Croce P. Background to fatigue load models for Eurocode 1: Part 2 Traffic Loads. *Progress in Structural Engineering and Materials.* 2001;3:335-345.

64.   Szabó B, Babuška I. Finite Element Analysis: Method, Verification and Validation. 2021.

65.   Cui C, Xu Y-L, Zhang Q-H. Multiscale fatigue damage evolution in orthotropic steel deck of cable-stayed bridges. *Engineering Structures.* 2021;237:112144.

66.   Wang C, Duan L, Zhai M, Zhang Y, Wang S. Steel bridge long-term performance research technology framework and research progress. *Advances in Structural Engineering.* 2017;20(1):51-68.

67.   Ye X, Su Y, Han J. A state-of-the-art review on fatigue life assessment of steel bridges. *Mathematical Problems in Engineering.* 2014;2014.

68.   Yu S, Li D, Ou J. Digital twin-based structure health hybrid monitoring and fatigue evaluation of orthotropic steel deck in cable-stayed bridge. *Structural Control and Health Monitoring.* 2022:e2976.

69.   Fisher JW, Barsom JM. Evaluation of cracking in the rib-to-deck welds of the Bronx–Whitestone Bridge. *Journal of Bridge Engineering.* 2016;21(3):04015065.

70.   De Jong F. Overview fatigue phenomenon in orthotropic bridge decks in the Netherlands. Paper presented at: Orthotropic Bridge Conference2004.

11. Appendices

A. Creating model

A.1. Design drawings

Figure 40 Appendix: Design drawings of the box girder. (B) The 12 mm thick deck plate. (C) The U-rib under the upper deck. (D) The rib-to-deck welded joint.
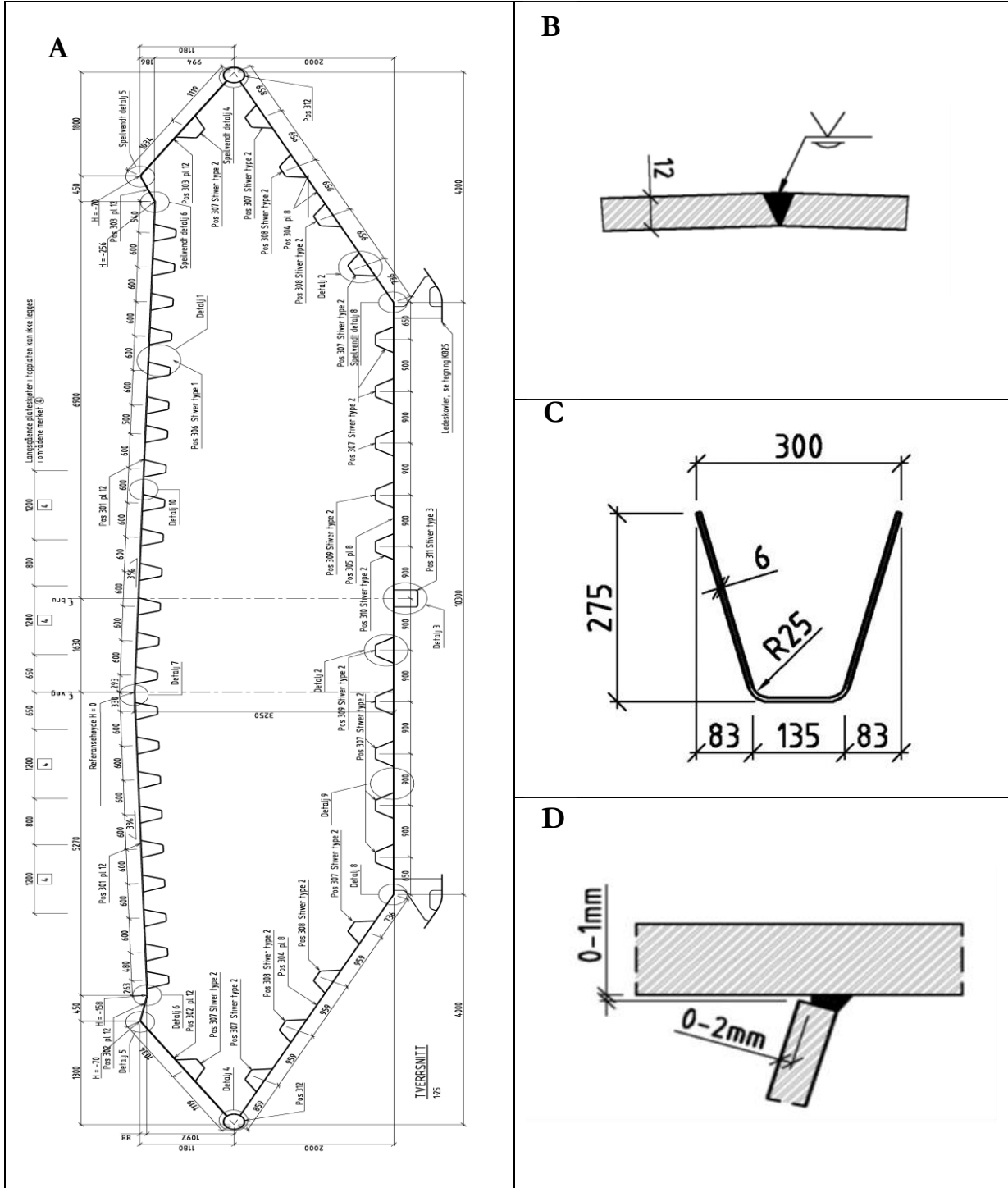
A.2.   The FEM of ribs and deck

U-ribs and upper deck.
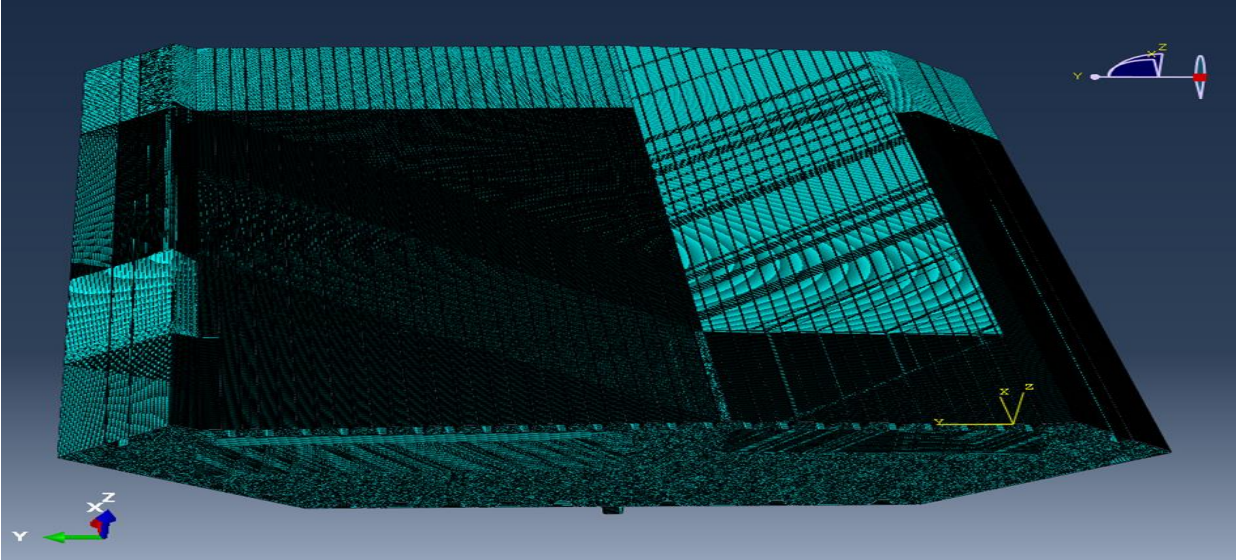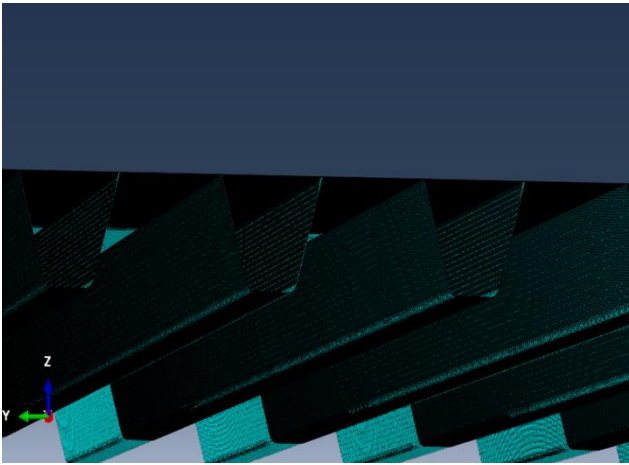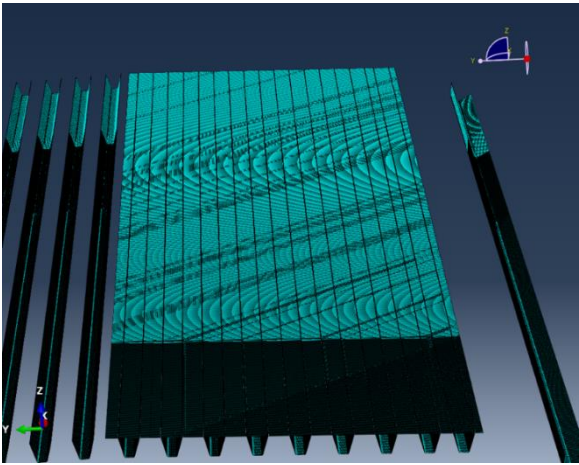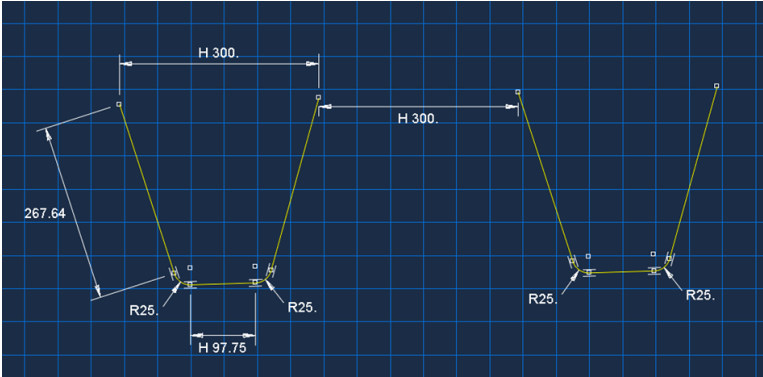
Figure 41 The spacing between the ribs is 300 mm. The rib to deck assemblage is demonstrated. The potential for analysis of the box-girder with very fine mesh is illustrated.

A.3. Partitioning and Meshing

Complex geometry requires special care for partitioning, to achieve linear S4R meshing. Datum planes are used to parallel partition several diaphragms using the same plane.
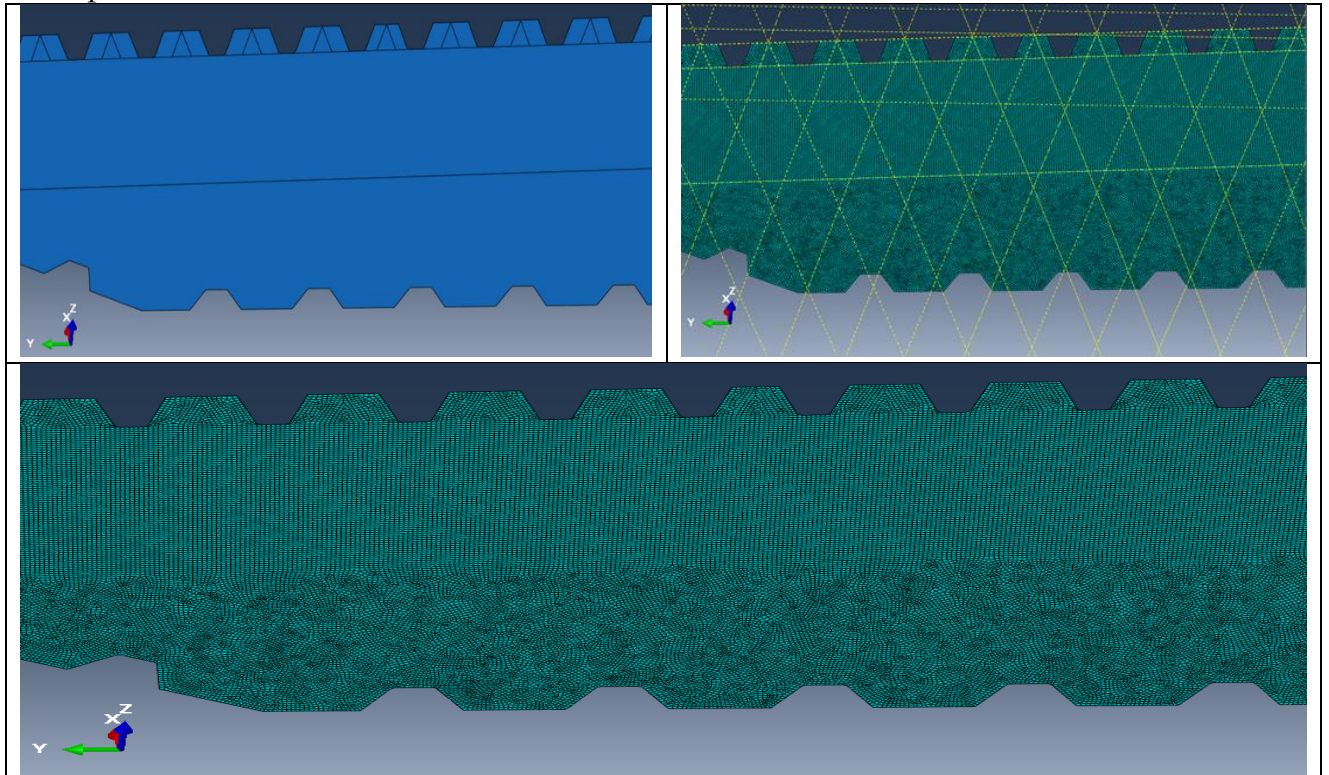
A.4. Boundary conditions

Tie connections
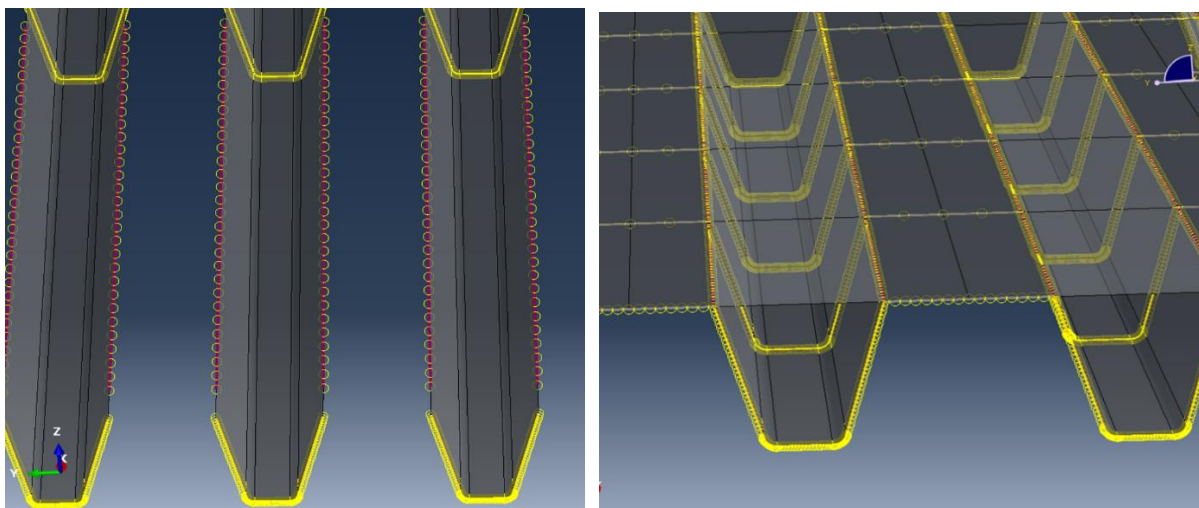
Suspension
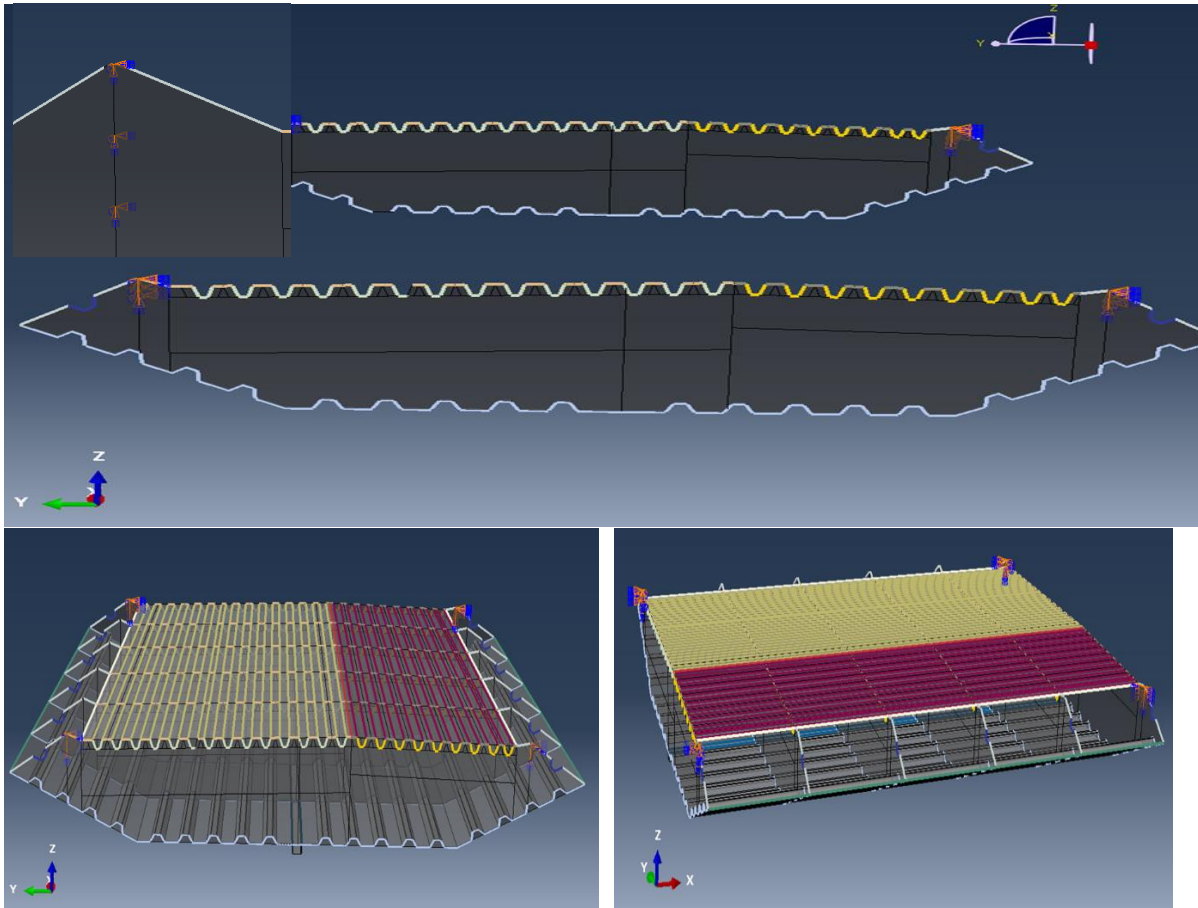
A.5. Location of Hot Spot in relation to wheel load
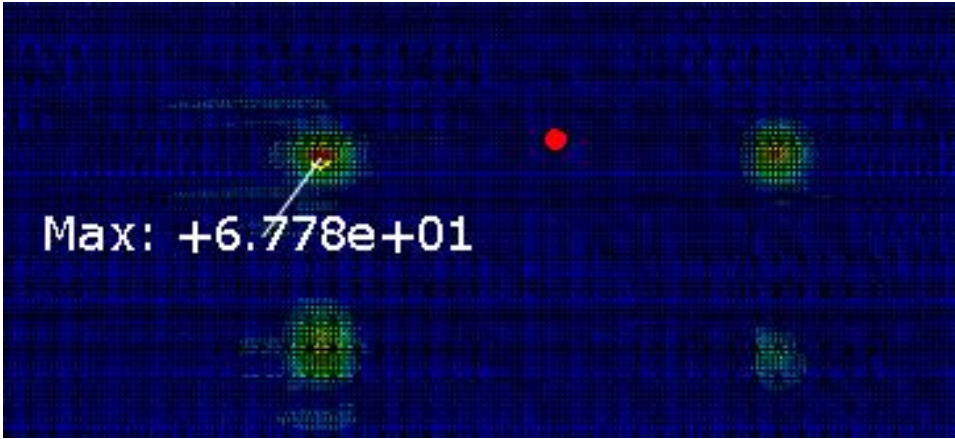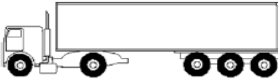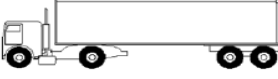
Figure 42 Hot Spot (red node) is located at midspan of the box girder and under the wheel loading surface.

B. Loading mechanism (Fortran Codes)

B.1. Dimensions of the fatigue load models

Dimensions of FLM 4

Vehicle type				Traffic type		
				Lorry percentage		
Lorry	Axle spacing [m]	Equivalent axle loads [kN]	Wheel type*	Long distance	Medium distance	Local traffic
(truck image)	4,5	70	A	20,0	40,0	20,0
		130	B			
(truck image)	4,20	70	A	5,0	10,0	5,0
	1,30	120	B			
		120	B			
(truck image)	3,20	70	A	50,0	30,0	5,0
	5,20	150	B			
	1,30	90	C			
	1,30	90	C			
		90	C			
(truck image)	3,40	70	A	15,0	15,0	5,0
	6,00	140	B			
	1,80	90	B			
		90	B			
(truck image)	4,80	70	A	10,0	5,0	5,0
	3,60	130	B			
	4,40	90	C			
	1,30	80	C			
		80	C			

Figure 43 Appendix: Dimension of fatigue load models [62].

Dimensions of FLM-N

Figur 5: Lasttype V1

F	BREDDE AV FORTAU
S	BREDDE AV SKULDER
K	BREDDE AV KJØREBANE
M	BREDDE AV MIDTDELER
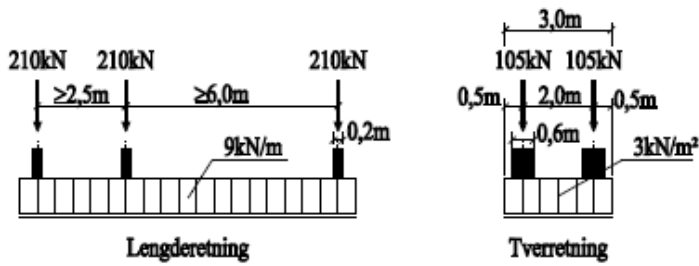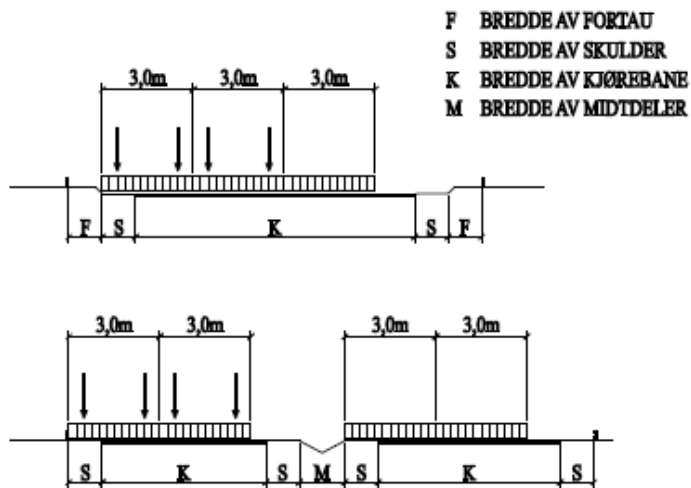
Figur 6: Eksempler på plassering av lasttype V1

B.2. Eccentricity

Lorry 5 was run on the lane with different eccentricities axle centerline from the bridge centerline. Eccentricity that gave the strongest stress concentration at Hot Spot was found after testing 7 different offsets. A closer look at the wheel center point will show small shifts in transversal location between images. Each image is a single frame from the seven different simulations.
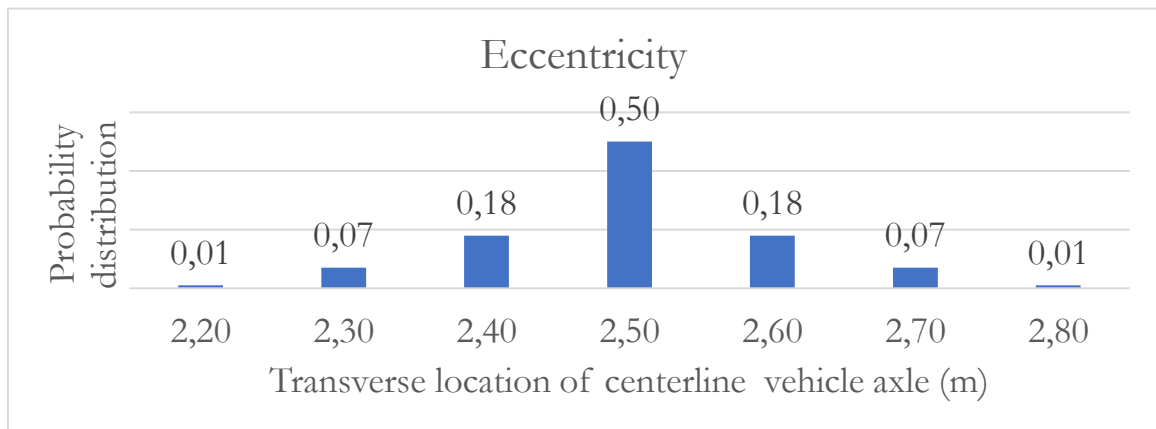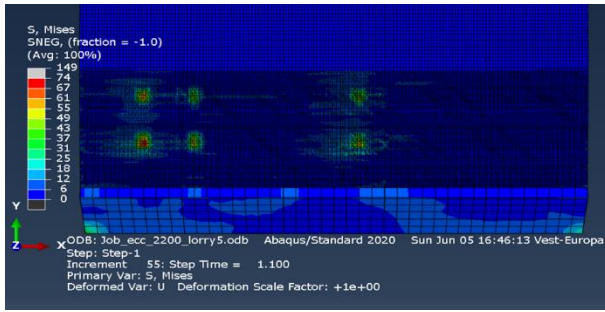
2.20 m
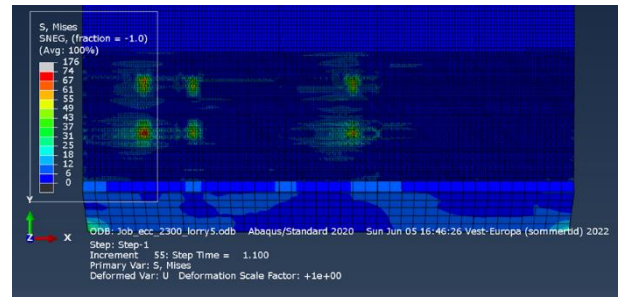
2.30 m
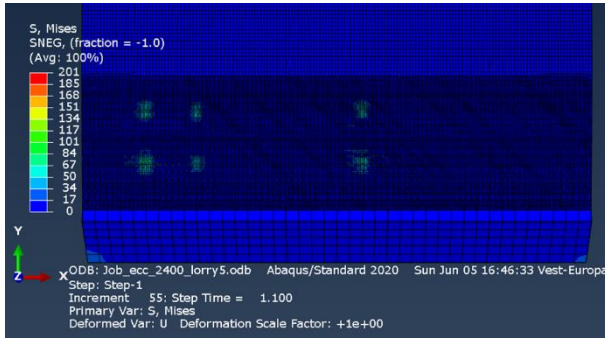
2.40 m
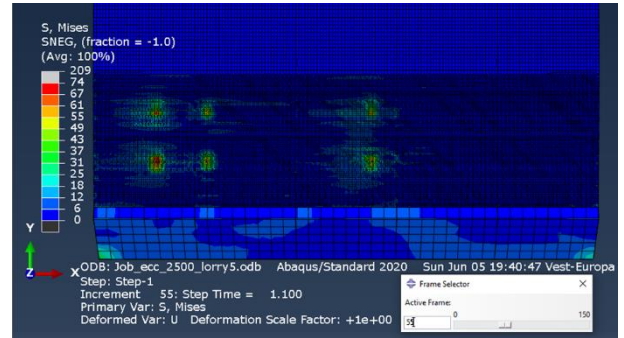
2.50 m
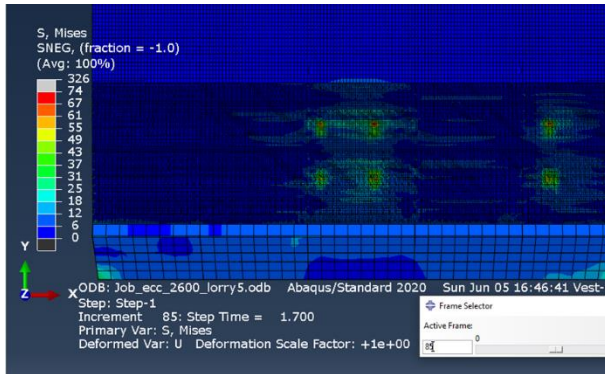
2.60 m
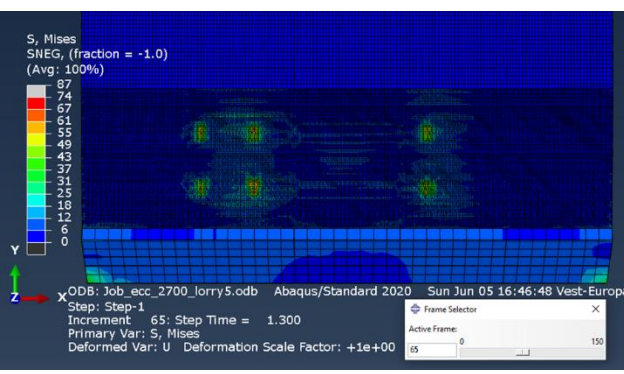
2.70 m
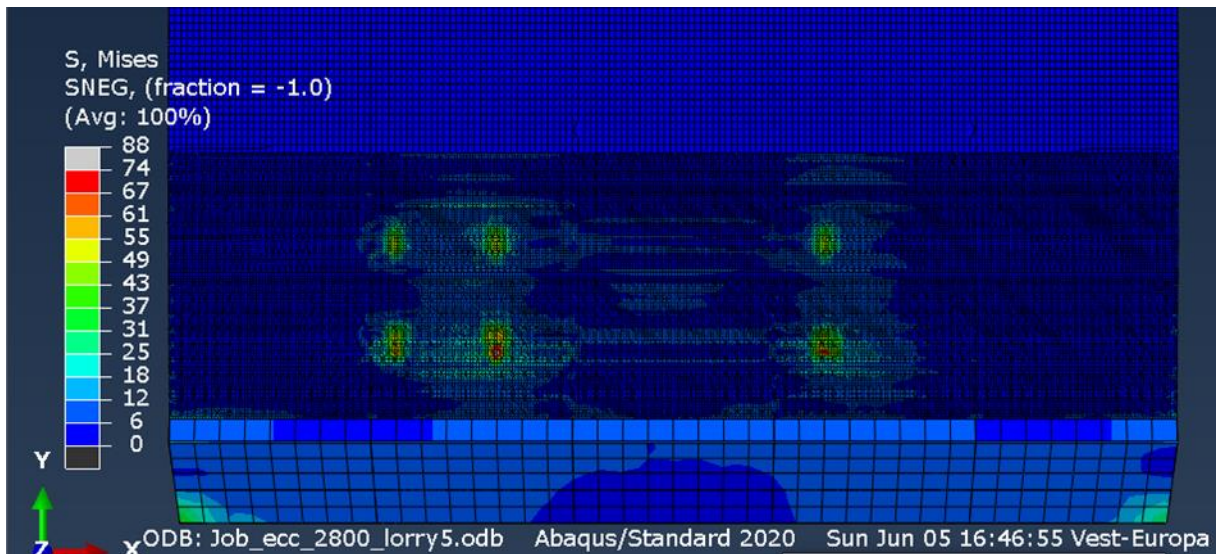
2.80 m

Figure 44 Appendix. Determining the eccentricity that gave the maximal damage.

B.3. Loading FLM-N

Lorry 1

```fortran
      subroutine DLOAD(F,KSTEP,KINC,TIME,NOEL,NPT,LAYER,KSPT,
     &                 COORDS,JLTYP,SNAME)

      include 'ABA_PARAM.INC'
      dimension TIME(2), COORDS (3)
      CHARACTER*80 SNAME
      X=COORDS(1)
      Y=COORDS(2)
      Z=COORDS(3)

         !variable definitionc
      Velocity = 10000
         ecc=2179 !4679 is the distance from local orgin to centerline
 (4679-2500=2179)
         Y_ax=2000
         X_ax1=6500 !distance between axle1 and axle2
         X_ax2=2000 !distance between axle2 and axle3

      !longitudinal position
      X_position = Velocity * TIME(1)

         !1st axle
      if (X.le.(X_position+100).and.X.ge.(X_position-
 100).and.Y.le.(ecc+300+Y_ax/2).and.Y.ge.(ecc-300+Y_ax/2)) then
         F=0.25
            elseif (X.le.(X_position+100).and.X.ge.(X_position-
 100).and.Y.le.(ecc+300-Y_ax/2).and.Y.ge.(ecc-300-Y_ax/2)) then
         F=0.25

      !2nd axle
      elseif (X.le.(X_position-6500+100).and.X.ge.(X_position-6500-
 100).and.Y.le.(ecc+300+Y_ax/2).and.Y.ge.(ecc-300+Y_ax/2)) then
         F=0.25
            elseif (X.le.(X_position-6500+100).and.X.ge.(X_position-6500-
 100).and.Y.le.(ecc+300-Y_ax/2).and.Y.ge.(ecc-300-Y_ax/2)) then
         F=0.25

      !3rd axle
      elseif (X.le.(X_position-8500+100).and.X.ge.(X_position-8500-
 100).and.Y.le.(ecc+300+Y_ax/2).and.Y.ge.(ecc-300+Y_ax/2)) then
         F=0.25
            elseif (X.le.(X_position-8500+100).and.X.ge.(X_position-8500-
 100).and.Y.le.(ecc+300-Y_ax/2).and.Y.ge.(ecc-300-Y_ax/2)) then
         F=0.25
      else
         F=0.0
      endif
      RETURN
      END
```

Lorry 2

```fortran
      subroutine DLOAD(F,KSTEP,KINC,TIME,NOEL,NPT,LAYER,KSPT,
     &                  COORDS,JLTYP,SNAME)

      include 'ABA_PARAM.INC'

      dimension TIME(2), COORDS (3)
      CHARACTER*80 SNAME

      X=COORDS(1)
      Y=COORDS(2)
      Z=COORDS(3)

         !variable definitionc
      Velocity = 10000
         ecc=2179 !4679 is the distance from local orgin to centerline (4679-
2500=2179)
         Y_ax=2000
         X_ax1=6500 !distance between axle1 and axle2
         X_ax2=2000 !distance between axle1 and axle2

      !longitudinal position
      X_position = Velocity * TIME(1)

         !1st axle
      if (X.le.(X_position+100).and.X.ge.(X_position-
100).and.Y.le.(ecc+300+Y_ax/2).and.Y.ge.(ecc-300+Y_ax/2)) then
         F=0.33
         elseif (X.le.(X_position+100).and.X.ge.(X_position-
100).and.Y.le.(ecc+300-Y_ax/2).and.Y.ge.(ecc-300-Y_ax/2)) then
         F=0.33

      !2nd axle
      elseif (X.le.(X_position-6500+100).and.X.ge.(X_position-6500-
100).and.Y.le.(ecc+300+Y_ax/2).and.Y.ge.(ecc-300+Y_ax/2)) then
         F=0.33
         elseif (X.le.(X_position-6500+100).and.X.ge.(X_position-6500-
100).and.Y.le.(ecc+300-Y_ax/2).and.Y.ge.(ecc-300-Y_ax/2)) then
         F=0.33

      !3rd axle
      elseif (X.le.(X_position-8500+100).and.X.ge.(X_position-8500-
100).and.Y.le.(ecc+300+Y_ax/2).and.Y.ge.(ecc-300+Y_ax/2)) then
         F=0.33
         elseif (X.le.(X_position-8500+100).and.X.ge.(X_position-8500-
100).and.Y.le.(ecc+300-Y_ax/2).and.Y.ge.(ecc-300-Y_ax/2)) then
         F=0.33
      else
         F=0.0
      endif
      RETURN
      END
```

Lorry 3

```fortran
      subroutine DLOAD(F,KSTEP,KINC,TIME,NOEL,NPT,LAYER,KSPT,
     &              COORDS,JLTYP,SNAME)

      include 'ABA_PARAM.INC'

      dimension TIME(2), COORDS (3)
      CHARACTER*80 SNAME

      X=COORDS(1)
      Y=COORDS(2)
      Z=COORDS(3)

          !variable definitionc
      Velocity = 10000
          ecc=2179 !4679 is the distance from local orgin to centerline (4679-
2500=2179)
          Y_ax=2000
          X_ax1=6500 !distance between axle1 and axle2
          X_ax2=2000 !distance between axle1 and axle2

      !longitudinal position
      X_position = Velocity * TIME(1)

          !1st axle
      if (X.le.(X_position+100).and.X.ge.(X_position-
100).and.Y.le.(ecc+300+Y_ax/2).and.Y.ge.(ecc-300+Y_ax/2)) then
         F=0.417
           elseif (X.le.(X_position+100).and.X.ge.(X_position-
100).and.Y.le.(ecc+300-Y_ax/2).and.Y.ge.(ecc-300-Y_ax/2)) then
         F=0.417

      !2nd axle
      elseif (X.le.(X_position-6500+100).and.X.ge.(X_position-6500-
100).and.Y.le.(ecc+300+Y_ax/2).and.Y.ge.(ecc-300+Y_ax/2)) then
         F=0.417
           elseif (X.le.(X_position-6500+100).and.X.ge.(X_position-6500-
100).and.Y.le.(ecc+300-Y_ax/2).and.Y.ge.(ecc-300-Y_ax/2)) then
         F=0.417

      !3rd axle
      elseif (X.le.(X_position-8500+100).and.X.ge.(X_position-8500-
100).and.Y.le.(ecc+300+Y_ax/2).and.Y.ge.(ecc-300+Y_ax/2)) then
         F=0.417
           elseif (X.le.(X_position-8500+100).and.X.ge.(X_position-8500-
100).and.Y.le.(ecc+300-Y_ax/2).and.Y.ge.(ecc-300-Y_ax/2)) then
         F=0.417
      else
         F=0.0
      endif
      RETURN
      END
```

Lorry 4

```fortran
      subroutine DLOAD(F,KSTEP,KINC,TIME,NOEL,NPT,LAYER,KSPT,
     &                 COORDS,JLTYP,SNAME)

      include 'ABA_PARAM.INC'

      dimension TIME(2), COORDS (3)
      CHARACTER*80 SNAME

      X=COORDS(1)
      Y=COORDS(2)
      Z=COORDS(3)

         !variable definitionc
      Velocity = 10000
         ecc=2179 !4679 is the distance from local orgin to centerline (4679-
2500=2179)
         Y_ax=2000
         X_ax1=6500 !distance between axle1 and axle2
         X_ax2=2000 !distance between axle1 and axle2

      !longitudinal position
      X_position = Velocity * TIME(1)

         !1st axle
      if (X.le.(X_position+100).and.X.ge.(X_position-
100).and.Y.le.(ecc+300+Y_ax/2).and.Y.ge.(ecc-300+Y_ax/2)) then
         F=0.5208
           elseif (X.le.(X_position+100).and.X.ge.(X_position-
100).and.Y.le.(ecc+300-Y_ax/2).and.Y.ge.(ecc-300-Y_ax/2)) then
         F=0.5208

      !2nd axle
      elseif (X.le.(X_position-6500+100).and.X.ge.(X_position-6500-
100).and.Y.le.(ecc+300+Y_ax/2).and.Y.ge.(ecc-300+Y_ax/2)) then
         F=0.5208
           elseif (X.le.(X_position-6500+100).and.X.ge.(X_position-6500-
100).and.Y.le.(ecc+300-Y_ax/2).and.Y.ge.(ecc-300-Y_ax/2)) then
         F=0.5208

      !3rd axle
      elseif (X.le.(X_position-8500+100).and.X.ge.(X_position-8500-
100).and.Y.le.(ecc+300+Y_ax/2).and.Y.ge.(ecc-300+Y_ax/2)) then
         F=0.5208
           elseif (X.le.(X_position-8500+100).and.X.ge.(X_position-8500-
100).and.Y.le.(ecc+300-Y_ax/2).and.Y.ge.(ecc-300-Y_ax/2)) then
         F=0.5208
      else
         F=0.0
      endif
      RETURN
      END
```

Lorry 5

```fortran
      subroutine DLOAD(F,KSTEP,KINC,TIME,NOEL,NPT,LAYER,KSPT,
     &                 COORDS,JLTYP,SNAME)

      include 'ABA_PARAM.INC'

      dimension TIME(2), COORDS (3)
      CHARACTER*80 SNAME

      X=COORDS(1)
      Y=COORDS(2)
      Z=COORDS(3)

         !variable definitionc
      Velocity = 10000
         ecc=2179 !4679 is the distance from local orgin to centerline (4679-
2500=2179)
         Y_ax=2000
         X_ax1=6500 !distance between axle1 and axle2
         X_ax2=2000 !distance between axle1 and axle2

      !longitudinal position
      X_position = Velocity * TIME(1)

         !1st axle
      if (X.le.(X_position+100).and.X.ge.(X_position-
100).and.Y.le.(ecc+300+Y_ax/2).and.Y.ge.(ecc-300+Y_ax/2)) then
         F=0.6042
         elseif (X.le.(X_position+100).and.X.ge.(X_position-
100).and.Y.le.(ecc+300-Y_ax/2).and.Y.ge.(ecc-300-Y_ax/2)) then
         F=0.6042

      !2nd axle
      elseif (X.le.(X_position-6500+100).and.X.ge.(X_position-6500-
100).and.Y.le.(ecc+300+Y_ax/2).and.Y.ge.(ecc-300+Y_ax/2)) then
         F=0.6042
         elseif (X.le.(X_position-6500+100).and.X.ge.(X_position-6500-
100).and.Y.le.(ecc+300-Y_ax/2).and.Y.ge.(ecc-300-Y_ax/2)) then
         F=0.6042

      !3rd axle
      elseif (X.le.(X_position-8500+100).and.X.ge.(X_position-8500-
100).and.Y.le.(ecc+300+Y_ax/2).and.Y.ge.(ecc-300+Y_ax/2)) then
         F=0.6042
         elseif (X.le.(X_position-8500+100).and.X.ge.(X_position-8500-
100).and.Y.le.(ecc+300-Y_ax/2).and.Y.ge.(ecc-300-Y_ax/2)) then
         F=0.6042
      else
         F=0.0
      endif
      RETURN
      END
```
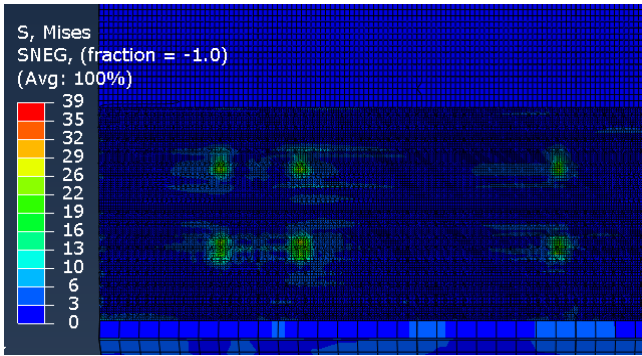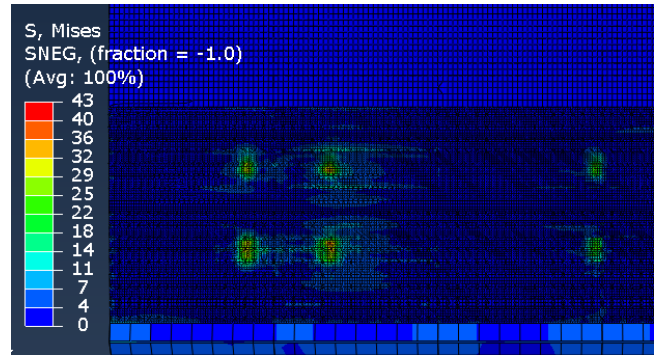
Lorry 1
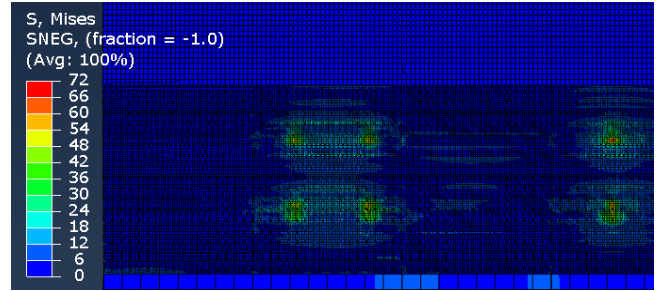
Lorry 2
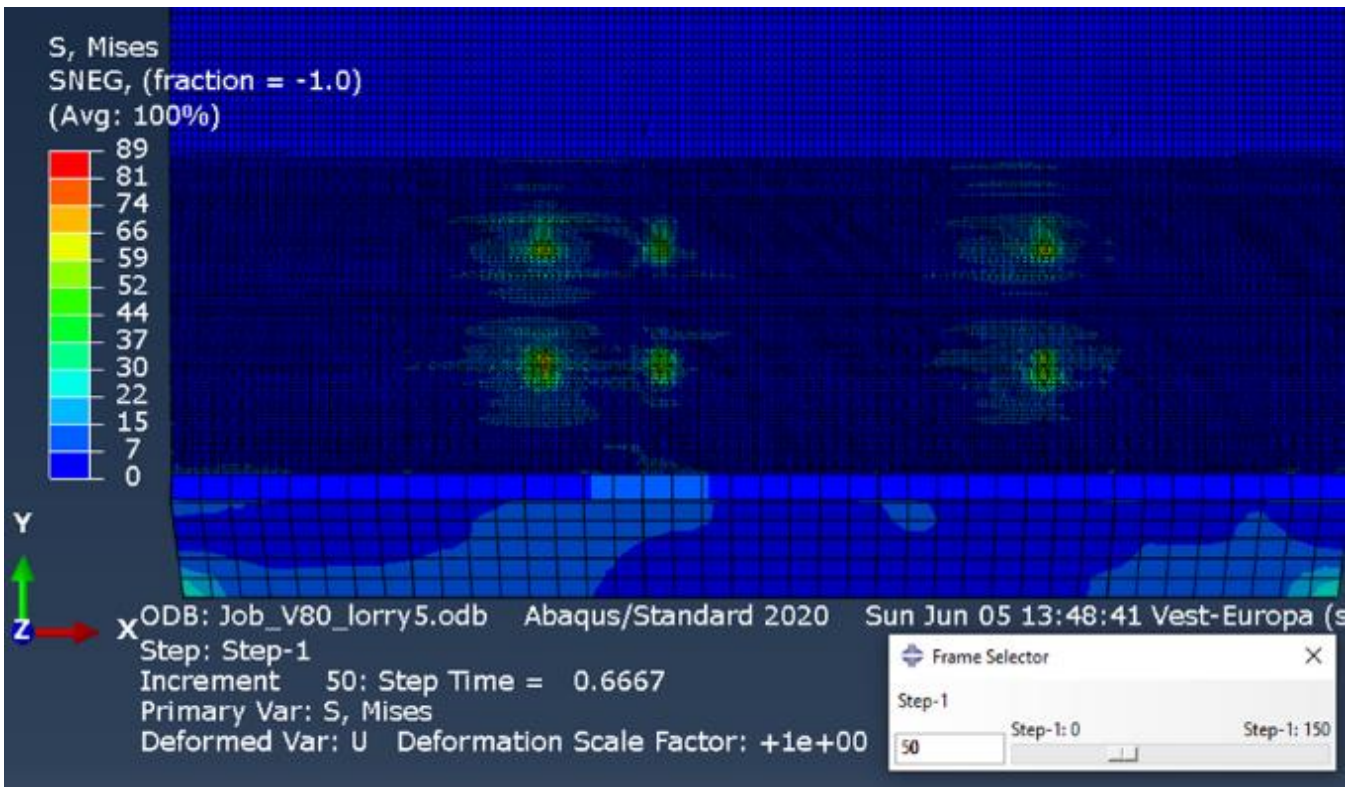
Lorry 3

Lorry 4

Lorry 5

Figure 45 von Mises wheel stress distribution of the five lorries in FLM-N.

B.4. Loading FLM 4

Lorry 1

```fortran
      subroutine DLOAD(F,KSTEP,KINC,TIME,NOEL,NPT,LAYER,KSPT,
     &                 COORDS,JLTYP,SNAME)

      include 'ABA_PARAM.INC'

      dimension TIME(2), COORDS (3)
      CHARACTER*80 SNAME

      X=COORDS(1)
      Y=COORDS(2)
      Z=COORDS(3)

          !variable definitionc
      Velocity = 10000
          ecc=2179 !4679 is the distance from local orgin to centerline
(4679-2500=2179)
          Y_ax=2000
          X_ax1=4500 !distance between axle1 and axle2

      !longitudinal position
      X_position = Velocity * TIME(1)

          !1st axle (Axle type 1A)
      if (X.le.(X_position+160).and.X.ge.(X_position-
160).and.Y.le.(ecc+110+Y_ax/2).and.Y.ge.(ecc-110+Y_ax/2)) then
        F=0.5
          elseif (X.le.(X_position+160).and.X.ge.(X_position-
160).and.Y.le.(ecc+110-Y_ax/2).and.Y.ge.(ecc-110-Y_ax/2)) then
        F=0.5

      !2nd axle (Axle type 1B)
      elseif (X.le.(X_position-4500+160).and.X.ge.(X_position-4500-
160).and.Y.le.(ecc+220+Y_ax/2).and.Y.ge.(ecc-220+Y_ax/2)) then
        F=0.46
          elseif (X.le.(X_position-4500+160).and.X.ge.(X_position-4500-
160).and.Y.le.(ecc+220-Y_ax/2).and.Y.ge.(ecc-220-Y_ax/2)) then
        F=0.46
      else
        F=0.0
      endif
      RETURN
      END
```

Lorry 2

```fortran
      subroutine DLOAD(F,KSTEP,KINC,TIME,NOEL,NPT,LAYER,KSPT,
     &                  COORDS,JLTYP,SNAME)

      include 'ABA_PARAM.INC'

      dimension TIME(2), COORDS (3)
      CHARACTER*80 SNAME

      X=COORDS(1)
      Y=COORDS(2)
      Z=COORDS(3)


         !variable definitionc
      Velocity = 10000
         ecc=2179 !4679 is the distance from local orgin to centerline
(4679-2500=2179)
         Y_ax=2000
         X_ax1=4200 !distance between axle1 and axle2
      X_ax2=1300 !distance between axle2 and axle3 (distance )

      !longitudinal position
      X_position = Velocity * TIME(1)

         !1st axle
      if (X.le.(X_position+160).and.X.ge.(X_position-
160).and.Y.le.(ecc+110+Y_ax/2).and.Y.ge.(ecc-110+Y_ax/2)) then
         F=0.994318/2
         elseif (X.le.(X_position+160).and.X.ge.(X_position-
160).and.Y.le.(ecc+110-Y_ax/2).and.Y.ge.(ecc-110-Y_ax/2)) then
         F=0.994318/2

      !2nd axle
      elseif (X.le.(X_position-4200+160).and.X.ge.(X_position-4200-
160).and.Y.le.(ecc+220+Y_ax/2).and.Y.ge.(ecc-220+Y_ax/2)) then
         F=0.923295/2
         elseif (X.le.(X_position-4200+160).and.X.ge.(X_position-4200-
160).and.Y.le.(ecc+220-Y_ax/2).and.Y.ge.(ecc-220-Y_ax/2)) then
         F=0.923295/2

      !3rd axle
      elseif (X.le.(X_position-5500+160).and.X.ge.(X_position-5500-
160).and.Y.le.(ecc+220+Y_ax/2).and.Y.ge.(ecc-220+Y_ax/2)) then
         F=0.923295/2
         elseif (X.le.(X_position-5500+160).and.X.ge.(X_position-5500-
160).and.Y.le.(ecc+220-Y_ax/2).and.Y.ge.(ecc-220-Y_ax/2)) then
         F=0.923295/2
      else
        F=0.0
      endif
      RETURN
      END
```

11-15

Lorry 3

```fortran
      subroutine DLOAD(F,KSTEP,KINC,TIME,NOEL,NPT,LAYER,KSPT,
     &                  COORDS,JLTYP,SNAME)

      include 'ABA_PARAM.INC'

      dimension TIME(2), COORDS (3)
      CHARACTER*80 SNAME

      X=COORDS(1)
      Y=COORDS(2)
      Z=COORDS(3)

         !variable definitionc
      Velocity = 10000
         ecc=2179 !4679 is the distance from local orgin to centerline
(4679-2500=2179)
         Y_ax=2000

      !longitudinal position
      X_position = Velocity * TIME(1)

         !1st axle (Wheel type A)
      if (X.le.(X_position+160).and.X.ge.(X_position-
160).and.Y.le.(ecc+110+Y_ax/2).and.Y.ge.(ecc-110+Y_ax/2)) then
        F=0.49715
         elseif (X.le.(X_position+160).and.X.ge.(X_position-
160).and.Y.le.(ecc+110-Y_ax/2).and.Y.ge.(ecc-110-Y_ax/2)) then
        F=0.49715

      !2nd axle (Wheel type B)
       elseif (X.le.(X_position-3200+160).and.X.ge.(X_position-3200-
160).and.Y.le.(ecc+220+Y_ax/2).and.Y.ge.(ecc-220+Y_ax/2)) then
        F=0.53267
         elseif (X.le.(X_position-3200+160).and.X.ge.(X_position-3200-
160).and.Y.le.(ecc+220-Y_ax/2).and.Y.ge.(ecc-220-Y_ax/2)) then
        F=0.53267

      !3rd axle (Wheel type C)
       elseif (X.le.(X_position-8400+160).and.X.ge.(X_position-8400-
160).and.Y.le.(ecc+220+Y_ax/2).and.Y.ge.(ecc-220+Y_ax/2)) then
        F=0.52083
         elseif (X.le.(X_position-8400+160).and.X.ge.(X_position-8400-
160).and.Y.le.(ecc+220-Y_ax/2).and.Y.ge.(ecc-220-Y_ax/2)) then
        F=0.52083
```

```
      !4th axle (Wheel type C)
      elseif (X.le.(X_position-9700+160).and.X.ge.(X_position-9700-
160).and.Y.le.(ecc+220+Y_ax/2).and.Y.ge.(ecc-220+Y_ax/2)) then
        F=0.52083
          elseif (X.le.(X_position-9700+160).and.X.ge.(X_position-9700-
160).and.Y.le.(ecc+220-Y_ax/2).and.Y.ge.(ecc-220-Y_ax/2)) then
        F=0.52083

      !5th axle (Wheel type C)
      elseif (X.le.(X_position-11000+160).and.X.ge.(X_position-11000-
160).and.Y.le.(ecc+220+Y_ax/2).and.Y.ge.(ecc-220+Y_ax/2)) then
        F=0.52083
          elseif (X.le.(X_position-11000+160).and.X.ge.(X_position-11000-
160).and.Y.le.(ecc+220-Y_ax/2).and.Y.ge.(ecc-220-Y_ax/2)) then
        F=0.52083
      else
        F=0.0
      endif
      RETURN
      END
```

Lorry 4

```fortran
      subroutine DLOAD(F,KSTEP,KINC,TIME,NOEL,NPT,LAYER,KSPT,
     &                 COORDS,JLTYP,SNAME)

      include 'ABA_PARAM.INC'
      dimension TIME(2), COORDS (3)
      CHARACTER*80 SNAME
      X=COORDS(1)
      Y=COORDS(2)
      Z=COORDS(3)
      Velocity = 10000
         ecc=2179
         Y_ax=2000
      X_position = Velocity * TIME(1)

         !1st axle (Wheel type 4A)
      if (X.le.(X_position+160).and.X.ge.(X_position-
160).and.Y.le.(ecc+110+Y_ax/2).and.Y.ge.(ecc-110+Y_ax/2)) then
        F=0.5
           elseif (X.le.(X_position+160).and.X.ge.(X_position-
160).and.Y.le.(ecc+110-Y_ax/2).and.Y.ge.(ecc-110-Y_ax/2)) then
        F=0.5

      !2nd axle (Wheel type 4B)
        elseif (X.le.(X_position-3400+160).and.X.ge.(X_position-3400-
160).and.Y.le.(ecc+220+Y_ax/2).and.Y.ge.(ecc-220+Y_ax/2)) then
        F=0.5
           elseif (X.le.(X_position-3400+160).and.X.ge.(X_position-3400-
160).and.Y.le.(ecc+220-Y_ax/2).and.Y.ge.(ecc-220-Y_ax/2)) then
        F=0.5

      !3rd axle (Wheel type 4B)
        elseif (X.le.(X_position-9400+160).and.X.ge.(X_position-9400-
160).and.Y.le.(ecc+220+Y_ax/2).and.Y.ge.(ecc-220+Y_ax/2)) then
        F=0.32
           elseif (X.le.(X_position-9400+160).and.X.ge.(X_position-9400-
160).and.Y.le.(ecc+220-Y_ax/2).and.Y.ge.(ecc-220-Y_ax/2)) then
        F=0.32

      !4th axle (Wheel type 4B)
        elseif (X.le.(X_position-11200+160).and.X.ge.(X_position-11200-
160).and.Y.le.(ecc+220+Y_ax/2).and.Y.ge.(ecc-220+Y_ax/2)) then
        F=0.32
           elseif (X.le.(X_position-11200+160).and.X.ge.(X_position-11200-
160).and.Y.le.(ecc+220-Y_ax/2).and.Y.ge.(ecc-220-Y_ax/2)) then
        F=0.32

      else
        F=0.0
      endif
      RETURN
      END
```

Lorry 5

```fortran
      subroutine DLOAD(F,KSTEP,KINC,TIME,NOEL,NPT,LAYER,KSPT,
     &                 COORDS,JLTYP,SNAME)

      include 'ABA_PARAM.INC'

      dimension TIME(2), COORDS (3)
      CHARACTER*80 SNAME

      X=COORDS(1)
      Y=COORDS(2)
      Z=COORDS(3)

         !variable definitionc
      Velocity = 10000
         ecc=2179 !4679 is the distance from local orgin to centerline
(4679-2500=2179)
         Y_ax=2000

      !longitudinal position
      X_position = Velocity * TIME(1)

         !1st axle (Wheel type 5A)
      if (X.le.(X_position+160).and.X.ge.(X_position-
160).and.Y.le.(ecc+110+Y_ax/2).and.Y.ge.(ecc-110+Y_ax/2)) then
        F=0.5
         elseif (X.le.(X_position+160).and.X.ge.(X_position-
160).and.Y.le.(ecc+110-Y_ax/2).and.Y.ge.(ecc-110-Y_ax/2)) then
        F=0.5

      !2nd axle (Wheel type 5B)
       elseif (X.le.(X_position-4800+160).and.X.ge.(X_position-4800-
160).and.Y.le.(ecc+220+Y_ax/2).and.Y.ge.(ecc-220+Y_ax/2)) then
        F=0.46
         elseif (X.le.(X_position-4800+160).and.X.ge.(X_position-4800-
160).and.Y.le.(ecc+220-Y_ax/2).and.Y.ge.(ecc-220-Y_ax/2)) then
        F=0.46

      !3rd axle (Wheel type 5C)
       elseif (X.le.(X_position-8400+160).and.X.ge.(X_position-8400-
160).and.Y.le.(ecc+135+Y_ax/2).and.Y.ge.(ecc-135+Y_ax/2)) then
        F=0.52
         elseif (X.le.(X_position-8400+160).and.X.ge.(X_position-8400-
160).and.Y.le.(ecc+135-Y_ax/2).and.Y.ge.(ecc-135-Y_ax/2)) then
        F=0.52
```

```
      !4th axle (Wheel type 5C)
      elseif (X.le.(X_position-12800+160).and.X.ge.(X_position-12800-
160).and.Y.le.(ecc+135+Y_ax/2).and.Y.ge.(ecc-135+Y_ax/2)) then
        F=0.46
          elseif (X.le.(X_position-12800+160).and.X.ge.(X_position-12800-
160).and.Y.le.(ecc+135-Y_ax/2).and.Y.ge.(ecc-135-Y_ax/2)) then
        F=0.46

      !5th axle (Wheel type 5C)
      elseif (X.le.(X_position-14100+160).and.X.ge.(X_position-14100-
160).and.Y.le.(ecc+135+Y_ax/2).and.Y.ge.(ecc-135+Y_ax/2)) then
        F=0.46
          elseif (X.le.(X_position-14100+160).and.X.ge.(X_position-14100-
160).and.Y.le.(ecc+135-Y_ax/2).and.Y.ge.(ecc-135-Y_ax/2)) then
        F=0.46
      else
        F=0.0
      endif
      RETURN
      END
```
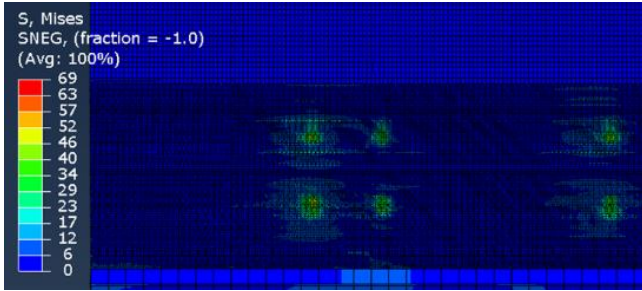
Lorry 1

Lorry 2

Lorry 3

Lorry 4

Lorry 5

11-21
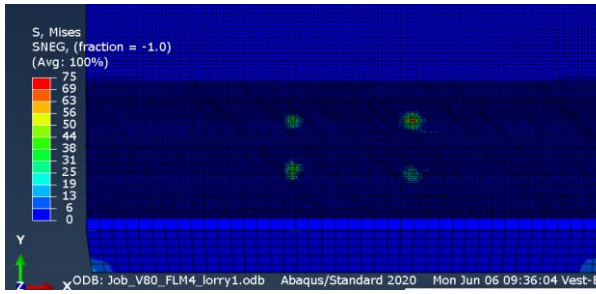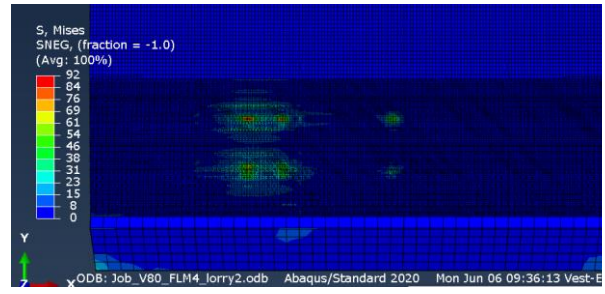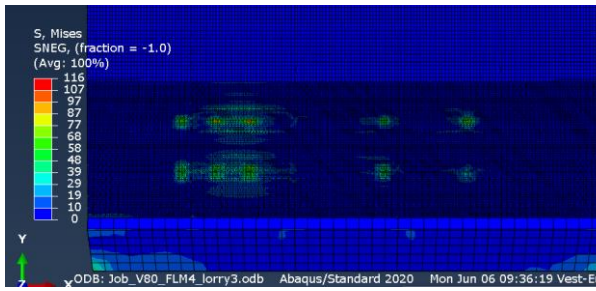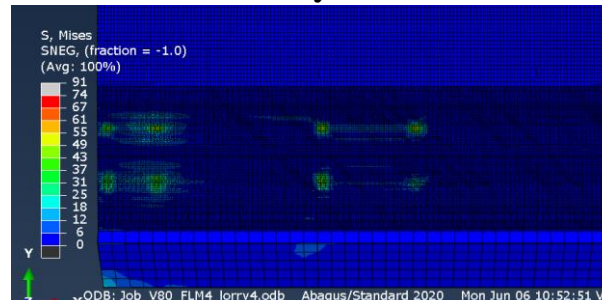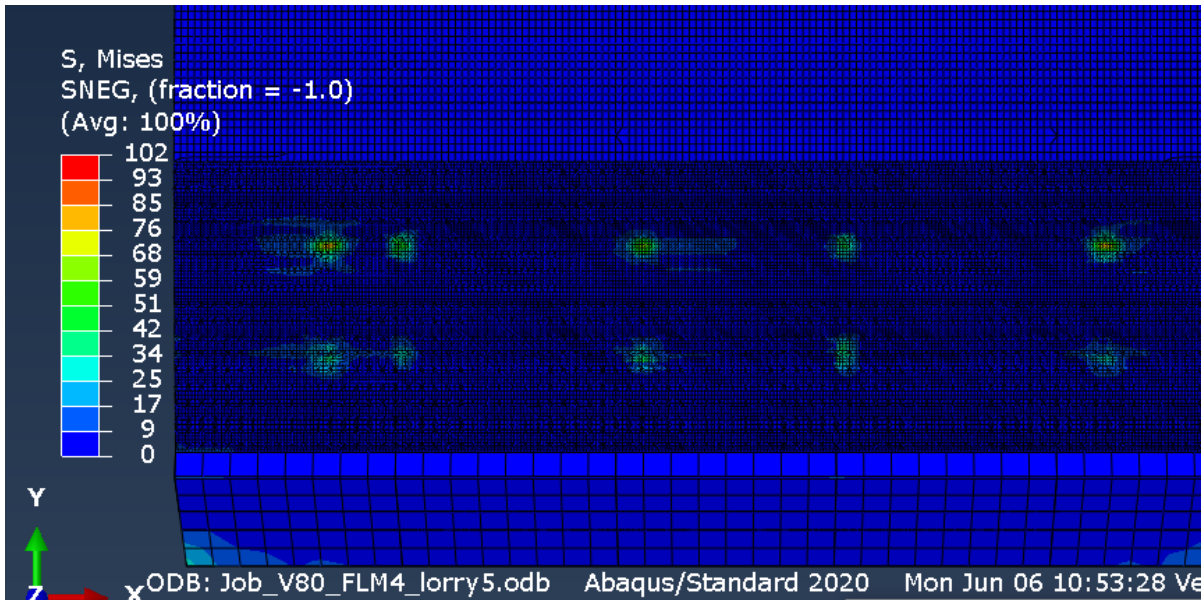
C.   Stress analysis (Python Codes)

C.1. Hot Spot Stress Extrapolation

```python
# -*- coding: mbcs -*-
# Do not delete the following import lines
from abaqus import *
from abaqusConstants import *
import __main__
```

Importing the Hot Spot reference points

```python
def part_0():
    import section
    import regionToolset
    import displayGroupMdbToolset as dgm
    import part
    import material
    import assembly
    import step
    import interaction
    import load
    import mesh
    import optimization
    import job
    import sketch
    import visualization
    import xyPlot
    import displayGroupOdbToolset as dgo
    import connectorBehavior
    session.linkedViewportCommands.setValues(_highlightLinkedViewports=False)
    odb = session.odbs['C:/Users/257796/OneDrive - Universitetet i
Stavanger/Masters_Thesis/Abaqus_mai/box_girder_mai/Job_test_V80_lorry3.odb']
    session.xyDataListFromField(odb=odb, outputPosition=NODAL, variable=(('S',
        INTEGRATION_POINT, ((COMPONENT, 'S11'), (COMPONENT, 'S22'), (COMPONENT,
        'S12'), )), ), nodeSets=("H0", ))
```

Linear extrapolation of Hot Spot stress from reference point plane stresses

```python
def part_1_creating_H0_S11_S22_S12():
    import section
    import regionToolset
    import displayGroupMdbToolset as dgm
    import part
    import material
    import assembly
    import step
    import interaction
    import load
    import mesh
    import optimization
    import job
    import sketch
    import visualization
    import xyPlot
    import displayGroupOdbToolset as dgo
    import connectorBehavior
    xy1 = session.xyDataObjects['S:S22 (Avg: 100%) SP:1 PI: STIVER_INTERN-1 N:
804']
    xy2 = decimateFilter(xyData=xy1, decimationFactor=2)
    xy2.setValues(
        sourceDescription='decimateFilter ( xyData="S:S22 (Avg: 100%) SP:1 PI:
STIVER_INTERN-1 N: 804" , decimationFactor= 2 )')
    tmpName = xy2.name
    session.xyDataObjects.changeKey(tmpName, 'RP2_S22')
    xy1 = session.xyDataObjects['S:S22 (Avg: 100%) SP:1 PI: STIVER_INTERN-1 N:
784']
    xy2 = decimateFilter(xyData=xy1, decimationFactor=2)
    xy2.setValues(
        sourceDescription='decimateFilter ( xyData="S:S22 (Avg: 100%) SP:1 PI:
STIVER_INTERN-1 N: 784" , decimationFactor= 2 )')
    tmpName = xy2.name
    session.xyDataObjects.changeKey(tmpName, 'RP1_S22')
    xy1 = session.xyDataObjects['RP1_S22']
    xy2 = session.xyDataObjects['RP2_S22']
    xy3 = 1.67*xy2-0.67*xy1
    xy3.setValues(sourceDescription='1.67 * "RP2_S22"-0.67 *"RP1_S22"')
    tmpName = xy3.name
    session.xyDataObjects.changeKey(tmpName, 'H0_S22')

    xy1 = session.xyDataObjects['S:S11 (Avg: 100%) SP:1 PI: STIVER_INTERN-1 N:
804']
    xy2 = decimateFilter(xyData=xy1, decimationFactor=2)
    xy2.setValues(
        sourceDescription='decimateFilter ( xyData="S:S11 (Avg: 100%) SP:1 PI:
STIVER_INTERN-1 N: 804" , decimationFactor= 2 )')
    tmpName = xy2.name
    session.xyDataObjects.changeKey(tmpName, 'RP2_S11')
    xy1 = session.xyDataObjects['S:S11 (Avg: 100%) SP:1 PI: STIVER_INTERN-1 N:
784']
    xy2 = decimateFilter(xyData=xy1, decimationFactor=2)
    xy2.setValues(
        sourceDescription='decimateFilter ( xyData="S:S11 (Avg: 100%) SP:1 PI:
STIVER_INTERN-1 N: 784" , decimationFactor= 2 )')
    tmpName = xy2.name
```

```
    session.xyDataObjects.changeKey(tmpName, 'RP1_S11')
    xy1 = session.xyDataObjects['RP1_S11']
    xy2 = session.xyDataObjects['RP2_S11']
    xy3 = 1.67*xy2-0.67*xy1
    xy3.setValues(sourceDescription='1.67 * "RP2_S11"-0.67 *"RP1_S11"')
    tmpName = xy3.name
    session.xyDataObjects.changeKey(tmpName, 'H0_S11')

    xy1 = session.xyDataObjects['S:S12 (Avg: 100%) SP:1 PI: STIVER_INTERN-1 N:
804']
    xy2 = decimateFilter(xyData=xy1, decimationFactor=2)
    xy2.setValues(
        sourceDescription='decimateFilter ( xyData="S:S12 (Avg: 100%) SP:1 PI:
STIVER_INTERN-1 N: 804" , decimationFactor= 2 )')
    tmpName = xy2.name
    session.xyDataObjects.changeKey(tmpName, 'RP2_S12')
    xy1 = session.xyDataObjects['S:S12 (Avg: 100%) SP:1 PI: STIVER_INTERN-1 N:
784']
    xy2 = decimateFilter(xyData=xy1, decimationFactor=2)
    xy2.setValues(
        sourceDescription='decimateFilter ( xyData="S:S12 (Avg: 100%) SP:1 PI:
STIVER_INTERN-1 N: 784" , decimationFactor= 2 )')
    tmpName = xy2.name
    session.xyDataObjects.changeKey(tmpName, 'RP1_S12')
    xy1 = session.xyDataObjects['RP1_S12']
    xy2 = session.xyDataObjects['RP2_S12']
    xy3 = 1.67*xy2-0.67*xy1
    xy3.setValues(sourceDescription='1.67 * "RP2_S12"-0.67 *"RP1_S12"')
    tmpName = xy3.name
    session.xyDataObjects.changeKey(tmpName, 'H0_S12')
```

Hot Spot Stress extrapolation

Stress in MPa and time in seconds.

Lorry 1
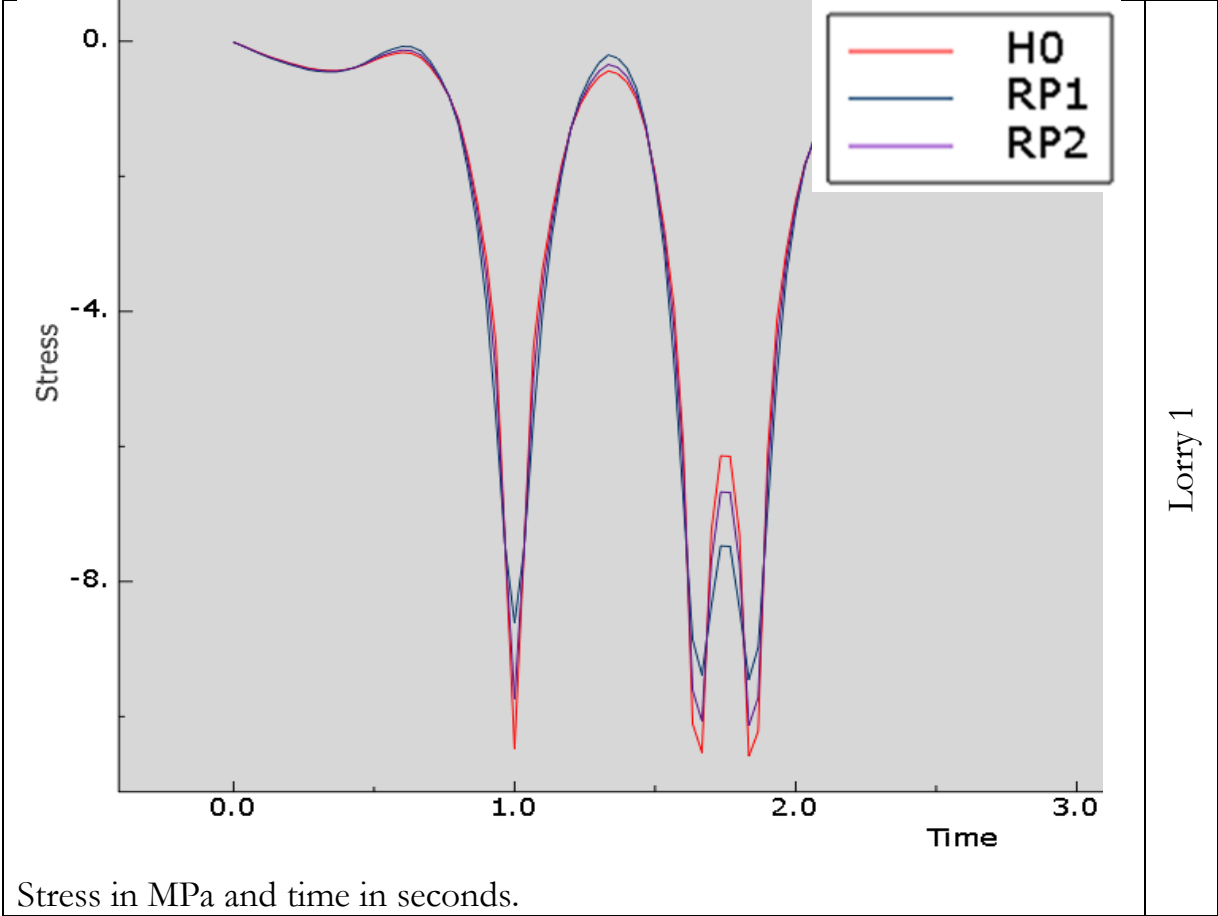
Calculating principal stresses from the Hot Spot plane stress

```python
def part_2_H0_SP_2_calculation():
    import section
    import regionToolset
    import displayGroupMdbToolset as dgm
    import part
    import material
    import assembly
    import step
    import interaction
    import load
    import mesh
    import optimization
    import job
    import sketch
    import visualization
    import xyPlot
    import displayGroupOdbToolset as dgo
    import connectorBehavior
    xy1 = session.xyDataObjects['H0_S11']
    xy2 = session.xyDataObjects['H0_S22']
    xy3 = session.xyDataObjects['H0_S12']
    xy4 =(xy1+xy2)/2+(0.5*sqrt((xy1-xy2)*(xy1-xy2)+4*(xy3)*(xy3)))
    xy4.setValues(
        sourceDescription='("H0_S11" + "H0_S22")/2 + (0.5 * sqrt( ( "H0_S11" -
"H0_S22" )*( "H0_S11" - "H0_S22" )   + 4 * ("H0_S12")* ("H0_S12")) )')
    tmpName = xy4.name
    session.xyDataObjects.changeKey(tmpName, 'SP_1')
    xy1 = session.xyDataObjects['H0_S11']
    xy2 = session.xyDataObjects['H0_S22']
    xy3 = session.xyDataObjects['H0_S12']
    xy4 =(xy1+xy2)/2-(sqrt((xy1-xy2)*(xy1-xy2)+4*(xy3)*(xy3)))
    xy4.setValues(
        sourceDescription='("H0_S11" + "H0_S22")/2 - (sqrt( ( "H0_S11" - "H0_S22"
)*( "H0_S11" - "H0_S22" )   + 4 * ("H0_S12")* ("H0_S12")) )')
    tmpName = xy4.name
    session.xyDataObjects.changeKey(tmpName, 'SP_2')
    xyp = session.xyPlots['XYPlot-1']
    chartName = xyp.charts.keys()[0]
    chart = xyp.charts[chartName]
    xy1 = session.xyDataObjects['SP_1']
    c1 = session.Curve(xyData=xy1)
    xy2 = session.xyDataObjects['SP_2']
    c2 = session.Curve(xyData=xy2)
    chart.setValues(curvesToPlot=(c1, c2, ), )
    session.charts[chartName].autoColor(lines=True, symbols=True)
    session.viewports['Viewport: 1'].setValues(displayedObject=xyp)
```

C.3. Stresses outputted from Abaqus

Stresses at one of the reference points for the Hot Spot (node 784) from Abaqus

```
—— S:Max In-Plane Principal (Abs) (Avg: 100%) SP:1 PI: STIVER_INTERN-1 N: 784
—— S:Max In-Plane Principal (Abs) (Avg: 100%) SP:5 PI: STIVER_INTERN-1 N: 784
—— S:Max In-Plane Principal (Avg: 100%) SP:1 PI: STIVER_INTERN-1 N: 784
—— S:Max In-Plane Principal (Avg: 100%) SP:5 PI: STIVER_INTERN-1 N: 784
—— S:Max Principal (Abs) (Avg: 100%) SP:1 PI: STIVER_INTERN-1 N: 784
—— S:Max Principal (Abs) (Avg: 100%) SP:5 PI: STIVER_INTERN-1 N: 784
—— S:Max Principal (Avg: 100%) SP:1 PI: STIVER_INTERN-1 N: 784
—— S:Max Principal (Avg: 100%) SP:5 PI: STIVER_INTERN-1 N: 784
—— S:Mid Principal (Avg: 100%) SP:1 PI: STIVER_INTERN-1 N: 784
—— S:Mid Principal (Avg: 100%) SP:5 PI: STIVER_INTERN-1 N: 784
—— S:Min In-Plane Principal (Avg: 100%) SP:1 PI: STIVER_INTERN-1 N: 784
—— S:Min In-Plane Principal (Avg: 100%) SP:5 PI: STIVER_INTERN-1 N: 784
—— S:Min Principal (Avg: 100%) SP:1 PI: STIVER_INTERN-1 N: 784
—— S:Min Principal (Avg: 100%) SP:5 PI: STIVER_INTERN-1 N: 784
—— S:Mises (Avg: 100%) SP:1 PI: STIVER_INTERN-1 N: 784
—— S:Mises (Avg: 100%) SP:5 PI: STIVER_INTERN-1 N: 784
—— S:Out-of-Plane Principal (Avg: 100%) SP:1 PI: STIVER_INTERN-1 N: 784
—— S:Out-of-Plane Principal (Avg: 100%) SP:5 PI: STIVER_INTERN-1 N: 784
—— S:Pressure (Avg: 100%) SP:1 PI: STIVER_INTERN-1 N: 784
—— S:Pressure (Avg: 100%) SP:5 PI: STIVER_INTERN-1 N: 784
—— S:S11 (Avg: 100%) SP:1 PI: STIVER_INTERN-1 N: 784
—— S:S11 (Avg: 100%) SP:5 PI: STIVER_INTERN-1 N: 784
—— S:S12 (Avg: 100%) SP:1 PI: STIVER_INTERN-1 N: 784
—— S:S12 (Avg: 100%) SP:5 PI: STIVER_INTERN-1 N: 784
—— S:S22 (Avg: 100%) SP:1 PI: STIVER_INTERN-1 N: 784
—— S:S22 (Avg: 100%) SP:5 PI: STIVER_INTERN-1 N: 784
—— S:S33 (Avg: 100%) SP:1 PI: STIVER_INTERN-1 N: 784
—— S:S33 (Avg: 100%) SP:5 PI: STIVER_INTERN-1 N: 784
—— S:Third Invariant (Avg: 100%) SP:1 PI: STIVER_INTERN-1 N: 784
—— S:Third Invariant (Avg: 100%) SP:5 PI: STIVER_INTERN-1 N: 784
—— S:Tresca (Avg: 100%) SP:1 PI: STIVER_INTERN-1 N: 784
—— S:Tresca (Avg: 100%) SP:5 PI: STIVER_INTERN-1 N: 784
```

11-27
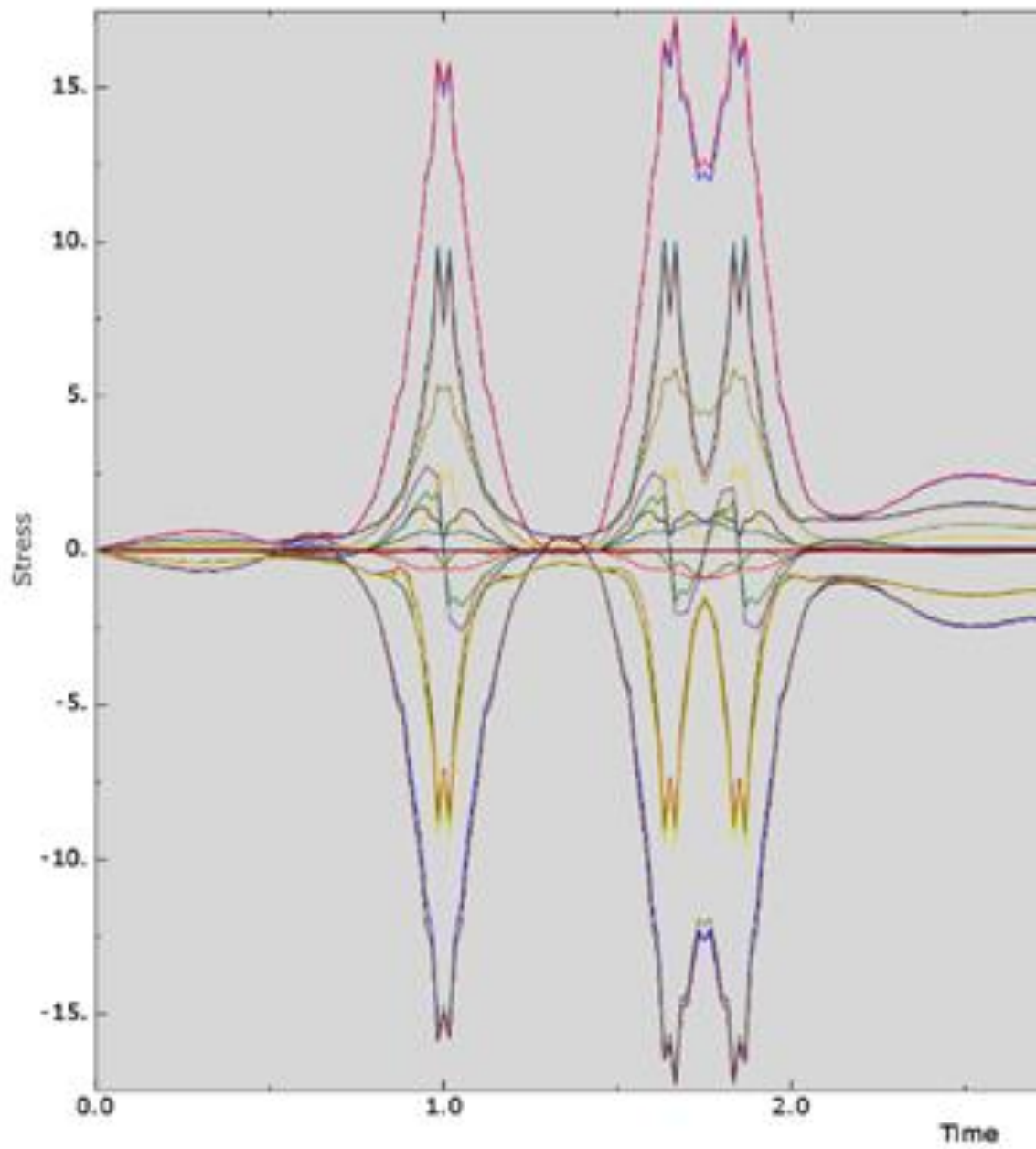
C.4. Plane stresses

Principal stresses were calculated from the plane stresses $\sigma 11$, $\sigma 12$, and $\sigma 22$. Figures below show example stress histories for these stresses. $\sigma 33 = 0$.
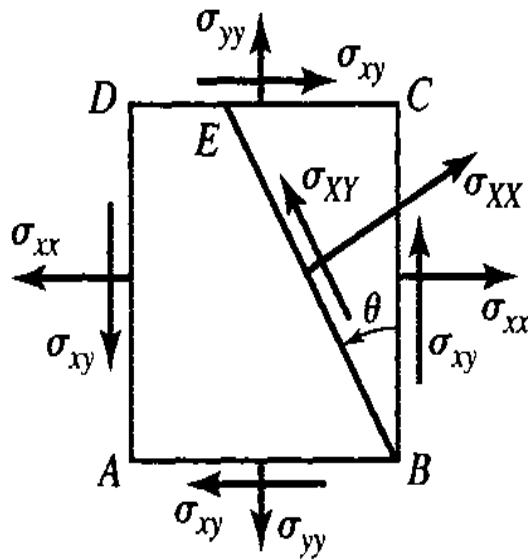
Figure 46 Plane stress components. Where σ_{11}, σ_{22} and σ_{12} are σ_{xx}, σ_{yy}, and σ_{xy}

σ33

σ 22

σ 12

σ 11
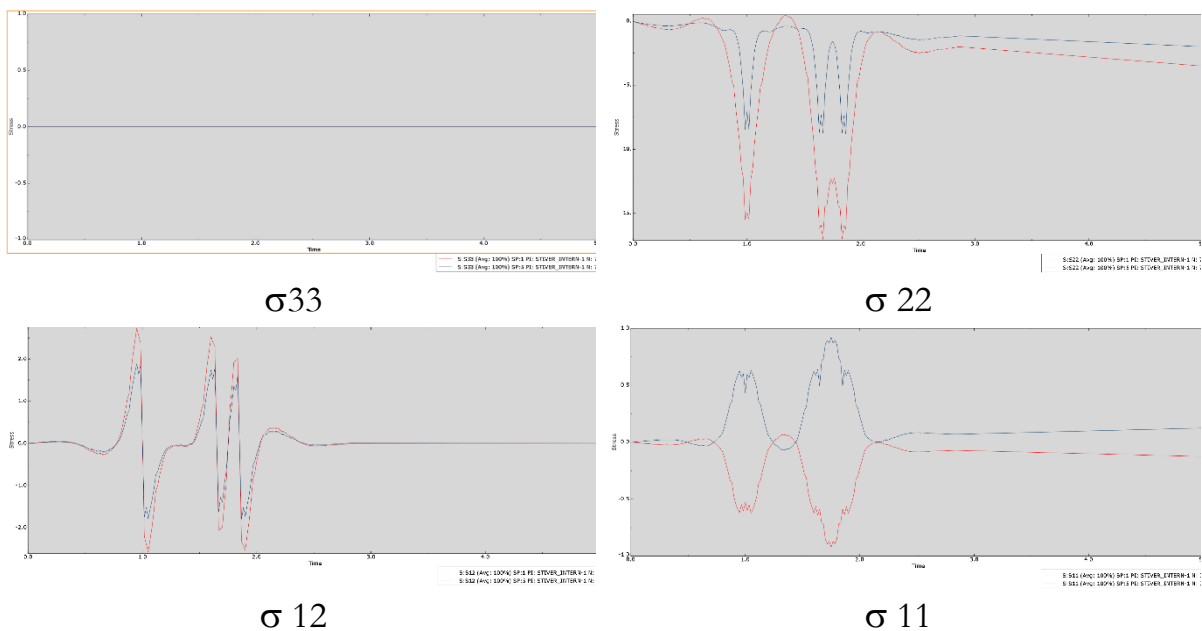
C.5. Cycle Counting

```python
import pandas as pd
import matplotlib.pyplot as plt
import scipy.stats as stats
import numpy as np
import rainflow
# Requires installing Rainflow using Conda
# conda install -c conda-forge rainflow

StressLorry1 = lorry1["Stress"]
cyclesLorry1 = rainflow.count_cycles(StressLorry1)
StressRangesLorry1 = pd.DataFrame(cyclesLorry1,
columns=["StressRangesLorry1","cycles"])

StressLorry2 = lorry2["Stress"]
cyclesLorry2 = rainflow.count_cycles(StressLorry2)
StressRangesLorry2= pd.DataFrame(cyclesLorry2,
columns=["StressRangesLorry2","cycles"])

StressLorry3 = lorry3["Stress"]
cyclesLorry3 = rainflow.count_cycles(StressLorry3)
StressRangesLorry3= pd.DataFrame(cyclesLorry3,
columns=["StressRangesLorry3","cycles"])

StressLorry4 = lorry4["Stress"]
cyclesLorry4 = rainflow.count_cycles(StressLorry4)
StressRangesLorry4= pd.DataFrame(cyclesLorry4,
columns=["StressRangesLorry4","cycles"])

StressLorry5 = lorry5["Stress"]
cyclesLorry5 = rainflow.count_cycles(StressLorry5)
StressRangesLorry5= pd.DataFrame(cyclesLorry5,
columns=["StressRangesLorry5","cycles"])
```

D.   Calculation of fatigue life

D.1.   Detail Category

Nominal stress
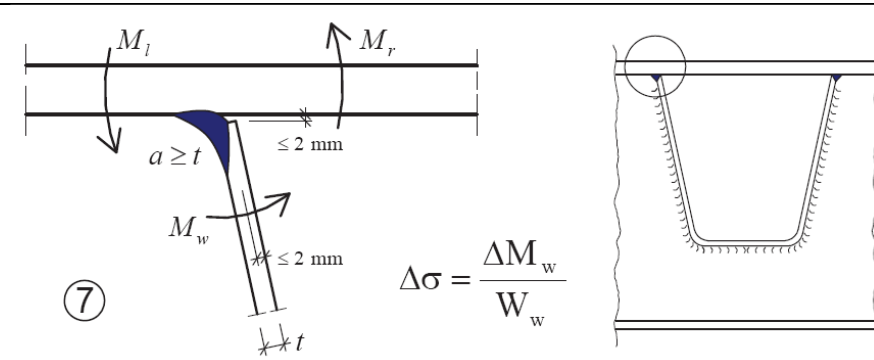
Detail Category	Constructional detail
71	$$\Delta\sigma = \frac{\Delta M_w}{W_w}$$

Figure 47 Detail category for Orthotropic decks Table 8.8 NS-EN 1993-1-9.

Hot Spot
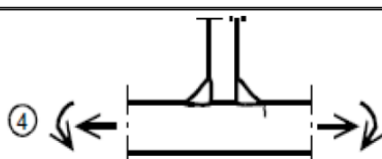
Detail category	Constructional detail	Description	Requirements
100		4) Non load-carrying fillet welds.	4) - Weld toe angle ≤60°. - See also NOTE 2.

Figure 48 Detail category for Hot spot stress used in this thesis
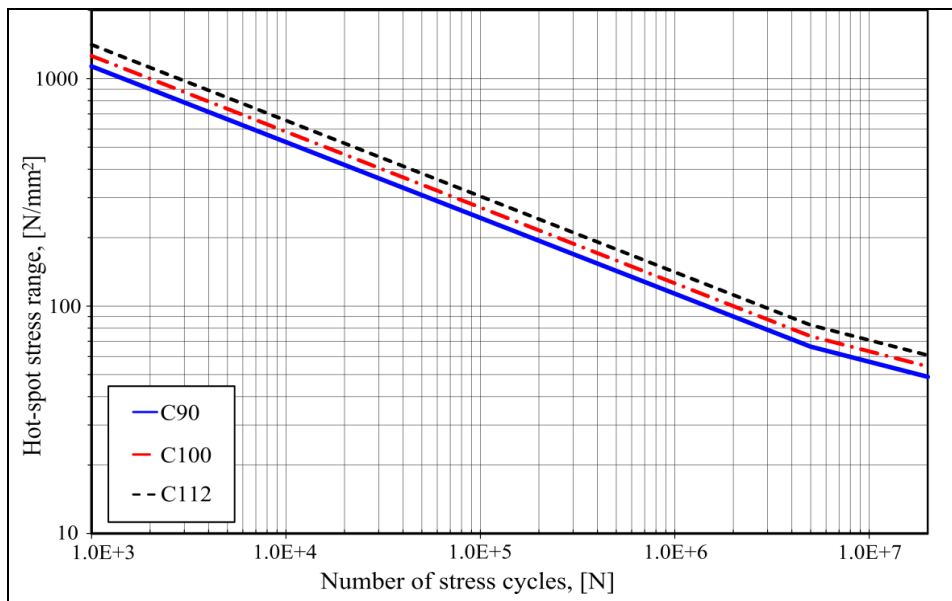
Figure 49 Structural hot-spot stress-based S-N curves recommended by EN 1993-1-9:2005

11-31

D.2. Hot Spot stress method

FLM-N

Rib-to-Deck					
σ_C	100	MPa	Detail category for Hot Spot		
σ_D	73,7				
σ_L	40,4613				
γ_{mf}	1,35		High consequence		
γ_{Ff}	1				
DAF	1,00				
NOBS	1332250	Total yearly number of lorries in each slow line (FLM-N)			
					Yearly damage

Lorry 1	75 %	of NOBS			
Stress range	Adjusted stress range	Cycles pr.lorry	Cycles pr.year (ni)	Cycle to fail (Ni)	ni/Ni
17,24	23,27	0,75	999187,50	1E+100	9,99188E-95
14,97	20,21	0,75	999187,50	1E+100	9,99188E-95
14,22	19,20	0,75	999187,50	1E+100	9,99188E-95
				SUM LORRY 1	7,99E-94

Lorry 2	10 %	of NOBS			
Stress range	Adjusted stress range	Cycles pr.lorry	Cycles pr.year (ni)	cycle to fail (Ni)	ni/Ni
21,98163798	29,7	0,10	133225	1E+100	1,33225E-95
19,88381758	26,8	0,10	133225	1E+100	1,33225E-95
18,8088427	25,4	0,10	133225	1E+100	1,33225E-95
				SUM LORRY 1	1,0658E-94

Lorry 3	5 %	of NOBS			
Stress range	Adjusted stress range	Cycles pr.lorry	Cycles pr.year (nie)	cycle to fail (Ni)	ni/Ni
27,1	36,63	0,05	66612,5	1E+100	6,66125E-96
25,2	34,03	0,05	66612,5	1E+100	6,66125E-96
23,8	32,16	0,05	66612,5	1E+100	6,66125E-96
				SUM LORRY 3	5,33E-95

Lorry 4	5 %	of NOBS			
Stress range	Adjusted stress range	Cycles pr.lorry	Cycles pr.year (nie)	cycle to fail (Ni)	ni/Ni
33	45	0,05	66612,5	59209318,78	0,001125034
32	43	0,05	66612,5	77727770,15	0,000856997
30	40	0,05	66612,5	1E+100	6,66125E-96
				SUM LORRY 1	0,001982031

lorry5	5 %	of NOBS gives			
Stress range	Adjusted stress range	Cycles pr.lorry	Cycles pr.year (nie)	cycle to fail (Ni)	ni/Ni
38,3	51,7	0,05	66612,5	29553745,4	0,002253944
36,6	49,4	0,05	66612,5	36929045,7	0,001803797
34,7	46,8	0,05	66612,5	48426233,4	0,001375546
				SUM Lorry 5	0,0054
			Sum yearly damage all lorries		0,0074
			Fatigue life (years)		135

FLM 4

Rib-to-Deck					
σ_C	100	MPa	Detail category for Hot Spot		
σ_D	73,7				
σ_L	40,4613				
γ_{mf}	1,35		High consequence		
γ_{Ff}	1				
DAF	1,00				
NOBS	500000	Total yearly number of lorries in each slow line (FLM4), medium distance			

					Yearly damage
Lorry 1	40 %	of NOBS	200000		
Stress range	**Adjusted stress range**	**Cycles pr.lorry**	**Cycles pr.year (nie)**	**Cycle to fail (Ni)**	**ni/Ni**
35,00	47,25	0,40	200000,00	46163462,89	0,004332431
23,42	31,62	0,40	200000,00	1E+100	2E-95
3,87	5,22	0,40	200000,00	1E+100	2E-95
				SUM LORRY 1	**4,33E-03**
Lorry 2	10 %	of NOBS gives	50000		
Stress range	**Adjusted stress range**	**Cycles pr.lorry**	**Cycles pr.year (nie)**	**Cycle to fail (Ni)**	**ni/Ni**
44,74215155	60,4	0,10	50000	13522415,57	0,003697564
23,6836175	32,0	0,10	50000	1E+100	5E-96
16,43571397	22,2	0,10	50000	1E+100	5E-96
				SUM LORRY 1	**0,003697564**
Lorry 3	30 %	of NOBS gives	150000		
Stress range	**Adjusted stress range**	**Cycles pr.lorry**	**Cycles pr.year (nie)**	**Cycle to fail (Ni)**	**ni/Ni**
50,4	68,04	0,3	150000	7455656,983	0,020118951
42,4	57,26	0,3	150000	17667715,31	0,008490062
20,3	27,40	0,3	150000	1E+100	1,5E-95
18,5	24,95	0,3	150000	1E+100	1,5E-95
18,1	24,39	0,3	150000	1E+100	1,5E-95
				SUM LORRY 3	**2,86E-02**
Lorry 4	15 %	of NOBS gives	75000		
Stress range	**Adjusted stress range**	**Cycles pr.lorry**	**Cycles pr.year (nie)**	**Cycle to fail (Ni)**	**ni/Ni**
41	55	0,15	75000	21979025,52	0,003412344
27	36	0,15	75000	1E+100	7,5E-96
20	27	0,15	75000	1E+100	7,5E-96
15	20	0,15	75000	1E+100	7,5E-96
				SUM LORRY 1	**0,003412344**
lorry5	5 %	of NOBS gives	25000		
Stress range	**Adjusted stress range**	**Cycles pr.lorry**	**Cycles pr.year (nie)**	**Cycle to fail (Ni)**	**ni/Ni**
36,4	49,1	0,05	25000	37943001,49	0,000658883
31,2	42,1	0,05	25000	82583779,47	0,000302723
24,4	33,0	0,05	25000	1E+100	2,5E-96
23,7	32,0	0,05	25000	1E+100	2,5E-96
13,5	18,2	0,05	25000	1E+100	2,5E-96
				SUM Lorry 5	**0,0010**
			Sum yearly damage all lorries		0,0410
			Fatigue life (years)		**24**

D.3. Nominal stress method

FLM-N

Rib-to-Deck					
σ_C	71	MPa	Detail category for Hot Spot		
σ_D	52,33				
σ_L	28,73				
γ_{mf}	1,35		High consequence		
γ_{Ff}	1				
DAF	1,00				
NOBS	1332250	Total yearly number of lorries in each slow line (FLM-N)			
					Yearly damage
Lorry 1	75 %	of NOBS			
Stress range	Adjusted stress range	Cycles pr.lorry	Cycles pr.year (ni)	Cycle to fail (Ni)	ni/Ni
8,97	12,11	0,75	999187,50	1E+100	9,99188E-95
4,16	5,61	0,75	999187,50	1E+100	9,99188E-95
2,87	3,88	0,75	999187,50	1E+100	9,99188E-95
				SUM LORRY 1	7,99E-94
Lorry 2	10 %	of NOBS			
Stress range	Adjusted stress range	Cycles pr.lorry	Cycles pr.year (ni)	cycle to fail (Ni)	ni/Ni
11,97	16,2	0,10	133225	1E+100	1,33225E-95
5,54	7,5	0,10	133225	1E+100	1,33225E-95
3,81	5,1	0,10	133225	1E+100	1,33225E-95
				SUM LORRY 2	1,0658E-94
Lorry 3	5 %	of NOBS			
Stress range	Adjusted stress range	Cycles pr.lorry	Cycles pr.year (nie)	cycle to fail (Ni)	ni/Ni
15,2	20,58	0,05	66612,5	1E+100	6,66125E-96
7,1	9,53	0,05	66612,5	1E+100	6,66125E-96
4,8	6,52	0,05	66612,5	1E+100	6,66125E-96
				SUM LORRY 3	5,33E-95
Lorry 4	5 %	of NOBS			
Stress range	Adjusted stress range	Cycles pr.lorry	Cycles pr.year (nie)	cycle to fail (Ni)	ni/Ni
19	26	0,05	66612,5	1E+100	6,66125E-96
9	12	0,05	66612,5	1E+100	6,66125E-96
6	8	0,05	66612,5	1E+100	6,66125E-96
				SUM LORRY 4	5,33E-95
lorry5	5 %	of NOBS gives			
Stress range	Adjusted stress range	Cycles pr.lorry	Cycles pr.year (nie)	cycle to fail (Ni)	ni/Ni
22,3	30,1	0,05	66612,5	79047384,31	0,000842691
10,4	14,0	0,05	66612,5	1E+100	6,66125E-96
7,0	9,5	0,05	66612,5	1E+100	6,66125E-96
				SUM LORRY 5	0,0008
			Sum yearly damage all lorries		0,0008
			Fatigue life (years)		1187

D.4.   Comparing RP from Stiffener wall vs Deck plate

Comparing fatigue life between the two reference points of the Hot Spot Stress at the rib-to-deck welded joint.
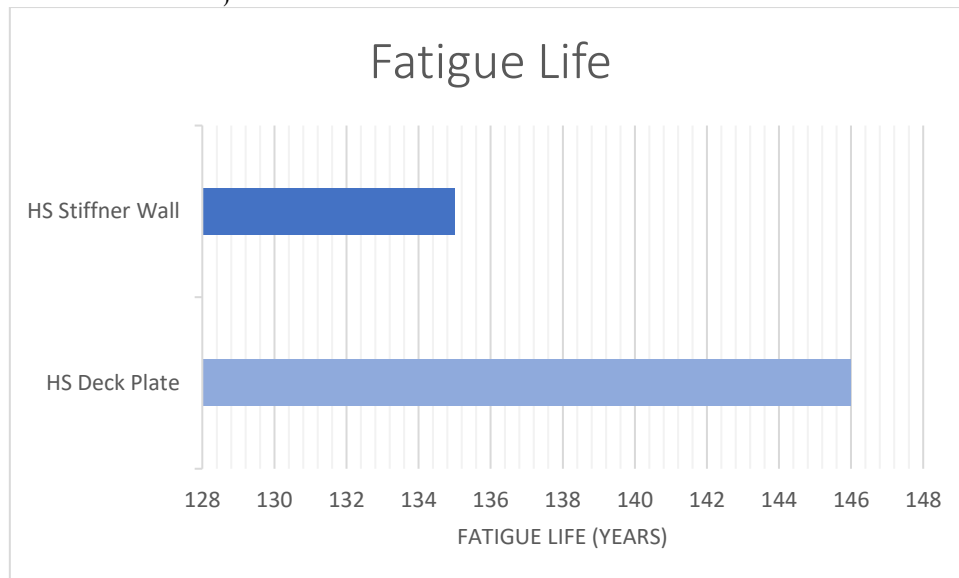
Figure 50 Fatigue life of the rib-to-deck welded joints from RPs at Stiffener wall vs RPs at the deck plate.

E. Global model

E.1. Z-value that gave the maximal stress

The longitudinal normal stress of a node at x = 282 m
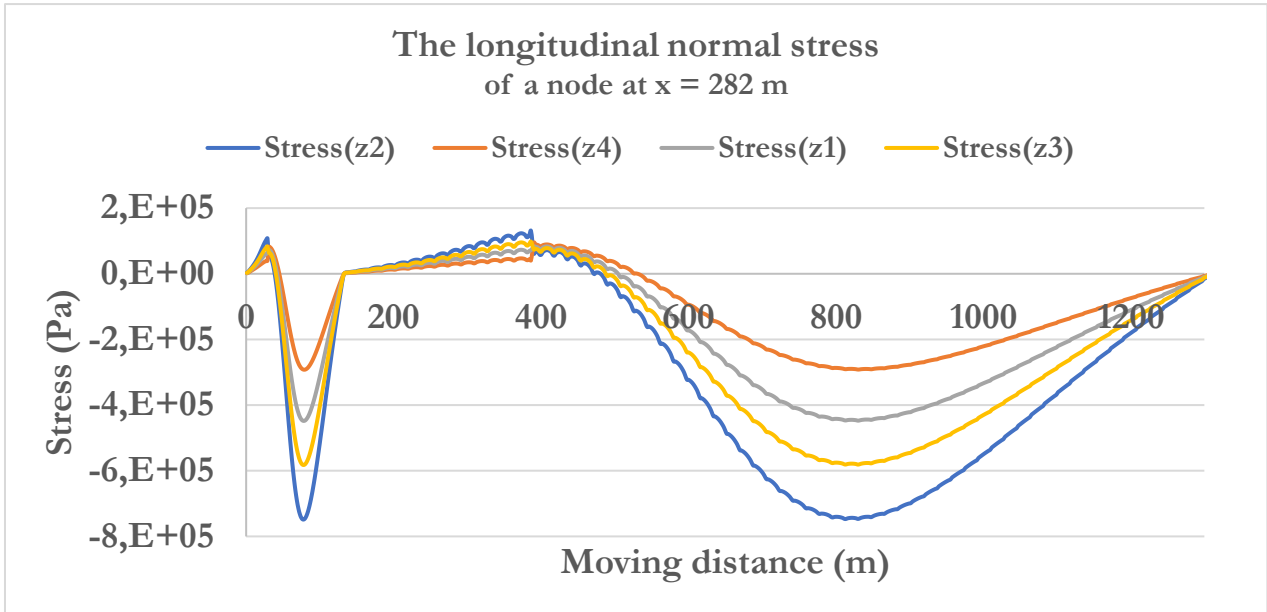
Figure 51 Finding the Z-value that gave the maximum stress.

Label	Z-value (m)	Max tensile stress (Pa)	Max compressive stress (Pa)
z1	5,27	83465	-448042
z2	**8,53**	**131150**	**-748384**
z3	6,727	98230	-581993
z4	3,575	94883	-292243

E.2. Influence lines

Loading the global model with lorry 5 (FLM-N) = 3x 145 kN = 435 kN, measurements (SF1, SM2, SM3) from node 198 (at X=218 m, L/6, where L = 1310 m). Stress (σ) is calculated using the equations below at each node in the global model in Abaqus: N = SF1 (axial force), A= cross-section area of the box girder, M_y = SM2 (moment about the weak axis y), M_z = SM3 (moment about the strong axis z). se input table for values of A, Iy, Iz, y and z. SF1, SM2 and SM3 are from Abaqus output, see results section for stress.

$$\sigma = \frac{axial\ foce\ (SF1)}{A_{box-girder}} + \frac{M\ about\ weak\ axis\ (SM2) * y}{I_y} + \frac{M\ about\ strong\ axis\ (SM3) * z}{I_z}$$

$$\sigma = \frac{SF1}{0.5813} + \frac{SM2 \times 1.953}{0.972} + \frac{SM3 \times 8.53}{16.448}$$

11-36

X	SF1	SM2	SM3	Stress
1	16	352	-41	3111
3	1062	-75	-14606	-564
5	2509	-669	-35189	-5734
7	3829	-1188	-55340	-10414
9	4965	-1558	-74996	-14038
11	5888	-1626	-94132	-15314
13	6596	-1057	-112748	-11313
15	7123	867	-130890	4323
17	7550	5620	-148718	44647
19	8032	16019	-166724	134594
21	8819	36953	-186419	317325
23	10214	75594	-212481	655736
25	2875	21351	825887	290383
27	4029	-1711	800642	86984
29	4408	-13734	782571	-20023
31	4294	-20085	766673	-77837
33	3920	-23902	751336	-113800
35	3429	-26803	736055	-141917
37	2896	-29551	720672	-168777
39	2357	-32478	705130	-197238
41	1829	-35710	689405	-228373
43	1319	-39272	673484	-262405
45	833	-43144	657359	-299134
47	370	-47275	641026	-338125
49	-68	-51600	624482	-378798
51	-481	-56041	607731	-420468
53	-869	-60511	590778	-462376
55	-1232	-64919	573630	-503714
57	-1570	-69169	556297	-543651
59	-1884	-73167	538794	-581360
61	-2173	-76825	521134	-616055
63	-2439	-80062	503335	-647029
65	-2682	-82809	485415	-673682
67	-2902	-85015	467394	-695559
69	-3101	-86646	449296	-712366
71	-3278	-87688	431143	-723974
73	-3434	-88146	412962	-730415
75	-3571	-88037	394780	-731853
77	-3687	-87393	376625	-728562
79	-3785	-86255	358528	-720888
81	-3863	-84667	340520	-709224
83	-3923	-82676	322633	-693985
85	-3965	-80332	304900	-675586
87	-3988	-77679	287353	-654431
89	-3994	-74763	270027	-630905
91	-3982	-71624	252954	-605368
93	-3952	-68302	236166	-578156
95	-3905	-64831	219696	-549573
97	-3840	-61245	203575	-519900
99	-3758	-57571	187832	-489391
101	-3659	-53838	172496	-458277
103	-3544	-50068	157594	-426766
105	-3411	-46284	143151	-395045
107	-3262	-42505	129192	-363281
109	-3096	-38748	115739	-331624
111	-2914	-35029	102812	-300207

113	-2716	-31361	90430	-269147
115	-2502	-27756	78608	-238545
117	-2272	-24224	67361	-208490
119	-2026	-20774	56701	-179056
121	-1765	-17412	46637	-150305
123	-1488	-14146	37176	-122284
125	-1196	-10977	28315	-95025
127	-890	-7906	20041	-68533
129	-570	-4929	12318	-42773
131	-238	-2031	5064	-17636
133	0	-37	180	-306
135	128	320	-1606	2839
137	240	288	-3170	2565
139	353	255	-4734	2282
141	465	221	-6298	1987
143	615	171	-8383	1565
145	764	117	-10468	1098
147	913	63	-12554	633
149	1210	-147	-16688	-1192
151	1358	-110	-18748	-857
153	1505	-116	-20807	-898
155	1651	-135	-22866	-1058
157	1797	-169	-24925	-1348
159	1941	-219	-26984	-1782
161	2085	-286	-29043	-2372
163	2227	-372	-31102	-3128
165	2369	-490	-33162	-4165
167	2648	-690	-37226	-5921
169	2786	-580	-39242	-4956
171	2922	-544	-41257	-4648
173	3056	-535	-43273	-4579
175	3189	-555	-45288	-4762
177	3321	-605	-47304	-5210
179	3450	-685	-49320	-5934
181	3579	-798	-51337	-6946
183	3705	-975	-53354	-8516
185	3952	-1153	-57326	-10123
187	4073	-964	-59292	-8495
189	4191	-881	-61257	-7796
191	4308	-838	-63223	-7454
193	4423	-837	-65189	-7480
195	4535	-879	-67155	-7885
197	4646	-965	-69122	-8681
199	4755	-1096	-71089	-9876
201	4861	-1321	-73058	-11901
203	5068	-1456	-76928	-13194
205	5167	-1180	-78842	-10827
207	5265	-1039	-80755	-9647
209	5361	-950	-82668	-8928
211	5454	-914	-84582	-8679
213	5545	-932	-86497	-8910
215	5634	-1006	-88411	-9629
217	5721	-1135	-90327	-10845
219	5806	-1387	-92243	-13139
221	5969	-1436	-96010	-13735
223	6047	-1051	-97872	-10441
225	6122	-827	-99733	-8563
227	6196	-663	-101594	-7225
229	6268	-562	-103456	-6431

231	6338	-523	-105319	-6189
233	6406	-546	-107182	-6501
235	6472	-633	-109045	-7374
237	6535	-867	-110910	-9536
239	6657	-733	-114578	-8584
241	6715	-188	-116392	-3922
243	6771	175	-118206	-854
245	6826	473	-120020	1645
247	6879	707	-121835	3577
249	6931	877	-123650	4942
251	6981	984	-125465	5744
253	7030	1026	-127281	5985
255	7078	906	-129098	4796
257	7169	1427	-132688	9104
259	7213	2239	-134471	16093
261	7257	2860	-136254	21400
263	7299	3422	-138037	26198
265	7342	3928	-139820	30501
267	7384	4379	-141604	34321
269	7426	4777	-143388	37675
271	7468	5124	-145172	40577
273	7510	5306	-146957	42031
275	7593	6622	-150533	53306
277	7636	7920	-152335	64553
279	7680	9033	-154136	74184
281	7725	10112	-155937	83511
283	7771	11159	-157739	92568
285	7819	12179	-159540	101389
287	7870	13176	-161342	110008
289	7922	14153	-163143	118459
291	7976	14984	-164946	125633
293	8093	17850	-168710	150537
295	8156	20038	-170681	169614
297	8223	22073	-172651	187353
299	8294	24119	-174622	205199
301	8370	26183	-176592	223208
303	8450	28271	-178562	241436
305	8534	30390	-180532	259940
307	8624	32546	-182502	278778
309	8720	34600	-184473	296738
311	8930	40259	-189044	346212
313	9046	44001	-191652	378945
315	9168	47644	-194259	410812
317	9297	51362	-196866	443356
319	9433	55163	-199473	476633
321	9576	59052	-202080	510701
323	9726	63036	-204688	545617
325	9882	67123	-207295	581440
327	10046	71161	-209904	616849
329	11575	81543	-354547	693410
330	5972	65239	320122	620802
332	387	46363	994916	525668
334	1741	45025	854267	499551
336	1941	40885	849528	463003
338	2138	36833	844789	427223
340	2332	32863	840051	392154
342	2520	28969	835313	357739
344	2703	24975	830573	322443
346	3030	18727	823352	267316

348	3175	16541	820827	248088
350	3311	14211	818304	227575
352	3439	11913	815779	207321
354	3558	9637	813254	187254
356	3669	7375	810729	167299
358	3772	5120	808202	147385
360	3866	2863	805675	127440
362	3953	419	803146	105838
364	4100	-2899	798831	76460
366	4161	-3725	797025	69102
368	4214	-4779	795218	59736
370	4261	-5876	793411	49969
372	4301	-7024	791604	39750
374	4334	-8228	789795	29027
376	4362	-9494	787986	17750
378	4383	-10828	786176	5869
380	4400	-12419	784365	-8279
382	4417	-14132	780977	-23690
384	4419	-14224	779387	-24679
386	4417	-14599	777798	-28164
388	4410	-15069	776208	-32491
390	4400	-15638	774617	-37690
392	4386	-16309	773027	-43791
394	4368	-17085	771435	-50823
396	4347	-17970	769844	-58813
398	4323	-19155	768252	-69445
400	4268	-20103	765135	-78227
402	4237	-19850	763600	-76244
404	4204	-19912	762066	-77027
406	4169	-20098	760531	-78898
408	4132	-20409	758997	-81872
410	4093	-20847	757462	-85965
412	4053	-21414	755928	-91191
414	4011	-22111	754393	-97563
416	3967	-23131	752858	-106776
418	3877	-23764	749803	-112850
420	3831	-23378	748272	-109721
422	3784	-23321	746743	-109480
424	3736	-23401	745214	-110446
426	3687	-23619	743685	-112628
428	3637	-23976	742157	-116031
430	3586	-24473	740628	-120662
432	3535	-25111	739100	-126524
434	3484	-26082	737572	-135316
436	3380	-26621	734512	-140587
438	3327	-26205	732970	-137217
440	3274	-26123	731430	-136767
442	3221	-26184	729891	-137572
444	3168	-26387	728352	-139636
446	3114	-26735	726813	-142960
448	3060	-27226	725274	-147546
450	3006	-27861	723736	-153393
452	2952	-28832	722199	-162190
454	2844	-29376	719113	-167516
456	2790	-28981	717554	-164330
458	2736	-28917	715998	-164043
460	2682	-28997	714443	-165020
462	2628	-29220	712887	-167261
464	2574	-29588	711333	-170765

466	2520	-30100	709779	-175532
468	2466	-30755	708225	-181558
470	2413	-31743	706672	-190510
472	2306	-32333	703553	-196243
474	2252	-31981	701975	-193434
476	2199	-31954	700401	-193468
478	2146	-32068	698827	-194751
480	2093	-32325	697253	-197282
482	2040	-32724	695681	-201058
484	1988	-33264	694108	-206078
486	1935	-33945	692537	-212336
488	1883	-34955	690966	-221468
490	1779	-35604	687809	-227722
492	1728	-35304	686211	-225368
494	1676	-35319	684617	-225777
496	1625	-35473	683023	-227406
498	1574	-35766	681430	-230253
500	1523	-36197	679838	-234314
502	1472	-36767	678246	-239587
504	1422	-37473	676655	-246065
506	1372	-38499	675066	-255341
508	1272	-39208	671868	-262115
510	1223	-38963	670250	-260237
512	1173	-39021	668635	-261024
514	1124	-39213	667021	-262991
516	1075	-39541	665408	-266137
518	1027	-40001	663795	-270457
520	979	-40596	662183	-275947
522	930	-41323	660571	-282600
524	883	-42358	658962	-291958
526	788	-43120	655722	-299192
528	741	-42927	654083	-297778
530	694	-43025	652448	-298915
532	647	-43253	650813	-301186
534	601	-43610	649178	-304590
536	554	-44095	647545	-309120
538	508	-44708	645912	-314772
540	463	-45448	644280	-321538
542	417	-46483	642649	-330899
544	327	-47287	639368	-338495
546	283	-47144	637708	-337513
548	238	-47277	636052	-338955
550	194	-47534	634396	-341480
552	150	-47913	632740	-345084
554	106	-48415	631086	-349762
556	63	-49039	629432	-355507
558	20	-49784	627779	-362313
560	-23	-50810	626127	-371592
562	-108	-51642	622804	-379430
564	-150	-51542	621124	-378830
566	-192	-51704	619447	-380518
568	-234	-51983	617770	-383234
570	-275	-52378	616094	-386971
572	-317	-52888	614419	-391724
574	-358	-53515	612744	-397487
576	-398	-54255	611070	-404253
578	-439	-55262	609398	-413359
580	-519	-56106	606034	-421302
582	-558	-56043	604333	-421021

11-41

584	-598	-56225	602636	-422887
586	-637	-56517	600939	-425721
588	-676	-56919	599243	-429515
590	-715	-57430	597547	-434265
592	-753	-58049	595852	-439964
594	-791	-58775	594158	-446604
596	-829	-59752	592465	-455446
598	-904	-60591	589062	-463342
600	-941	-60557	587342	-463309
602	-978	-60751	585625	-465277
604	-1015	-61048	583909	-468149
606	-1051	-61447	582194	-471920
608	-1087	-61948	580478	-476583
610	-1123	-62550	578764	-482133
612	-1159	-63252	577050	-488560
614	-1194	-64189	575338	-497044
616	-1265	-65005	571896	-504738
618	-1299	-64990	570158	-504873
620	-1334	-65187	568424	-506861
622	-1368	-65479	566689	-509689
624	-1402	-65866	564955	-513352
626	-1435	-66348	563222	-517844
628	-1469	-66923	561489	-523158
630	-1502	-67592	559756	-529286
632	-1535	-68478	558025	-537323
634	-1600	-69253	554548	-544655
636	-1632	-69248	552794	-544874
638	-1664	-69438	551042	-546799
640	-1696	-69716	549290	-549500
642	-1728	-70081	547539	-552972
644	-1759	-70534	545789	-557208
646	-1790	-71074	544038	-562202
648	-1821	-71698	542289	-567947
650	-1851	-72524	540539	-575452
652	-1911	-73241	537029	-582268
654	-1941	-73237	535260	-582488
656	-1971	-73410	533493	-584269
658	-2000	-73664	531726	-586762
660	-2029	-73999	529960	-589962
662	-2058	-74414	528193	-593864
664	-2087	-74909	526427	-598460
666	-2115	-75481	524662	-603743
668	-2143	-76238	522896	-610640
670	-2199	-76881	519357	-616797
672	-2226	-76867	517574	-616938
674	-2253	-77016	515794	-618498
676	-2280	-77238	514013	-620709
678	-2307	-77534	512233	-623565
680	-2333	-77903	510452	-627060
682	-2360	-78344	508672	-631189
684	-2386	-78857	506892	-635944
686	-2411	-79537	505112	-642168
688	-2462	-80091	501546	-647539
690	-2487	-80061	499753	-647530
692	-2512	-80177	497960	-648803
694	-2537	-80360	496168	-650668
696	-2561	-80610	494375	-653118
698	-2585	-80927	492583	-656148
700	-2609	-81308	490791	-659752

11-42

702	-2633	-81755	488998	-663923
704	-2656	-82353	487205	-669426
706	-2703	-82806	483617	-673911
708	-2725	-82752	481815	-673689
710	-2748	-82830	480013	-674624
712	-2770	-82968	478210	-676091
714	-2793	-83167	476408	-678088
716	-2815	-83426	474605	-680607
718	-2836	-83743	472803	-683644
720	-2858	-84119	471000	-687193
722	-2879	-84631	469196	-691943
724	-2921	-84976	465591	-695469
726	-2941	-84893	463781	-694989
728	-2962	-84928	461971	-695546
730	-2982	-85018	460161	-696582
732	-3002	-85161	458351	-698093
734	-3022	-85359	456541	-700074
736	-3041	-85609	454730	-702520
738	-3060	-85912	452919	-705425
740	-3079	-86337	451107	-709406
742	-3117	-86569	447488	-711934
744	-3135	-86453	445674	-711166
746	-3154	-86443	443859	-711322
748	-3172	-86482	442044	-711908
750	-3190	-86569	440229	-712919
752	-3207	-86704	438413	-714350
754	-3225	-86886	436596	-716197
756	-3242	-87116	434779	-718454
758	-3259	-87455	432961	-721673
760	-3292	-87572	429334	-723193
762	-3308	-87422	427517	-722120
764	-3325	-87366	425701	-721870
766	-3340	-87353	423883	-722003
768	-3356	-87384	422065	-722514
770	-3372	-87457	420246	-723400
772	-3387	-87573	418427	-724657
774	-3402	-87730	416606	-726279
776	-3417	-87985	414784	-728757
778	-3446	-87990	411154	-729288
780	-3461	-87806	409338	-727909
782	-3475	-87704	407522	-727259
784	-3489	-87642	405704	-726949
786	-3503	-87618	403886	-726976
788	-3516	-87631	402067	-727336
790	-3529	-87683	400247	-728024
792	-3543	-87771	398426	-729037
794	-3555	-87946	396603	-730810
796	-3581	-87844	392976	-730396
798	-3593	-87626	391164	-728719
800	-3605	-87482	389350	-727687
802	-3617	-87372	387536	-726956
804	-3629	-87296	385720	-726524
806	-3641	-87253	383904	-726387
808	-3652	-87244	382086	-726541
810	-3663	-87267	380268	-726982
812	-3674	-87367	378447	-728095
814	-3695	-87166	374828	-726796
816	-3706	-86917	373022	-724838
818	-3716	-86732	371215	-723450

11-43

820	-3726	-86578	369407	-722328
822	-3736	-86453	367597	-721470
824	-3746	-86359	365786	-720872
826	-3755	-86294	363974	-720532
828	-3764	-86258	362161	-720446
830	-3773	-86289	360345	-720953
832	-3791	-85996	356741	-718841
834	-3799	-85718	354945	-716625
836	-3808	-85496	353147	-714911
838	-3816	-85302	351347	-713432
840	-3824	-85134	349547	-712186
842	-3832	-84992	347745	-711169
844	-3839	-84877	345942	-710380
846	-3847	-84786	344137	-709815
848	-3854	-84755	342329	-709772
850	-3868	-84380	338746	-706926
852	-3874	-84076	336963	-704478
854	-3881	-83821	335177	-702471
856	-3887	-83591	333390	-700672
858	-3893	-83384	331601	-699078
860	-3899	-83200	329811	-697686
862	-3905	-83039	328020	-696494
864	-3910	-82900	326227	-695500
866	-3915	-82814	324431	-694965
868	-3926	-82365	320875	-691466
870	-3930	-82038	319108	-688813
872	-3935	-81755	317338	-686548
874	-3939	-81493	315566	-684466
876	-3944	-81251	313793	-682564
878	-3948	-81030	312019	-680841
880	-3952	-80829	310242	-679293
882	-3955	-80648	308465	-677919
884	-3959	-80512	306683	-676948
886	-3965	-79999	303162	-672876
888	-3968	-79653	301413	-670046
890	-3971	-79345	299662	-667557
892	-3974	-79055	297909	-665229
894	-3976	-78784	296155	-663059
896	-3979	-78530	294399	-661045
898	-3981	-78294	292642	-659187
900	-3983	-78075	290882	-657480
902	-3984	-77897	289119	-656128
904	-3987	-77329	285638	-651559
906	-3988	-76966	283912	-648579
908	-3989	-76637	282183	-645899
910	-3990	-76324	280453	-643359
912	-3991	-76027	278720	-640959
914	-3991	-75745	276986	-638696
916	-3992	-75479	275251	-636569
918	-3992	-75229	273513	-634575
920	-3992	-75013	271771	-632892
922	-3991	-74398	268338	-627900
924	-3990	-74021	266638	-624795
926	-3990	-73675	264934	-621954
928	-3989	-73342	263229	-619236
930	-3988	-73023	261522	-616640
932	-3986	-72719	259813	-614165
934	-3985	-72427	258103	-611809
936	-3983	-72149	256391	-609570

11-44

938	-3981	-71902	254674	-607604
940	-3977	-71248	251294	-602255
942	-3975	-70861	249623	-599051
944	-3972	-70500	247948	-596077
946	-3969	-70151	246271	-593212
948	-3967	-69815	244593	-590454
950	-3963	-69490	242913	-587801
952	-3960	-69178	241231	-585253
954	-3957	-68877	239547	-582807
956	-3953	-68603	237858	-580600
958	-3945	-67917	234539	-574958
960	-3941	-67522	232899	-571676
962	-3937	-67149	231256	-568597
964	-3933	-66788	229612	-565612
966	-3928	-66437	227965	-562721
968	-3923	-66097	226317	-559923
970	-3918	-65767	224666	-557216
972	-3913	-65447	223014	-554599
974	-3908	-65152	221357	-552191
976	-3897	-64440	218104	-546313
978	-3891	-64039	216500	-542974
980	-3885	-63658	214892	-539813
982	-3878	-63287	213282	-536735
984	-3872	-62925	211670	-533739
985	-3866	-62572	210056	-530824
987	-3859	-62229	208441	-527989
989	-3852	-61894	206824	-525233
991	-3845	-61580	205201	-522660
993	-3830	-60849	202021	-516597
995	-3823	-60445	200454	-513221
997	-3815	-60058	198884	-510001
999	-3807	-59680	197312	-506853
1001	-3799	-59309	195738	-503777
1003	-3791	-58947	194162	-500772
1005	-3782	-58593	192585	-497836
1007	-3774	-58247	191005	-494970
1009	-3765	-57919	189421	-492263
1011	-3747	-57174	186319	-486064
1013	-3737	-56768	184793	-482668
1015	-3728	-56378	183263	-479408
1017	-3718	-55995	181732	-476212
1019	-3709	-55619	180199	-473078
1021	-3699	-55250	178663	-470007
1023	-3688	-54888	177127	-466997
1025	-3678	-54533	175588	-464047
1027	-3668	-54194	174044	-461236
1029	-3646	-53440	171027	-454943
1031	-3635	-53035	169544	-451542
1033	-3624	-52643	168057	-448261
1035	-3613	-52258	166569	-445036
1037	-3601	-51879	165079	-441865
1039	-3590	-51506	163588	-438749
1041	-3578	-51139	162094	-435686
1043	-3566	-50778	160599	-432676
1045	-3554	-50431	159099	-429787
1047	-3529	-49673	156171	-423439
1049	-3516	-49269	154733	-420049
1051	-3503	-48878	153293	-416763
1053	-3490	-48492	151851	-413526

11-45

1055	-3477	-48112	150407	-410336
1057	-3464	-47737	148961	-407195
1059	-3450	-47367	147514	-404099
1061	-3437	-47003	146064	-401050
1063	-3423	-46650	144611	-398107
1065	-3395	-45892	141776	-391738
1067	-3380	-45492	140387	-388372
1069	-3366	-45103	138995	-385096
1071	-3351	-44718	137601	-381863
1073	-3336	-44339	136205	-378671
1075	-3321	-43964	134808	-375521
1077	-3306	-43594	133409	-372412
1079	-3291	-43228	132009	-369342
1081	-3275	-42873	130604	-366365
1083	-3244	-42117	127868	-360007
1085	-3228	-41723	126529	-356675
1087	-3212	-41337	125187	-353423
1089	-3195	-40956	123844	-350208
1091	-3179	-40579	122499	-347029
1093	-3162	-40205	121152	-343886
1095	-3145	-39836	119804	-340779
1097	-3128	-39471	118454	-337706
1099	-3111	-39115	117100	-334713
1101	-3076	-38366	114467	-328393
1103	-3059	-37978	113181	-325108
1105	-3041	-37598	111891	-321891
1107	-3023	-37221	110600	-318706
1109	-3005	-36847	109308	-315552
1111	-2987	-36478	108014	-312430
1113	-2968	-36112	106718	-309339
1115	-2950	-35749	105421	-306278
1117	-2931	-35394	104120	-303286
1119	-2893	-34654	101594	-297029
1121	-2874	-34273	100362	-293798
1123	-2854	-33899	99126	-290627
1125	-2835	-33528	97890	-287483
1127	-2815	-33160	96652	-284367
1129	-2795	-32795	95412	-281278
1131	-2775	-32433	94171	-278216
1133	-2755	-32074	92929	-275180
1135	-2734	-31722	91683	-272203
1137	-2693	-30994	89267	-266029
1139	-2672	-30621	88090	-262861
1141	-2651	-30254	86911	-259745
1143	-2630	-29890	85730	-256652
1145	-2609	-29529	84548	-253583
1147	-2587	-29170	83364	-250538
1149	-2565	-28814	82180	-247515
1151	-2544	-28460	80994	-244516
1153	-2522	-28112	79804	-241567
1155	-2477	-27398	77502	-235496
1157	-2455	-27034	76382	-232398
1159	-2432	-26675	75260	-229344
1161	-2409	-26319	74136	-226310
1163	-2386	-25965	73012	-223297
1165	-2363	-25613	71886	-220304
1167	-2340	-25264	70759	-217331
1169	-2317	-24917	69631	-214377
1171	-2293	-24574	68499	-211467

1173	-2246	-23876	66313	-205514
1175	-2222	-23522	65251	-202492
1177	-2197	-23172	64187	-199508
1179	-2173	-22824	63123	-196541
1181	-2149	-22478	62057	-193591
1183	-2124	-22135	60990	-190658
1185	-2099	-21793	59921	-187743
1187	-2074	-21453	58852	-184843
1189	-2049	-21117	57780	-181980
1191	-1998	-20436	55712	-176159
1193	-1973	-20092	54709	-173218
1195	-1947	-19752	53705	-170308
1197	-1921	-19413	52699	-167413
1199	-1895	-19077	51693	-164533
1201	-1869	-18742	50686	-161667
1203	-1843	-18408	49677	-158815
1205	-1816	-18076	48668	-155977
1207	-1789	-17748	47656	-153169
1209	-1736	-17085	45708	-147491
1211	-1708	-16752	44765	-144634
1213	-1681	-16422	43820	-141804
1215	-1654	-16093	42875	-138985
1217	-1626	-15766	41928	-136179
1219	-1598	-15440	40981	-133385
1221	-1571	-15116	40033	-130602
1223	-1542	-14793	39085	-127830
1225	-1514	-14473	38134	-125084
1227	-1457	-13829	36305	-119555
1229	-1429	-13507	35422	-116785
1231	-1400	-13187	34537	-114036
1233	-1371	-12869	33651	-111298
1235	-1342	-12552	32765	-108569
1237	-1313	-12236	31878	-105849
1239	-1283	-11921	30990	-103139
1241	-1254	-11607	30102	-100437
1243	-1224	-11295	29212	-97756
1245	-1164	-10671	27502	-92380
1247	-1134	-10360	26677	-89698
1249	-1104	-10051	25850	-87031
1251	-1073	-9742	25023	-84372
1253	-1043	-9435	24195	-81721
1255	-1012	-9129	23367	-79077
1257	-981	-8823	22539	-76440
1259	-950	-8518	21710	-73810
1261	-919	-8215	20879	-71194
1263	-856	-7610	19283	-65969
1265	-825	-7310	18512	-63370
1267	-793	-7011	17740	-60782
1269	-761	-6712	16967	-58199
1271	-729	-6414	16195	-55622
1273	-697	-6117	15422	-53050
1275	-665	-5820	14649	-50483
1277	-632	-5524	13875	-47921
1279	-600	-5229	13100	-45368
1281	-535	-4642	11606	-40279
1283	-502	-4351	10881	-37753
1285	-469	-4060	10155	-35232
1287	-436	-3770	9430	-32716
1289	-403	-3480	8704	-30202

1291	-370	-3191	7978	-27691
1293	-336	-2902	7252	-25183
1295	-303	-2613	6525	-22677
1297	-269	-2325	5798	-20176
1299	-202	-1750	4377	-15184
1301	-169	-1464	3677	-12702
1303	-135	-1179	2978	-10222
1305	-101	-893	2279	-7742
1307	-76	-679	1754	-5883
1309	-50	-465	1230	-4024
1311	-25	-251	705	-2165

11-48